FRA24-92-0013
Contract DTFR53-91-C-00046

October 1992

Maglev Guideway Route Alignment and Right-of-Way Requirements

Final Report

U.S. Department of Transportation

Federal Railroad Administration

MARTIN MARIETTA

Air Traffic Systems

Technical Report Documentation Page

1. Report No.	2. Government Accession No.	3. Recipient's Catalog No.
DOT/FRA/NMI-92/10		

4. Title and Subtitle	5. Report Date
Maglev Guideway Route Alignment and Right of Way Requirements	October 2, 1992
	6. Performing Organization Code
	8. Performing Organization Report No. DTFR53-91-C00046
7. Author(s) S. Carlton, T. Andriola	
9. Performing Organization Name and Address Martin Marietta Corporation Air Traffic Systems Division 475 School Street, SW Washington, DC 20024	10. Work Unit No. (TRAIS) 11. Contract or Grant No. DTFR53-91-C-00046
12. Sponsoring Agency Name and Address US Dept of Transportation/Federal Railroad Administration 400 Seventh Street, SW, Room 8222 Washington, DC 20590	13. Type of Report and Period Covered Final Report 14. Sponsoring Agency Code RDV-9

15. Supplementary Notes

COTR: Peter Montague, Federal Railroad Administration

16. Abstract

The use of existing rights-of-way (ROW) is assessed for maglev systems by estimating trip times and land acquisition requirements for potential maglev corridors while meeting passenger comfort limits. Right-of-way excursions improve trip time but incur a cost for purchasing land. This final report documents findings of the eight tasks in establishing right-of-way feasibility by examining three city-pair corridors in detail and developing an approximation method for estimating route length and travel times in 20 additional city-pair corridor portions and 21 new corridors. The use of routes independent of existing railroad or highway rights-of-way have trip time advantages and significantly reduce the need for aggressive guideway geometries on intercity corridors.

Selection of the appropriate alignment is determined by many corridor specific issues. Use of existing intercity rights-of-way may be appropriate for parts of routes on a corridor-specific basis and for urban penetration where vehicle speeds are likely to be reduced by policy due to noise and safety considerations, and where land acquisition costs are high. Detailed aspects of available rights-of-way, land acquisition costs, geotechnical issues, land use, and population centers must be examined in more detail on a specific corridor basis before the proper or best maglev alignment can be chosen. Other issues affecting the viability of maglev transportation include ridership, fare structures, and competition which are outside the scope of this research.

17. Key Words	18. Distribution Statement
Maglev, right-of-way, travel times, guideway alignment	Document is available to the US public through the National Technical Information Service, Springfield, VA 22161

19. Security Classif. (of this report)	20. Security Classif. (of this page)	21. No. of Pages	22. Price
Unclassified	Unclassified		

FRA24-92-0013
Contract DTFR53-91-C-00046

Maglev Guideway Route Alignment and Right-of-Way Requirements

October 1992

Final Report

MARTIN MARIETTA
AIR TRAFFIC SYSTEMS

475 School Street, SW
Washington, DC 20024

FOREWORD

Martin Marietta Corporation, Air Traffic Systems, submits this Final Report to the Federal Railroad Administration (FRA) as required under Contract No. DTFR53 91-C-00046, Maglev Guideway Route Alignment and Right-of-Way Requirements.

The authors wish to acknowledge the important contributions made by others to the successful execution of this study and the preparation of this report.

Mr. Peter Montague, the contracting officer's technical representative, and Mr. Arrigo Mongini , both of the Federal Railroad Administration, Washington DC, who provided technical oversight, encouragement, and guidance throughout the study.

Dr. John Harding and Mr. James Milner of the National Maglev Initiative and Ron Mauri and Leonore Katz-Rhoads of the Volpe National Transportation Systems Center, Cambridge, Massachusetts, who provided valuable inputs, attended periodic reviews, and served as an advisory group during the study effort and in the review of draft reports.

Messrs.Dave Muenkle, Ernie Zaloznik, and Jim Buzbee of Martin Marietta Astronautics, Denver, CO for their energetic and timely contributions of information and support during the study analysis.

We also wish to thank the other members of Martin Marietta Air Traffic Systems who dedicated many hours of their time to ensure the high quality and appropriate focus of this study. We thank Mr. Daniel Schaeffer and his staff for technical support, Mr. James Harbaugh for technical reviews and quality control, Mr. Carl Sara for his system and programmatic insights, and the support services personnel at Air Traffic Systems.

The Authors
Steven G. Carlton
Thomas Andriola
Principal Investigator:
Kenneth E. Ekman

CONTENTS

computer mapping

1.0 SUMMARY (ABSTRACT)

The use of existing rights-of-way (ROW) is assessed for maglev systems by estimating trip times and land acquisition requirements for potential maglev corridors while meeting passenger comfort limits. Potential excursions from and routes independent of existing ROW are found to reduce trip time but incur a cost for purchasing and clearing land for new ROW. This research documents the findings of eight tasks defined to assess the feasibility of maglev transportation alignments using existing rights-of-way. Three city-pair corridors are examined in detail, and an approximation method for 20 additional city-pair corridors is developed. The findings indicate that routes independent of existing railroad or highway rights-of-way have significant trip time advantages and significantly reduce the need for aggressive guideway geometries (high bank angles, rapid roll rates, etc.) on intercity corridors.

Ride comfort limits are recommended and used to derive maximum speeds with respect to guideway alignment characteristics, namely horizontal curvature, grade and vertical curvature, bank angle, and their rates of change. Segment speed profiles are developed, and non-default span lengths (i.e., bridges and alternative structures) are identified, for rail and highway routes in three corridors: (1) Syracuse-Albany-New York City, (2) Detroit-Chicago, and (3) San Francisco-Los Angeles. Trip times are estimated in both directions with 110, 134, and 150 m/s maximum speed constraints using simulated vehicle operations. Efforts to reduce overall trip times include judicious departures from the existing rights-of-way and new routes. Excursion alignments are compared for effectiveness by examining reduced trip time with respect to route kilometers outside the existing right-of-way. Trip times, average speed and span length requirements are provided for the excursion and independent routes in the three detailed corridors. A method for approximating trip times along 20 other corridors for existing highway and railroad rights-of-way, excursions, and independent routes is developed using raster scanned topographic map images, alignment digitization and trip time analysis software, and a parametric estimator. Costs for a default span configuration of 25 meters and recommended alternative structures, where the default structure is not usable, are estimated on a per meter basis.

Alignment geometries constrained within existing rights-of-way require that passengers tolerate aggressive superelevation, roll rate and vertical acceleration comfort limits. Existing alignments are shown to include short-radius curvatures (many 2000 meters or less) which require using total banking of up to 30 degrees to control lateral loads at high speeds. However, this entails downward vertical accelerations of up to 1.3g and requires roll rates of up to 10 degrees per second to shorten transition spirals enough to stay within ROW constraints for most of the route.

In these alignment configurations, passengers are subjected to comfort attributes unprecedented in previously implemented public transportation systems.

The advantage of these aggressive alignment geometries is that intercity trip time reductions on the order of 30 percent from more conservative approaches using 12 degrees superelevation, 1.2g maximum downward vertical acceleration, and 5 degrees per second roll rate limits can be achieved. These travel time advantages can be reduced still further by using alignments largely independent of the existing ROW and the more conservative comfort limits. These independent alignments consist of relatively longer tangent segments and larger radius curved segments which eliminate the need for the high bank angles. The independent alignment also exhibits higher average speeds for a given maximum vehicle speed and therefore accommodates the high speed capabilities of maglev systems effectively However, this approach will require acquisition and clearing of land for new ROW. These new ROW costs are compensated for somewhat by savings in guideway construction costs resulting from shorter independent route lengths and potentially reduced column height requirements.

Selection of appropriate alignments is determined by many corridor specific issues. Use of existing intercity rights-of-way may be appropriate for parts of routes where alignments are relatively straight or terrain constraints limit alternatives, and for urban penetration where vehicle speeds are likely to be reduced by policy and where land acquisition costs are high. Detailed aspects of available rights-of-way, land acquisition costs, geotechnical issues, land use, and population centers must be examined in more detail on a specific corridor basis before the most appropriate maglev alignment can be chosen. These and other issues, including ridership, fare structures, and competition, are outside the scope of this research.

2.0 TASKS PERFORMED

This research on the Maglev Guideway Route Alignment and Right-of-Way Requirements study is provided under paragraph 5.1 of the statement of work (SOW). This report covers eight tasks specified in the SOW. Paragraph 5.2 specifies that results of the proposed maglev route analyses be delivered in map and printed-list format and that machine-readable output be included as part of, or in an appendix to, the final report. Table 2-1 shows the SOW requirements and the location of the report sections which fulfill those requirements. Table 2-2 shows the 23 corridors investigated in this study.

Table 2-1 Reference to SOW Requirements and Location of Response

SOW Requirement	Section
a. 4.1.1 Identify methods for assessing passenger comfort and recommend an approach for scoring route alignment using a method that is sensitive to transportation ride quality. The contractor shall: (1) identify various measures of passenger comfort relevant to ride conditions expected in maglev operating environments, and (2) recommend limits of these measures for passengers.	3.2
4.1.2 Use comfort experienced through and comfort standards used in other transport modes, e.g., railroad, airplanes, automobiles, elevators, etc., to derive limits that can be applied to maglev operations.	3.2
b. 4.2.1 Derive maximum speed as a function of guideway geometry, such that passenger comfort recommendations established in Task 1 are not exceeded. The term "guideway geometry" refers to characteristics of the guideway, including grade, horizontal curve radius, bank angle, and rates of change of these characteristics with respect to distance along the guideway. These derived speeds shall be reported in both table and graph format. Combinations of grade, curvature, and banking that result in maximum speeds as low as 10 m/s shall be considered. Grade and curve measures shall be reported in relatively small increments (e.g., 0.5 percent and 150 m, respectively) to facilitate detailed evaluations of vehicle speed and trip times over alternative route alignments. The maximum bank angle set by the government is 12 degrees.	3.3.3 Appendix C
4.2.2 Where applicable, the contractor shall derive minimum speeds. For certain bank angles and horizontal curvature combinations, it may be necessary to maintain a minimum speed to achieve acceptable lateral acceleration levels.	3.3.5

c. 4.3.1 Develop maximum maglev segment speed profiles for a rail and a highway route in each of three selected corridors identified by the COTR as shown in Table 2-2. Use geographical alignment information to divide the route into segments for which alignment parameters are approximately constant.	3.4.3
4.3.2 Assume that the maglev guideway follows the existing curve alignment of the highway or rail route, and that grade and vertical curvature variations can be minimized by varying guideway height with support columns up to 12 m high. Identify and report on the number, by length category, of required bridges, i.e., the number of cases in which standard maglev span lengths must be exceeded because of specific circumstances. The maximum segment speed is the highest speed that does not exceed the passenger comfort limits identified, and is not limited by technical considerations such as vehicle power. For level, straight guideway, a maximum speed of 150 m/s shall be used.	3.4.4
d. 4.4 Estimate trip time for each corridor-route combination . Calculate and report average and speed at standard intervals of 300 meters for each segment-direction. Three maximum speeds shall be analyzed: 110, 134, and 150 m/s.	3.5 Appendix D
e. 4.5.1 Estimate the improvements in baseline trip times that would be associated with realistic maglev alignment excursions outside the existing rail and highway alignments considered. Identify the segments that most lengthen trip time and explore options for reducing their impact by moving the guideway alignment outside the rail or highway right-of-way.	3.6
4.5.2 Develop a new route alignment that is not constrained by the requirement that it roughly follow the existing highway and rail routes. In defining a new route the contractor shall take into account the special curve banking and grade climbing characteristics of maglev, and passenger comfort identified in Tasks 1 and 2.	3.6.6
4.5.3 Route re-alignment projects (or groups of related projects for segments whose maximum speeds are closely related) shall be listed in order of trip time reduction per kilometer of route outside the existing right-of-way. Required area needed shall also be reported assuming a right-of-way width provided. Maglev right-of-way width is set by the COTR at 18.3 meters.	3.6 Appendix E

f. 4.6 Develop and document a method for approximating trip times along other defined routes and estimating trip time improvements from route excursions by extending the results of Tasks 3, 4, and 5 to 20 additional corridors. Additional land and structural requirements shall be similarly estimated. The 20 corridors set by the COTR are listed in Table 2-2.	3.7
g. 4.7.1 Establish a default or baseline value for guideway support pillar spacing and span length. A literature search shall be performed to summarize guideway configurations and construction techniques.	3.8.3
4.7.2 Solutions shall be recommended to cases where the default span length must be exceeded because of special circumstances.. Solutions shall be specified for incremental ranges of extra span length. Estimates for construction costs per meter shall be developed for each recommended solution.	3.8.4
h. 4.8 Based on the 23 routes analyzed, quantitative results shall be arrayed in such a manner that conclusions can be drawn regarding the advantages and disadvantages of utilizing the existing right-of-way.	3.9

Table 2-2 Corridors Studied for Right-of-Way Analysis

Region	Three Detailed Corridors	20 Additional Corridors (Highway and Railroad)
Northeast:	A. Highway and Railroad New York City- Albany - Utica - Syracuse	1. Boston - Hartford 2. Hartford - New York City 3. New York City - Philadelphia 4. Philadelphia - Wilmington 5. Wilmington - Baltimore 6. Baltimore - Washington,D.C. 7. Syracuse - Rochester - Buffalo 8. Buffalo - Niagara Falls
Mid-West:	B. Highway and Railroad Detroit - Ann Arbor - Kalamazoo - Chicago	9. Chicago - Milwaukee 10. Milwaukee - Madison
Southwest:		11. Dallas - Houston 12. Dallas - Waco 13. Waco - Austin 14. Austin - San Antonio 15. Houston - Austin
West:	C1. Highway Los Angeles - Buttonwillow - Santa Nella - San Francisco C2. Railroad Los Angeles - Bakersfield - Merced - San Francisco	16. Los Angeles - Las Vegas 17. Los Angeles - San Diego 18. Seattle - Tacoma - Olympia - Portland
Southeast:		19. Miami - Ft. Lauderdale - W. Palm Beach - Orlando 20. Orlando - Tampa

3.0 FINDINGS

3.1 INTRODUCTION

The Maglev Guideway Route Alignment and Right-of-Way Requirements study is divided into eight distinct tasks. Figure 3.1-1 shows the relationship of these tasks and the corresponding outputs of each task.

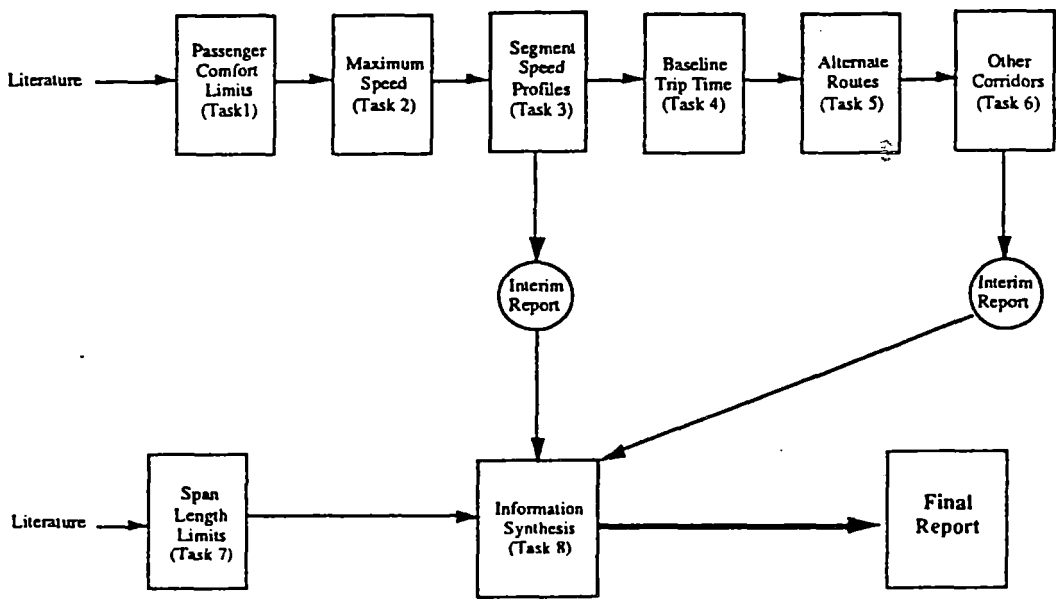

Figure 3.1-1 Relationship of Tasks

Subsection 3.2 identifies and evaluates methods used to assess ride comfort as a function of guideway alignment characteristics. This subsection defines comfort parameters due to guideway alignment with respect to a passenger-referenced coordinate system. Previous research in the area of passenger comfort is cited to assist in drawing conclusions on acceptable limits of forces for a maglev system. The subsection concludes with recommended limits for ride comfort which are used in subsequent tasks.

Subsection 3.3 derives maximum speeds with respect to guideway alignment characteristics, namely horizontal curvature, grade and vertical curvature, bank angle, and rates of change of these characteristics. Maximum speeds are derived for several curvature and bank angle combinations by constraining unbalanced forces acting on the passenger during vehicle motion along the guideway. Tables are produced (Appendix C) which tabulate speed limits with respect to combinations of guideway characteristics.

Subsection 3.4 develops segment speed profiles for a rail and highway route along three corridors: (1) New York City--Albany-Syracuse, (2) Detroit-Chicago, and (3) Los Angeles-San Francisco. Profiles are driven by the tables of subsection 3.3, and reflect maximum vehicle speeds along route segments containing similar guideway alignment characteristics. Speed profiles are displayed in graphical formats, and areas of severely restricted speed are identified and analyzed. Non-default span lengths (i.e., bridges and alternative structures) are also identified and reported.

Subsection 3.5 describes the findings obtained by examining vehicle trip times on the six route alignments developed previously. Vehicle motion is constrained by the geometric alignments represented in the speed profiles developed in subsection 3.4 and further by the longitudinal acceleration limits described in subsection 3.2. Each route is examined in both directions with 110, 134, and 150 m/s maximum speed constraints. The results of 36 computer runs (3 city-pair corridors * 2 routes * 3 maximum speeds * 2 directions) are described using tabulations of vehicle speed at 300-meter intervals and overall average speed.

Subsection 3.6 details the procedures used and the results obtained in efforts to reduce overall trip times by including judicious departures from the existing rights-of-way on the six route alignments. Route segments are identified which most limit speed and for which terrain and population density allow excursions. Excursion alignments are then compared for effectiveness by examining reduced trip time with respect to route kilometers outside the existing right-of-way. New routes not constrained by existing rights-of-way are identified. Trip times, average speed and span length requirements are provided for each independent route of the three detailed corridors.

Subsection 3.7 describes a method for approximating trip times along 20 other corridors for existing highway and railroad rights-of-way, excursions and independent routes. Land and extended span requirements are also identified. The approximation method uses raster scanned topographic map images, alignment digitization and trip time analysis software, and a parametric estimation trained against the three detailed corridors examined previously.

Subsection 3.8 provides costs for a default span configuration 25 meters. Alternative structures are identified for occasions along the guideway where the default structure is not usable. Length ranges are recommended and costs estimated (on a per meter basis) for all alternatives.

Subsection 3.9 includes a synthesis of the data generated in the previous tasks so that conclusions can be drawn from the research as a whole.

3.2 COMFORT PARAMETERS

3.2.1 Introduction

Maglev systems must provide appropriate comfort levels to attract sufficient ridership from existing transportation modes. Passengers may be exposed to unbalanced acceleration forces for longer periods of time during high-speed operation of the maglev system when compared to other forms of travel. It is projected that long radius curves, reaching several kilometers in length and requiring tens of seconds to traverse, will be prevalent in maglev system guideway alignments. High-speed travel and sustained unbalanced accelerations require that comfort limits be set to guide system designers and ensure an acceptable ride for passengers.

A literature search was performed which resulted in the identification of many aspects of passenger comfort. Comfort limits are recommended here for those aspects which directly affect the guideway alignment. These include linear acceleration, linear jerk, and roll rate. These parameters lead to guideway length, curvature radius, trip time and the need for right-of-way excursions. Levels for acoustic noise, temperature and pressure are not addressed, and no attempt has been made to establish the overall comfort limit or a budget for all contributing factors.

Several factors in the vehicle/guideway design and operation contribute to the overall comfort, including guideway curvature and banking; vehicle suspension and aerodynamics; and electromechanical vibrations. Design tolerances must be established for each portion of the maglev vehicle/guideway system to ensure passenger comfort. The total of these tolerance specifications define the comfort budget for a maglev system.

3.2.2 Passenger Comfort Parameters

Figure 3.2.2-1 identifies the parameters of passenger comfort. The discussion of passenger comfort considers both quantitative and qualitative measures. Quantitative measures are defined based on physical conditions and the effects of acceleration forces, and can be calculated or measured. Qualitative measures are assigned subjectively because they depend on passenger perception and feelings of comfort.

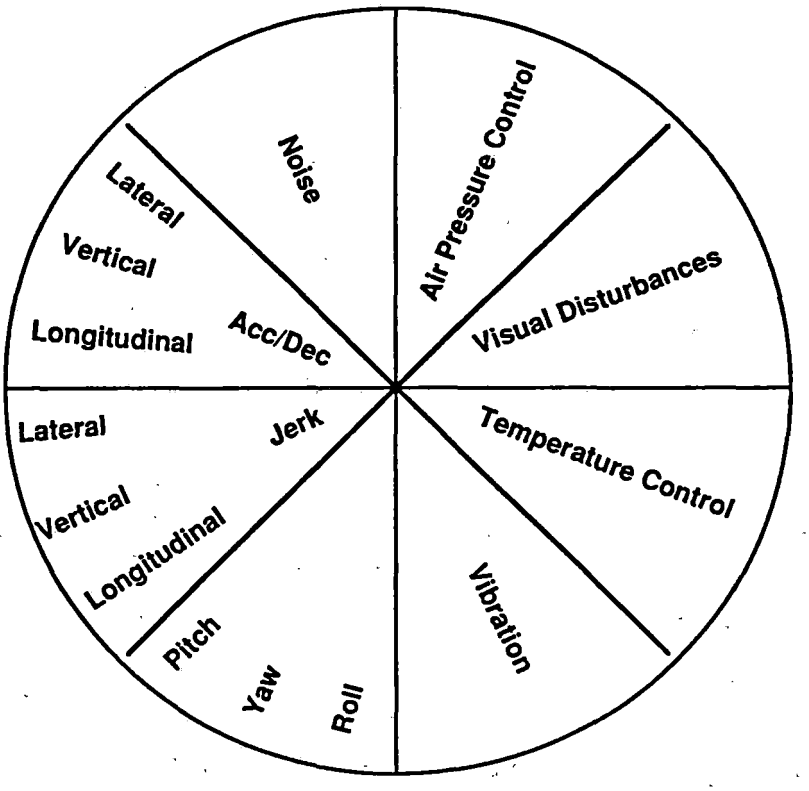

Figure 3.2.2-1 Comfort Parameters

An example of qualitative measures is the choice of speed and acceleration by automobile operators. The levels that are attained usually reflect the driver's subjective feeling of control and "may be the influence of visual contact with the forward environment ... The automobile rider sees the onset of curves, maneuvers, starts, and stops and is prepared for them. For the coach passenger, the behavior of the train comes without warning." (reference 1).

The focus of this report is on the acceleration, rates of change of acceleration (jerk), and rotational rates associated with passenger comfort. The six degrees of freedom for vehicle motion are shown in Table 3.2.2-1. These motions produce two types of acceleration forces, linear and rotational, which are relevant to passenger comfort. Linear forces are applied in the x, y, and z directions and are referred to as longitudinal, lateral, and vertical, respectively. Rotational forces are applied about the x, y, and z axes and are referred to as roll, pitch, and yaw, respectively. This is illustrated in Appendix B.

Table 3.2.2-1 Degrees of Freedom

Axis	Linear	Rotational
x	Longitudinal	Roll
y	Lateral	Pitch
z	Vertical	Yaw

3.2.2.1 Linear and Rotational Comfort Parameters

Lateral

Lateral acceleration contributes to a linear force felt by passengers as the vehicle traverses a curve. Passengers feel that they are either being pushed against the outside of the car, such as in flat curves, or falling in towards the center of the curve, such as when vehicle speed is too slow with respect to the degree of guideway superelevation. For flat curves, the important guideway parameters associated with calculating lateral forces are the degrees (or radius) of curvature and vehicle speed. The relationship of these variables can be shown by the equation for uniform circular motion.

$$a = v^2/r$$

where: a = centripetal acceleration
v = tangential velocity
r = radius of the circle

Lateral comfort limits depend on the level of lateral force that a passenger is willing to endure (both in magnitude and duration). Unbalanced lateral loads can be reduced through the application of guideway superelevation and proper vehicle speed control.

Vertical

The vertical comfort limits apply to variations in the net vertical forces relative to the constant gravity force acting downward. The primary cause of these variations is the vertical acceleration due to vehicle motion through a vertical guideway curve, which produces a force based on the direction and radius of curvature. Passengers are more sensitive to negative g-forces (e.g., coming out of the seat while cresting a hill) than to positive g-forces (e.g., pushed into the seat while traveling through a valley). Thus, different comfort limits could be set based on the direction of the vertical curvature.

Longitudinal

Longitudinal acceleration is the starting and stopping acceleration of the vehicle. Forward-facing passengers feel a sustained force pushing them backward, into their seat, during vehicle starting acceleration and pulling them forward, out of their seat, during deceleration.

Jerk

Jerk is the rate of change of acceleration expressed in meters per second cubed for linear accelerations. Table 3.2.2.1-1 shows the mathematical expressions for velocity, acceleration, and jerk with respect to linear displacement. Jerk measures the instantaneous pull (or push) associated with changing accelerations. Along with the initial change in acceleration, passengers experience

discomfort from the aperiodic motion of being thrown back and forth during vehicle motion. Horizontal and vertical transition curves are used to control jerk in lateral and vertical accelerations. Longitudinal jerk is controlled by the vehicle propulsion and braking subsystems to provide smooth starting and stopping accelerations.

Table 3.2.2.1-1 Derivatives of Linear Motion

Motion	Displacement	Velocity	Acceleration	Jerk
Longitudinal	dx	$V_x = \frac{dx}{dt}$	$A_x = \frac{dV_x}{dt}$	$r_x = \frac{dA_x}{dt}$
Lateral	dy	$V_y = \frac{dy}{dt}$	$A_y = \frac{dV_y}{dt}$	$r_y = \frac{dA_y}{dt}$
Vertical	dz	$V_z = \frac{dz}{dt}$	$A_z = \frac{dV_z}{dt}$	$r_z = \frac{dA_z}{dt}$

Roll

Roll is defined as the rotation of the vehicle with respect to the x-axis. Roll rate is the angular velocity in degrees per second. Passengers respond favorably to reduced roll conditions in maglev simulated environment studies (reference 2). Banking provides a precise angular positioning of the vehicle to gain advantages of higher speed in horizontal curves while controlling unbalanced lateral accelerations. Transition curves provide a gradual increase in bank angle until the desired angular positioning is reached for a given curve. Thus, the rate of this angular transition, the roll rate, can be equated to the increase in bank angle degrees per meter of guideway times the vehicle speed. The maximum bank angle and the roll rate are the principal parameters that contribute to comfort.

Pitch and Yaw

Pitch and yaw are the vehicle rotations about the y-axis and z-axis, respectively. They are defined relative to the passenger-centered coordinate system (reference Appendix B). In this coordinate system, the x-axis is always coincident with the direction of longitudinal vehicle motion.

Values for pitch and yaw are small because these motions are constrained tightly by the vehicle/guideway interaction. Pitch is limited by control of the levitation gap between the vehicle and guideway. Yaw is limited by control of vehicle guidance gap. Both pitch and yaw are susceptible to vibrational effects induced by vehicle aerodynamics, suspension operation and reaction of the gap control subsystems. These effects are not significant in defining the guideway alignment, and specific limits for these parameters are not recommended here.

3.2.2.2 Other Comfort Parameters

Vibration

Vibration is the rapid, oscillating movement of rigid bodies that is addressed extensively in the literature and is an important parameter for passenger comfort. Guideway alignment resulting in abrupt changes in acceleration rates can strain the counteracting effects of vehicle suspension systems. Smoothing of abrupt changes through the use of transition curves reduces route alignment contributions to vibration. As a result, vehicle design tolerances for vibration from aerodynamic, electromechanical, suspension, and gap control subsystem sources are more easily met.

Noise

Noise from a maglev system may be generated from electromechanical, aerodynamic, and aero-acoustic sources. Flow separation from appendages and structural vibrations account for the aero-acoustic noise. Research has shown that noise and vibration interact to affect the subjective assessment of passenger comfort (reference 3).

Visual Disturbances

Traveling at high speeds with high degrees of banking can cause passenger discomfort. The speed at which the adjacent terrain passes can cause motion sickness to those passengers who have access to a window. Furthermore, high degrees of banking may cause discomfort, because it is unknown how passengers will respond to unusual orientation with visual ground-level references at high speed (reference 4).

Other Factors

Many other measures can contribute to the overall comfort of passengers: temperature, pressure if the maglev is traveling through a tunnel, interior cabin design, and seat design. Exploring these human factors issues is necessary in the development of ride-quality standards.

3.2.3 Comfort Limits from Literature Search

There is considerable value gained in examining passenger comfort limits for other modes of transportation. Assessing these comfort limits allows conclusions to be drawn about the acceptable levels of acceleration, jerk, and rotational forces in the operational environment of a maglev system.

In the technical literature, two types of quantitative values for accelerations levels are presented. First, representative values are commonly found based on acceleration performance of a specific vehicle. Second, comfort limits are usually set based on experiments measuring subject responses to

different ride-quality situations. It is necessary to differentiate between the potential operational values of a system versus the acceptable level necessary for passenger comfort. Table 3.2.3-1 provides both representative values and comfort limits for linear accelerations.

Comfort limits for longitudinal acceleration ranged from 0.105g (electric train) to 0.26 (automobile). The relatively high accelerations for automobiles are attributed to the visual contact with the forward environment experienced by drivers and passengers. Passenger preparedness carries a significant weight in the judgement of acceptable acceleration levels (reference 1). Current high-speed maglev systems operate in the 0.153g range. However, if the maglev system could be designed to prepare passengers for periods of forward or backward acceleration, longitudinal limits could be raised to levels similar to that of aircraft.

Table 3.2.3-1 Comfort Parameter Values

Transportation System	Comfort Limit	Representative Value
	Start/Stop Acceleration (g)	**Start/Stop Acceleration (g)**
Transrapid (ref. 5,10)	.153	NA
Japanese Maglev	.163	NA
Trolley Car (ref. 1)	NA	.120
Electric Train (ref. 1)	.150	NA
Commercial Aircraft (ref. 1)	NA	.501
1992 Corvette	NA	.569 (1)
	Lateral Acceleration (g)	**Lateral Acceleration (g)**
Transrapid (ref. 5,10)	.102	NA
Electric Train (ref. 1)	.220 (2)	NA
General. Motors Testing (ref. 1)	.187 (3)	NA
Elevator (ref. 1)	NA	.010
Trolley Car (ref. 1)	.070	NA
Commercial Aircraft (ref. 1)	NA	.010
	Vertical Acceleration (g)	**Vertical Acceleration (g)**
Transrapid (ref. 5,10)	.051	NA
Elevators (ref. 1)	.300	.094 to .219 (4)
	Jerk (g/s)	**Jerk (g/s)**
Transrapid (ref. 5)	.05 (lateral)	NA
Elevators (ref. 1)	NA	.328 (vertical)
	Bank Angle(d)/ Roll Rate(d/s)	**Bank Angle(d)/ Roll Rate(d/s)**
Transrapid (ref. 10)	NA	12 / 12
Train (ref. 18, 20)	NA	6 / 1.1 - 2.5
Proposed (Grumman,et al)	NA	24 / 3

Note: NA (not available)
(1) Based on Dealer Information, 0 to 60 mph in 4.8 Seconds
(2) Seated Passenger Travel Only
(3) Average for Male Subjects over Different Age Groups
(4) Based on Discussion with Elevator Manufacturer

Lateral accelerations range from 0.06g to 0.22g. The literature did not break down the contributions to lateral accelerations from subsystem sources. Thus, all values reported were considered as total system accelerations.

3.2.4 Previous Research in Assessing Passenger Comfort

Documents pertaining to the assessment of passenger comfort were consulted to determine their applicability for ride quality in high-speed maglev systems. The descriptions below represent those reports that have shown value to evaluating the ride comfort of a maglev system.

Peplar, et al

In the late 1970's, Dr. Richard D. Peplar, et al, developed ride-quality models for subjects exposed to primarily vibrational accelerations for bus and train transportation (references 7, 8, 9). Subjects were asked to rate the ride using a predefined comfort scale as follows:

1 - Very Comfortable
2 - Comfortable
3 - Somewhat Comfortable
4 - Neutral
5 - Somewhat Uncomfortable
6 - Uncomfortable
7 - Very Uncomfortable

Models were generated using best-fit criteria to predict subjective responses for ride comfort. Peplar's approach is given in Figure 3.2.4-1.

Peplar's ride quality research addressed all six degrees of passenger motion. Best-fit regression models were chosen based on correlations among comfort parameters. For bus transportation, roll rate provided the best measure of passenger comfort on straight roads, while lateral forces, sustained and vibrational, were used to estimate comfort for curves. Roll rate and noise were the best measure for train transportation (reference 9). However, Peplar stated that for air travel, lateral and vertical forces are the important comfort parameters (reference 8).

Peplar estimated a mean comfort rating using best-fit parameters as compared to empirical results in passenger tests for the different modes. He also proposed an estimator for "new" modes using bus, train and aircraft results. In addition, he proposed an overall ride-quality model using a binomial distribution to predict the distribution of comfort ratings on the 7-level scale. Figure 3.2.4-2 shows the percentage of passengers satisfied as a function of the comfort rating scale. Finally, Peplar discussed the development of techniques and procedures needed in evaluating rider comfort. Suggestions were made regarding data collection, model choice, and model validation.

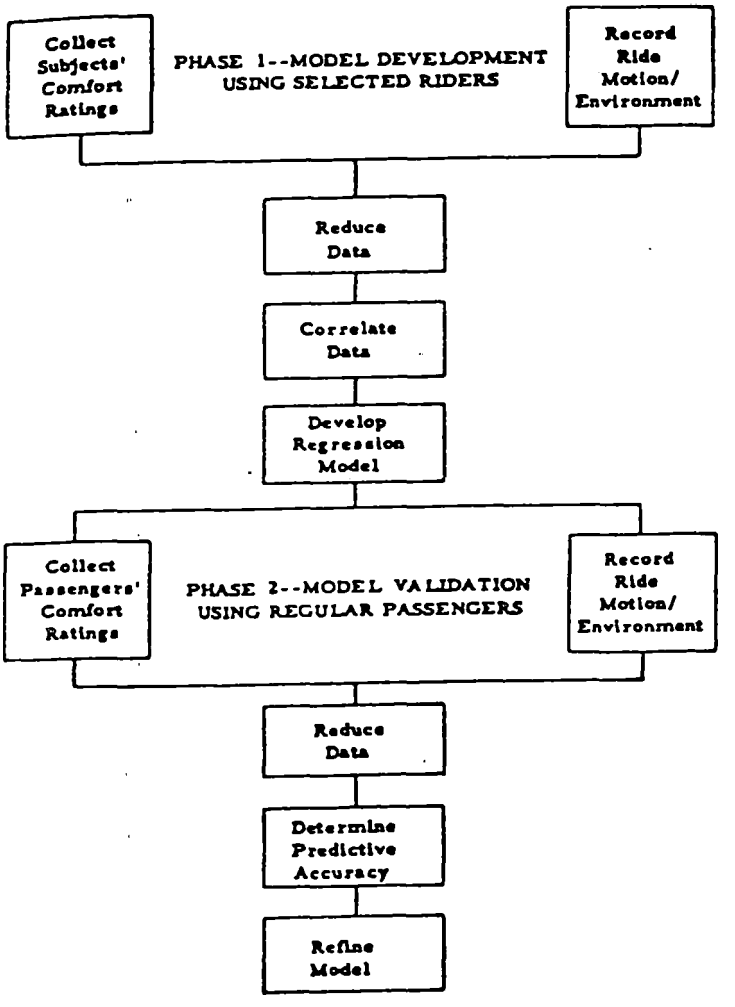

Source: Development of Techniques and Data for Evaluating Ride Quality, Peplar et al, February 1978

Figure 3.2.4-1 Peplar's Approach

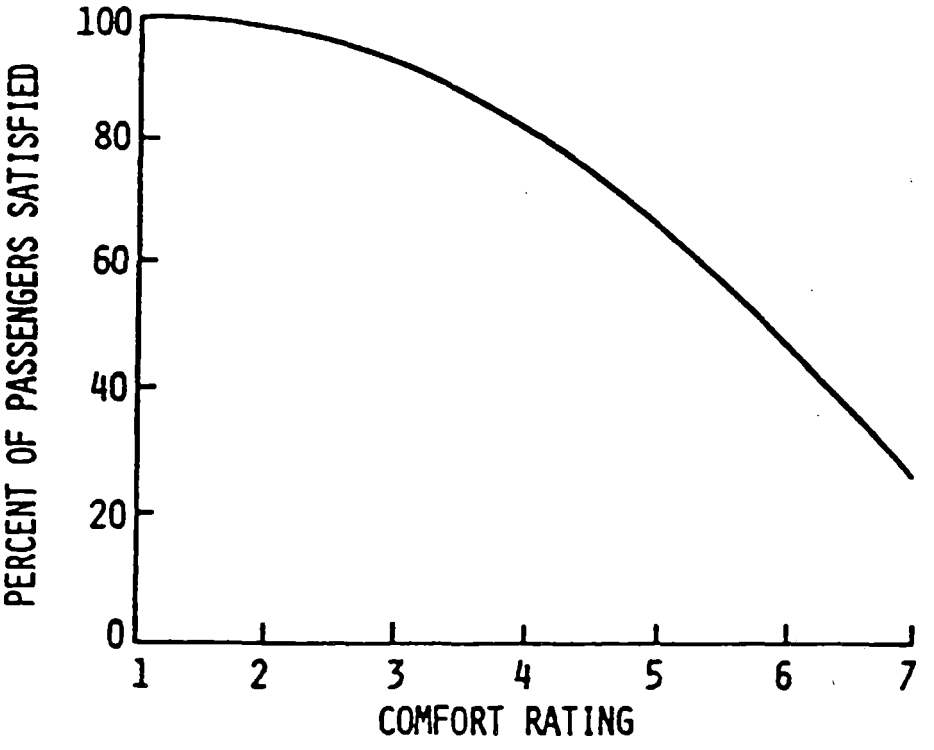

Figure 3.2.4-2 Percent Passengers Satisfied

Peplar's research focused on vibrational accelerations rather than sustained acceleration forces. Vibrational parameters were averaged (root mean square - RMS) for use in comfort estimation. His comfort mean estimator for new modes is represented below:

$$C' = 0.5 + 0.5 * r_r + 0.1[dB(A)-70] + 17 * A_t + 17 * A_v$$

where:
- r_r = Roll Rate (RMS)
- dB(A)= noise on the A-weighted scale inside vehicle
- A_t = Transverse Acceleration (RMS)
- A_v = Vertical Acceleration (RMS)
- C' = Mean Comfort Rating

This estimator is developed using data from tangent segments with some hills. The bus mode data for curved segments, in which sustained lateral acceleration is recognized as an important parameter, is not used to derive this estimator. Also, no mention is made of passenger orientation, such as standing, sitting, and facing direction. Other factors not included in Peplar's study that may influence maglev comfort ratings include relatively high total banking angles, high speed, rapid transitional roll rates (perhaps varying from one side to the other quickly in a successive curves), and frequent longitudinal acceleration/deceleration as may be required to reduce trip times within existing right-of-way constraints.

Limited data has been reported that quantifies noise levels and vibrational parameters to predict and evaluate comfort for maglev systems using Peplar's proposed estimator. These factors, and the

importance of ride comfort, indicate a need to simulate and/or empirically analyze maglev systems further.

United States - Germany Cooperative Study on Ride-Quality

In 1978 the U.S. Department of Transportation (DOT) and Federal Republic Germany Ministry of Research and Development (FRG) performed a cooperative study to research the ride-quality characteristics of potential magnetically levitated systems (reference 2). Subjects were placed in a NASA Passenger Ride Quality (PRQ) simulator and tested on three degrees of freedom: lateral acceleration (rms), vertical acceleration (rms), and roll rate (rms). Passengers rated the level of ride comfort while reading and writing.

The study was divided into two phases in measuring passenger comfort. Phase 1 placed 1 to 2 minutes of constant vibrational forces on subjects. Phase 2 was designed as a 45-minute trip with various degrees of vibrational forces being applied. These experiments were designed to have acceleration and banking characteristics similar to a maglev vehicle. The FRG provided input data from Transrapid05 vehicle runs at three separate speeds. These inputs were translated by the Passenger Ride Quality Apparatus (PRQA) into forces for the simulation runs. Vehicle longitudinal motion was simulated by visual projections of passing scenery outside the simulator windows.

The subject responses were rated on a 7-level comfort scale similar to that used by Peplar et al. Table 3.2.4-1 shows the mean passenger response for the different maglev conditions simulated. The longitudinal velocities indicated in the table refer to the vehicle speeds represented by the vibrational forces simulated. Then, using Peplar's binomial expansion equation, responses were converted to percentages of perceived ride satisfaction.

Table 3.2.4-1 US DOT/FRG Mean Comfort Ratings for Maglev Ride Characteristics

Test Condition	Mean Comfort Rating	Subjective Rating
55.5 m/s Reduced Roll	3.00	Good
55.5 m/s Base Case	3.58	Good/Comfortable
83.3 m/s Reduced Lateral	2.73	Good
83.3 m/s Reduced Roll	3.06	Good
83.3 m/s Base Case	4.25	Comfortable
111 m/s Reduced Roll/Lateral	4.15	Comfortable
111 m/s Reduced Lateral	4.46	Comfortable
111 m/s Reduced Roll	4.79	Comfortable
111 m/s Base Case	5.29	Comfortable/Poor

This study looked at parameters that were most closely related to passenger comfort. Statistical correlations were computed to determine the mathematical relationship between parameters. Lateral and vertical accelerations showed high correlation to perceived comfort. Table 3.2.4-2 shows the correlation matrix from the report. The study revealed that though there was little correlation between the roll rate and comfort, the subjective responses of passengers to reduced roll conditions were significant, especially in the 300 km/hr (83.3 m/s) speed range. Specific roll rate and lateral force reductions applied were not reported for this work.

Table 3.2.4-2 Statistical Correlation for Comfort Parameters

	Comfort	Noise	Lateral	Vertical	Roll
Comfort	1.00				
Noise	0.76	1.00			
Lateral	0.84	0.75	1.00		
Vertical	0.81	0.86	0.85	1.00	
Roll	0.64	0.52	0.52	0.66	1.00

As with Peplar's work, these results provide insight into the discussion of passenger comfort. However, the effect of sustained acceleration forces has not been fully explored. Current high speed maglev (or high speed rail) programs should be consulted to determine the research that has been performed in this area. Benefits may be realized through the construction of an apparatus to simulate sustained acceleration forces for six degrees of freedom and measure passenger responses to such conditions.

Acceleration and Comfort Work

Research was performed by Gebhard (Reference 1) at the Johns Hopkins University on the relationship between acceleration and comfort in ground public transportation systems. Values for linear accelerations and jerk were collected along with performance measures to establish acceptable ranges for acceleration. The resulting comfort ranges recommended are expressed in Table 3.2.4-3.

Table 3.2.4-3 Range Limits of Acceleration Forces

Acceleration	Comfort Range
Longitudinal	0.11g to 0.15g
Lateral	0.06g to 0.22g
Vertical	0.10g to 0.30g

Gebhard concluded that the tests he had examined (to 1970) may have been biased for low accelerations based on effects of the test designs. These biasing factors included the number of rating criteria, the title of the criteria, the instructions given to subjects before testing, and rating unimportant aspects of ride comfort as opposed to "ride choice." He suggested that ride choice may be a more appropriate means of evaluating a new mode of transportation if it were to include other aspects of the trip, such as the trip time.

Gebhard also asserted that acceleration values closer to that of the automobile could be acceptable to passengers if the proper seats were used (e.g., concave seat, concave back support, and arm rests), perhaps appropriate seat constraints, and a visual reference or other alerting system to forewarn of events so that motion accelerations might be anticipated and prepared for as they are in automobiles. He did suggest that more conservative accelerations would be required if operational conditions included standing passengers.

Noise and Vibration Criteria

In 1990 NASA published a report on the development of methodologies to measure ride quality. The methodology recommended the use of a ride-quality apparatus (mentioned above) to create force and noise variations and a ride-quality meter to collect experimental data. The models generated could be useful for "making ride comfort design tradeoffs and as a tool for comparative assessment of ride quality" (reference 3).

This document develops an important part of the ride-quality picture. Noise and vibration levels will need to be addressed for an operational system. Studies can define aerodynamic noise sources and develop design criteria. Vibration forces will be addressed in the guideway and vehicle designs. However, neither noise nor vibration plays a role in passenger comfort from a guideway-alignment standpoint. Therefore, comfort values were not collected.

3.2.5 Recommending Limits

Before setting limits for passenger comfort it is important to have a clear understanding of the operating environment of the maglev system. Questions need to be raised on issues such as ridership, travel time, maximum operating speeds, and passenger restrictions. Without these clarifications there is considerable room for interpretation in setting comfort limits.

Limits selected for this study benefited from FRA stewardship and consultation from many ride quality experts. The limits are the result of government consultation and are representative of current

expert opinions, but do not imply that they represent a Federal Standard Table 3.2.5-1 specifies the comfort limits for use in the subsequent route alignment steps in this study.

Table 3.2.5-1 Recommended Comfort Limits

Comfort Parameter	Acceleration Limit (g)	Jerk Limit (g/s)
Starting/Stopping	0.16	0.07
Lateral	0.10	0.07
Vertical	+0.20 to -0.05	0.10
Roll Rate	5 degrees per second	NA

The limit 0.16g was chosen for starting and stopping acceleration because it is consistent with values being used for maglev test vehicles and rail passenger transit. The limit is slightly higher than the range specified in the Johns Hopkins report. Higher longitudinal accelerations are allowable if jerk values are kept low. To allow for this high value, longitudinal jerk is set at 0.07g/s. Many sources allow that jerk is important, but few values are reported.

A stringent constraint was considered on unbalanced lateral loads (.03 g) to limit geometric contribution to the comfort budget, allow maximum flexibility in the design of other system components, and provide a ride more closely aligned with aircraft. The sustained and vibrational values for aircraft are on the order of .01g and may be important to retain when attracting air mode passengers to maglev.

However, review and consultation with technical experts suggests that a more aggressive approach to unbalanced lateral load (0.10g) is warranted. This will allow a better opportunity to align consistently with the existing right-or-way.

Tangent and curved guideway sections are joined by transition spirals to limit effects of lateral jerk. German studies have shown that using sinusoidal transitions, rather than cubic parabolas, can smooth steps of lateral jerk (reference 10). The limit for lateral jerk was set at 0.07g/s to be consistent with Transrapid (ref. 10) and values reported for railroads (ref. 1). The value for roll rate was chosen at 5 degrees per second. This value is a compromise between the aggressive value used by Transrapid and that experienced in railroads, and reflects some conservatism based on the lack of reported data.

Vertical acceleration forces are more difficult to assign limits to because of different passenger perceptions of forces applied through vertical curves. Passengers are more sensitive to the negative accelerations; therefore, vertical centripetal acceleration limits will range from +0.20g for valleys to -0.05g for crests. Vertical jerk is set at 0.10g/s limit as a representative value consistent with the

lateral jerk and with regard to little reported data. The relatively high value for elevators is discounted due to the high passenger awareness of expected vertical motion when riding an elevator. The only surprise encountered is when the elevator is expected to go one way and it goes the other, such as when one gets on the "wrong" elevator. Also, the passenger sensitivity to vertical acceleration reported (ref. 8) for the air mode indicates that control of vertical acceleration onset through stringent jerk limits is appropriate. Transrapid uses clothoidal vertical transition curves for this purpose (ref. 5).

The limits suggested here will be used in the subsequent steps of this study to align guideway within existing highway and railroad right-of-way. The high speed of maglev and the relatively constrained geometric configuration of right-of-ways will present a challenge to achieve competitive trip-times. High bank angles, rapid roll rates (in transition and from side-to-side), sustained accelerations, frequent longitudinal acceleration/deceleration, and effects with respect to passenger orientation can be expected to contribute to the comfort environment. In addition, aggressive alignments using simultaneous horizontal and vertical curvature may be required. Special seat design, passenger restraint systems, and early warning systems (ref. 1) could allow more aggressive comfort limits. Existing comfort research does not sufficiently address these issues. Further investigation and analysis of these effects for existing maglev prototypes and high-speed rail should be pursued. There is no current operational capability (the NASA PRQA system is out of service) to assess these passenger comfort issues for a maglev system. A realistic tool for evaluating ride quality is essential in the progression of maglev as a viable means of transportation in the United States.

3.3 MAXIMUM SPEED TABLES

3.3.1 Introduction

This section decomposes the components of guideway alignment to understand the forces involved with calculating vehicle speed. Maximum vehicle speeds are calculated here as a function of the following guideway alignment characteristics including grade, vertical curve radius, horizontal curve radius, bank angle, and rates of change of these characteristics with respect to distance along the guideway.

The following assumptions were used in the analysis:

1) Maglev trains consist of a one car vehicle. This simplification eliminates the effects of train coupling in the discussion of guideway alignment.
2) The maglev vehicle has no power constraints. However, a 10% maximum grade is used.
3) A maximum operating speed of 150 m/s is used.
4) A limited set of alternative bank angles is specified for the analysis of maximum speeds. This set includes 6, 12, 18, and 24 degrees.

3.3.2 Characteristics of Guideway Alignment

Horizontal Curvature

Horizontal curvature is the change in the lateral position relative to the change of longitudinal displacement. Horizontal curvature restricts vehicle speed due to passengers comfort limits set for lateral loads.

The rate of change of horizontal curvature measures the transitions from straight to curved path along the guideway. Sudden changes in horizontal curvature produce high levels of lateral jerk which can be deemed unacceptable for ride comfort. Spirals or easement curves are used to produce gradual changes in curvature which reduce the rate of change of the lateral loads. Clothoidal or sinusoidal transition curves can be used to further smooth effects of lateral jerk.

Bank Angle

Guideway banking can increase maximum vehicle speed by reducing the lateral forces felt by passengers while travelling along horizontally curved guideway. The bank angle used in this analysis is a measure of the angular rotation about the x-axis. Superelevation and vehicle tilting effects combine to provide a given bank angle with respect to the earth centered and passenger coordinate systems..

The rate of change of bank angle is referred to as the roll rate. Rotation of the vehicle to desirable bank angles is necessary to maintain vehicle speed while traversing curves. However, passengers are sensitive to sudden vehicle rotations. It is possible that higher roll rate limits can be tolerated by controlling the onset of roll such as through the use of sinusoidal transition curves.

Grade

Grade is the change in elevation per longitudinal distance. The maximum grade for a maglev system has been set at 10 percent for this study. This maximum is not expected to be exceeded while analyzing existing rights-of-way because highways and railroads rarely encounter gradients greater than 5 percent. However, in considering judicious excursions from the right-of-way and independent routes, the 10 percent maximum will be observed.

Grade has no effect on the maximum vehicle speed because vehicle power is not constrained in the initial detailed corridors. (Note that power requirements are substantial at grades approaching 10 percent, especially when high speeds are to be maintained or further longitudinal acceleration is desired. These effects where included in travel time analyses reported for new corridors in section 3.7.) Vehicle speed is limited by the rate of change of grade or vertical curvature. Small radii for vertical curvature can limit vehicle speeds by exceeding comfort levels in the vertical direction. Support columns are used to smooth terrain variations thus minimizing the effects of vertical curvatures.

3.3.3 Derivation of Equations for Maximum Vehicle Speeds

Maximum vehicle speeds for which recommended comfort limits are preserved can be derived through the decomposition and analysis of acceleration forces. Each guideway alignment characteristic and its contribution to the forces acting on the passenger is examined. When the vehicle is at rest, gravity is the only acceleration felt by passengers as shown in Figure 3.3.3-1. The magnitude of the acceleration is 1.0g.

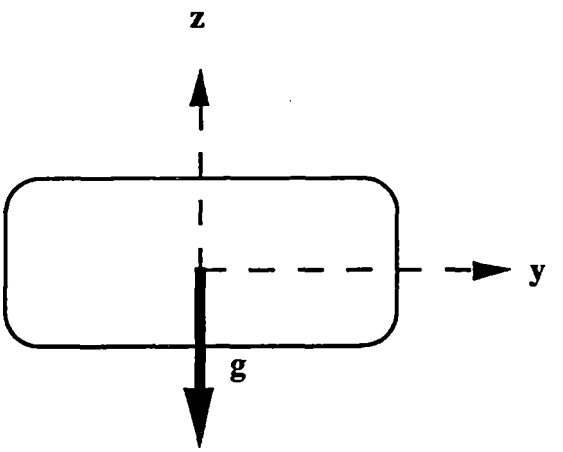

Figure 3.3.3-1 Vehicle At Rest

Once the vehicle is set in motion, other forces acting on the vehicle due to guideway alignment come into play. The most significant forces affecting comfort are the result of horizontal and vertical curvature. Guideway curvature can be defined by the equation for uniform circular motion which defines tangential velocity as a function of radius and centripetal acceleration (shown below). By using this equation vehicle speed can be constrained to meet passenger comfort criteria:

$$a_y = \frac{v^2}{r_h} \qquad a_z = \frac{v^2}{r_v}$$

where: a_y, a_z = lateral and vertical accelerations, respectively
r_h, r_v = horizontal and vertical radii values, respectively
v = vehicle speed

If the maglev vehicle is in motion on a flat, straight path, the force of gravity remains the only force acting on the vehicle (and its passengers). No lateral or vertical forces are being applied because motion is purely longitudinal (i.e., no y or z displacement). Stated another way, values for the horizontal and vertical radii are infinite.

Once lateral or vertical displacement is introduced into the guideway alignment, equations defining vehicle speed must reflect acceleration forces caused by guideway curvature. Equations for maximum vehicle speeds can then be expressed as a function of curve radii and passenger comfort limits.

The following subsections describe each of the guideway alignment characteristics and illustrate the effect on maximum vehicle speed.

3.3.3.1 Horizontal Curvature

Vehicle speed is dependent on the horizontal radius value. Speeds are restricted by the centrifugal force pulling passengers outward and the stringent tolerances set in subsection 3.2.5. For a horizontal curve with no superelevation, a radius of at least 23 kilometers is required before the vehicle can reach the maximum speed of 150 m/s without violating the lateral comfort constraint. Figure 3.3.3.1-1 shows the summations of acceleration forces for this case.

$$Y: \Sigma a_y = \frac{v^2}{r_h} = 0.10g \qquad Z: \Sigma a_z = 1.0g \text{ (gravity)}$$

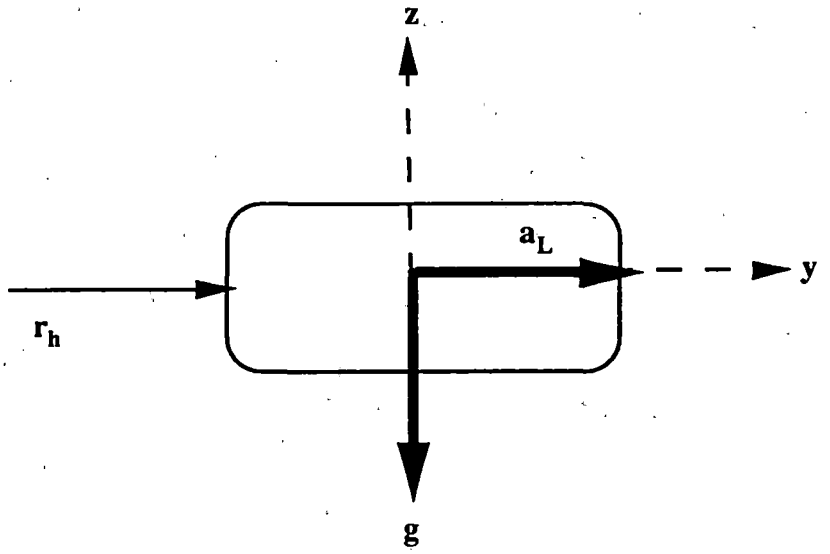

Figure 3.3.3.1-1 Horizontal Curvature

3.3.3.2 Bank Angle

Guideway banking allows vehicle speeds to be increased by reducing the unbalanced, lateral loads caused by horizontal curves.. Figure 3.3.3.2-1 shows the application of acceleration forces with regard to guideway banking. The centrifugal and gravitational forces are still applied in the reference coordinate system as in Figure 3.3.3.1-1. However, passengers will experience the forces through their own reference system which has now rotated ß degrees in the y-z plane due to the banking of the guideway. The dotted lines represent the passenger reference system (see also Appendix B).

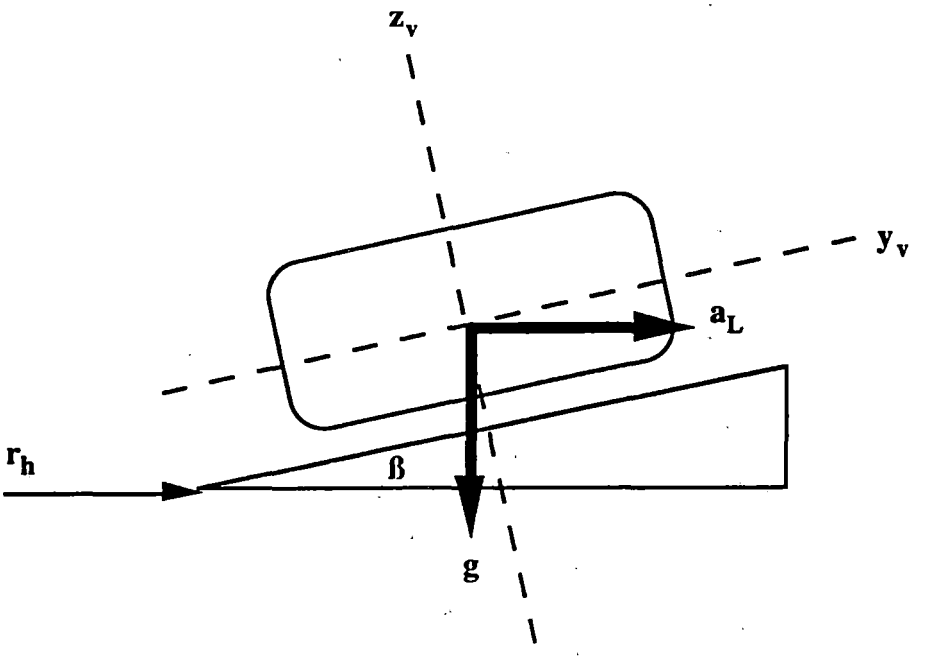

Figure 3.3.3.2-1 Effects Of Guideway Banking

Figure 3.3.3.2-2 shows the decomposed acceleration forces and equations for a banked guideway at angle ß. Contributions to the total lateral force consist of components for both the lateral and vertical directions. As the bank angle increases, the horizontal component of the centrifugal force lessens while the lateral component of the gravitational force increases. Lateral comfort is violated when the imbalance between the centrifugal force and the lateral component of the gravitational force exceeds the lateral limit. As an example, lateral comfort is violated when a vehicle (stationary or moving) is on straight guideway banked greater than 5.7 degrees. So it is possible to begin banking (up to 5.7 degrees) prior to the transition to a horizontal curve.

Figure 3.3.3.2-3 shows top operating speeds (150 m/s) as a function of horizontal radius and bank angle. As the bank angle is increased the minimum radii necessary to maintain the top speed decreases. The Transrapid 07 vehicle has a cruising speed of 400 km/hr and a minimum horizontal radius of 4000 meters for 12 degrees banking. The lateral acceleration for this example is 1.0m/s/s or 0.1g (reference 5,10).

Y: $\Sigma a_y = a_L\cos(\beta) - g\sin(\beta) = 0.10g$

$$\frac{v^2\cos(\beta)}{r_h} = g(0.10 + \sin(\beta))$$

Z: $\Sigma a_z = g\cos(\beta) + a_L\sin(\beta) = 1.2g$

$$\frac{v^2\sin(\beta)}{r_h} = g(1.20 - \cos(\beta))$$

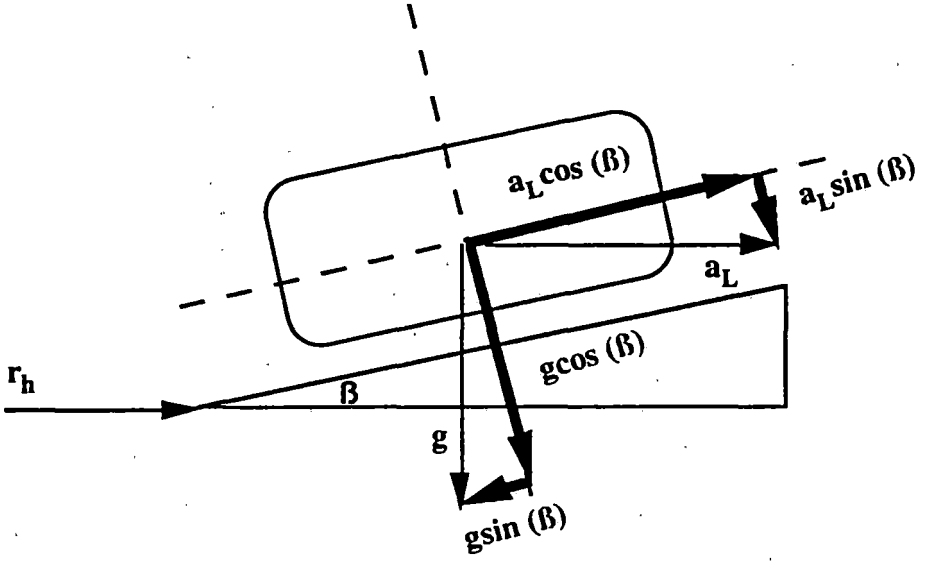

Figure 3.3.3.2-2 Force Decompositions Due To Banking

In addition to the maximum speeds, minimum speeds must be calculated when guideway banking is present. A minimum speed must be maintained in order not to exceed the lateral acceleration limit toward the inside of the curve. Therefore, the maglev vehicle has a speed range to which it must adhere to satisfy lateral comfort limits for any portion of the guideway that is banked. As the degree of banking increases, the allowable speed interval decreases. Figure 3.3.3.2-4 through 3.3.3.2-7 show the maximum and minimum speeds associated with adhering to the 0.10g lateral limit for 6, 12, 18, and 24 degrees of banking.

Vertical forces are also present as a result of guideway banking and must be balanced with respect to comfort constraints. The equation to resolve the vertical components has been provided in Figure 3.3.3.2-2. The sum of the vertical components cannot exceed the comfort constraint of 1.2g in the downward direction. This constraint is violated at the point where passengers feel a force 20 percent greater than gravity pressing down on them, which occurs for banking 33 degrees and greater with balanced lateral loads at 150 m/s. These bank angles are larger than will be examined for use of existing right-of way alignments in this study.

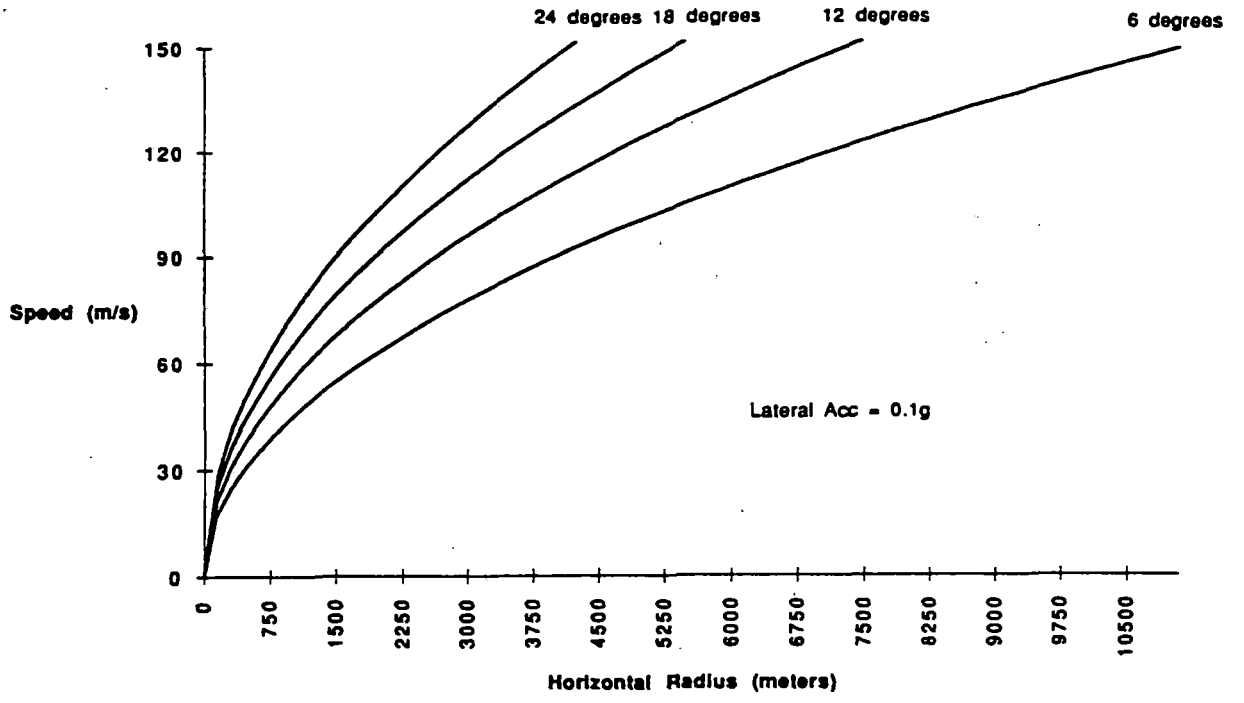

Figure 3.3.3.2-3 Vehicle Speed As Function of Bank Angle

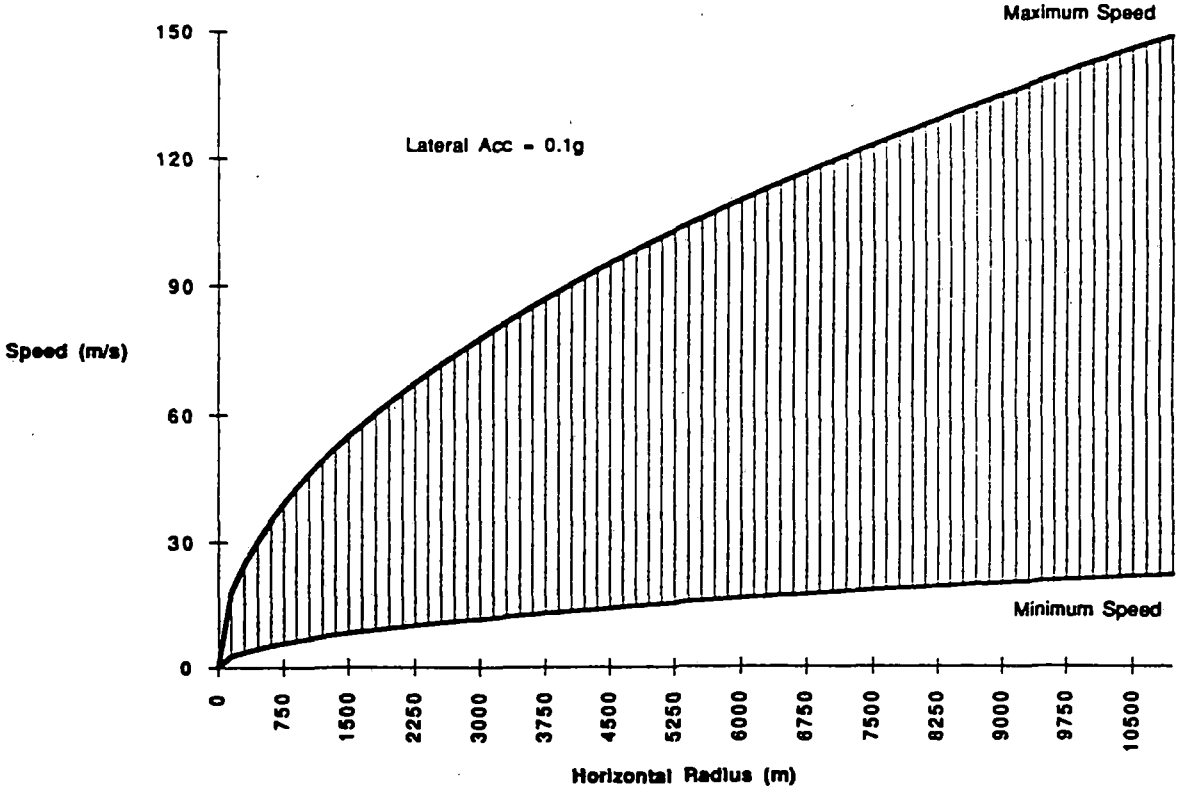

Figure 3.3.3.2-4 Speed Interval for 6 Degrees Banking

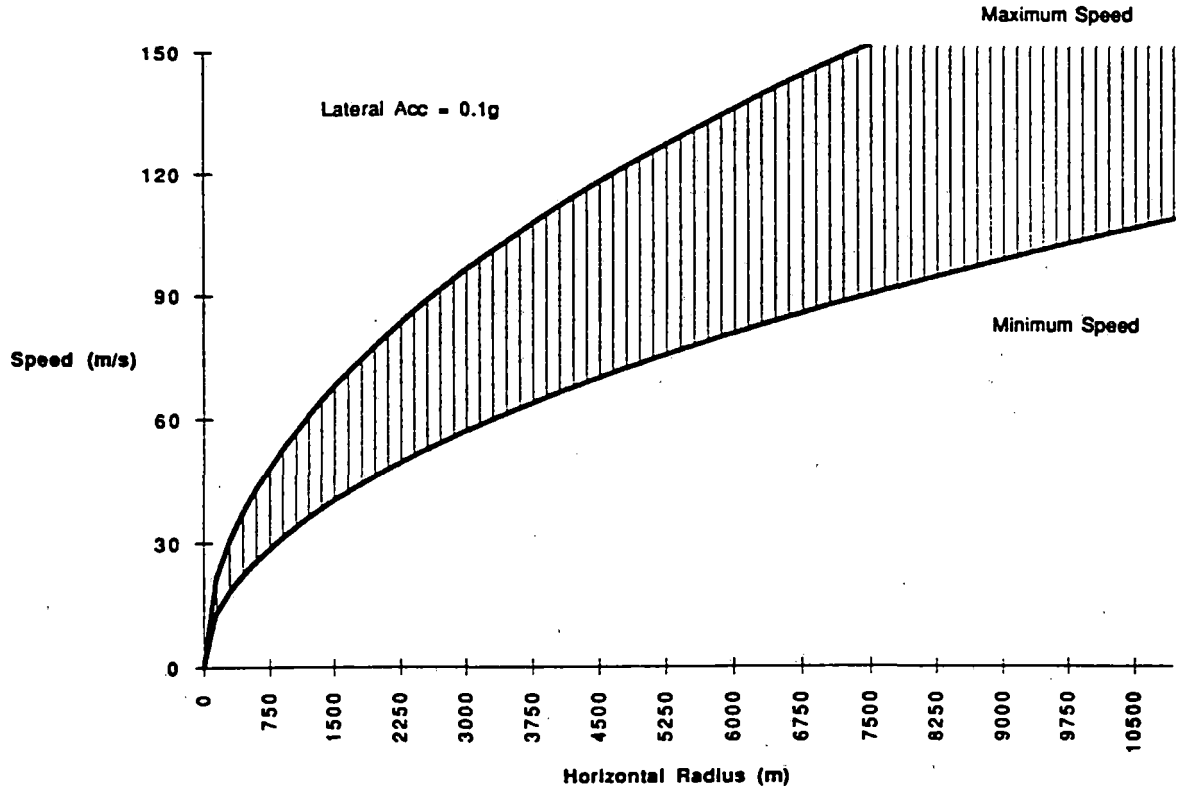

Figure 3.3.3.2-5 Speed Interval for 12 Degrees Banking

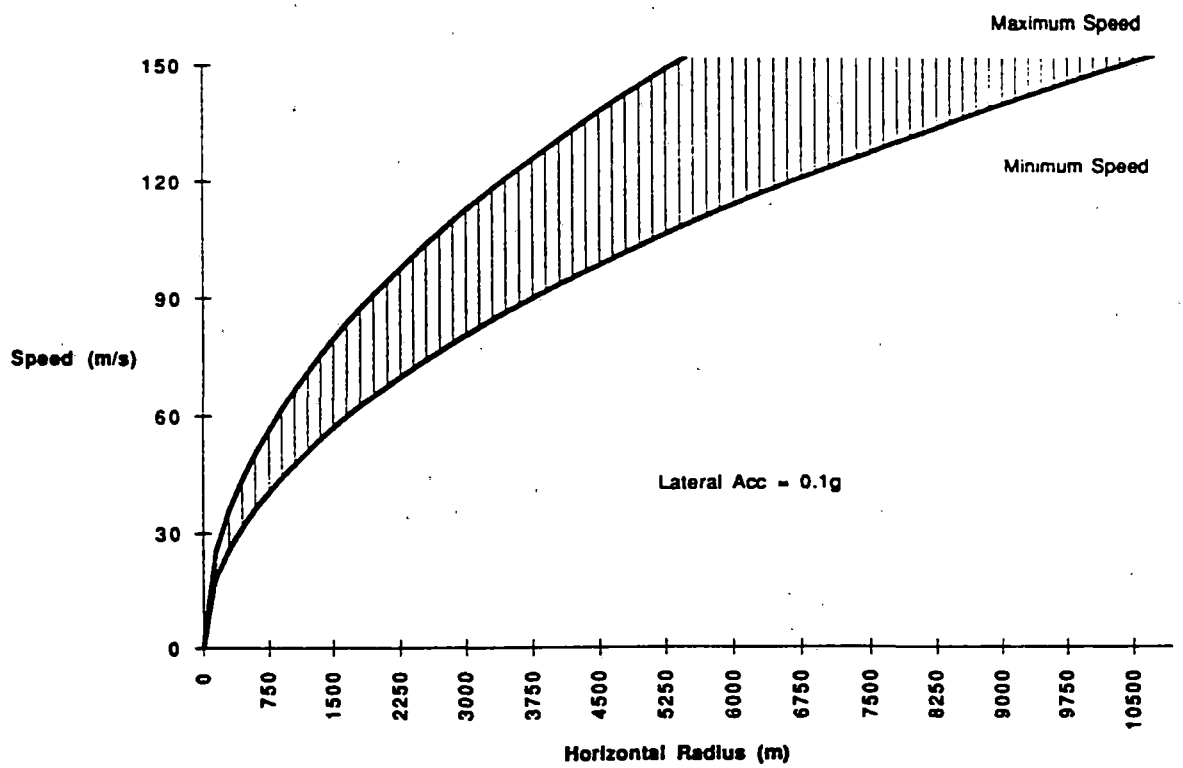

Figure 3.3.3.2-6 Speed Interval for 18 Degrees Banking

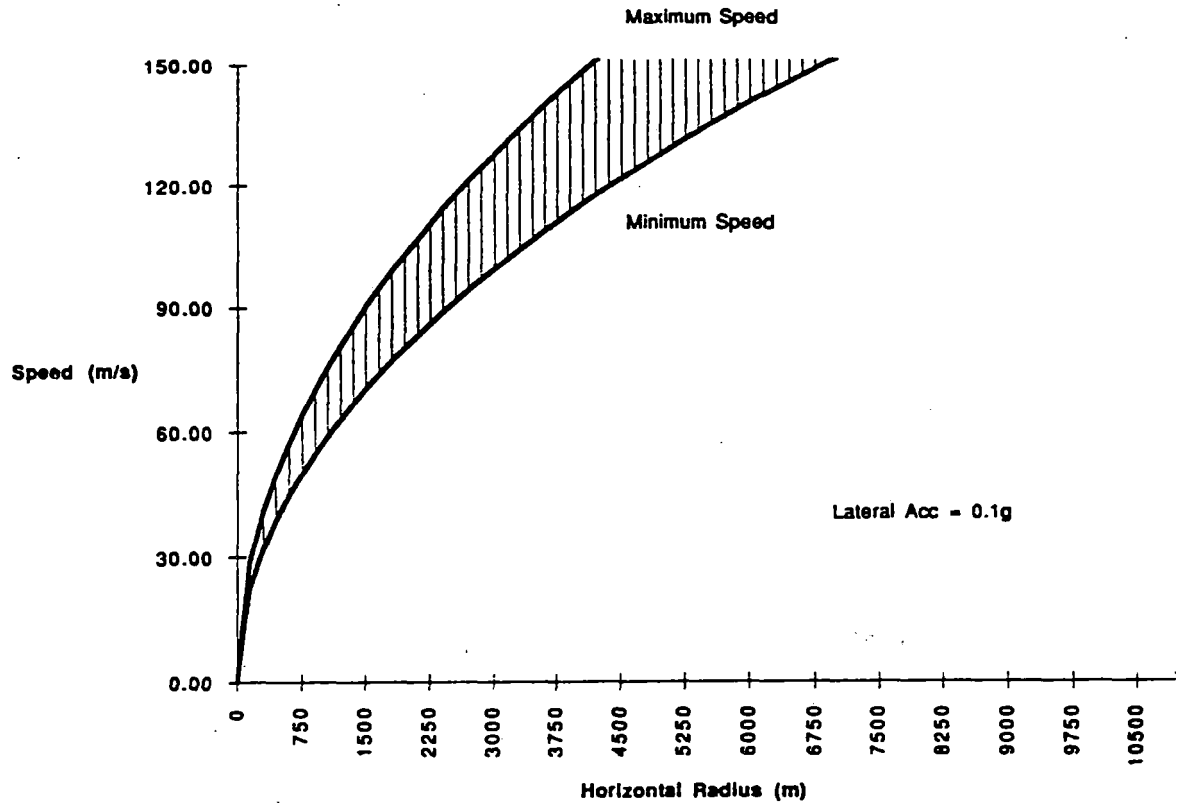

Figure 3.3.3.2-7 Speed Interval for 24 Degrees Banking

However, the relationship between the vertical components is such that as vehicle banking is increased, the gravity component of passenger-centered vertical force lessens while the vertical component of the centrifugal force increases. The net result is an increase in the vertical force experienced by the passenger. Figure 3.3.3.2-8 graphically depicts the vertical acceleration as a function of bank angle and horizontal radius for a vehicle speed set at 150 m/s. The curves are plotted for the range of horizontal radii which meet vertical comfort requirements for this case. At slower speeds, for a given bank angle, curves of lesser radii will allow permissible vertical comfort.

Looking at Figure 3.3.3.2-7 for the case of 24 degrees, the range of horizontal radii needed to meet the 0.10g comfort limit is between 4000 and 6800 meters at 150 m/s. The vertical sum of the accelerations in that range is 1.03g to 1.15g, which is within comfort limits. Lateral effects of banking and horizontal curvature determine the appropriate radius range for maximum vehicle speed when banking 28 degrees or less. Figure 3.3.3.2-9 shows that vertical acceleration is contained within comfort limits for balanced lateral loads and bank angles below 33 degrees. Bank angles up to 38 degrees can be used with negative lateral loads.

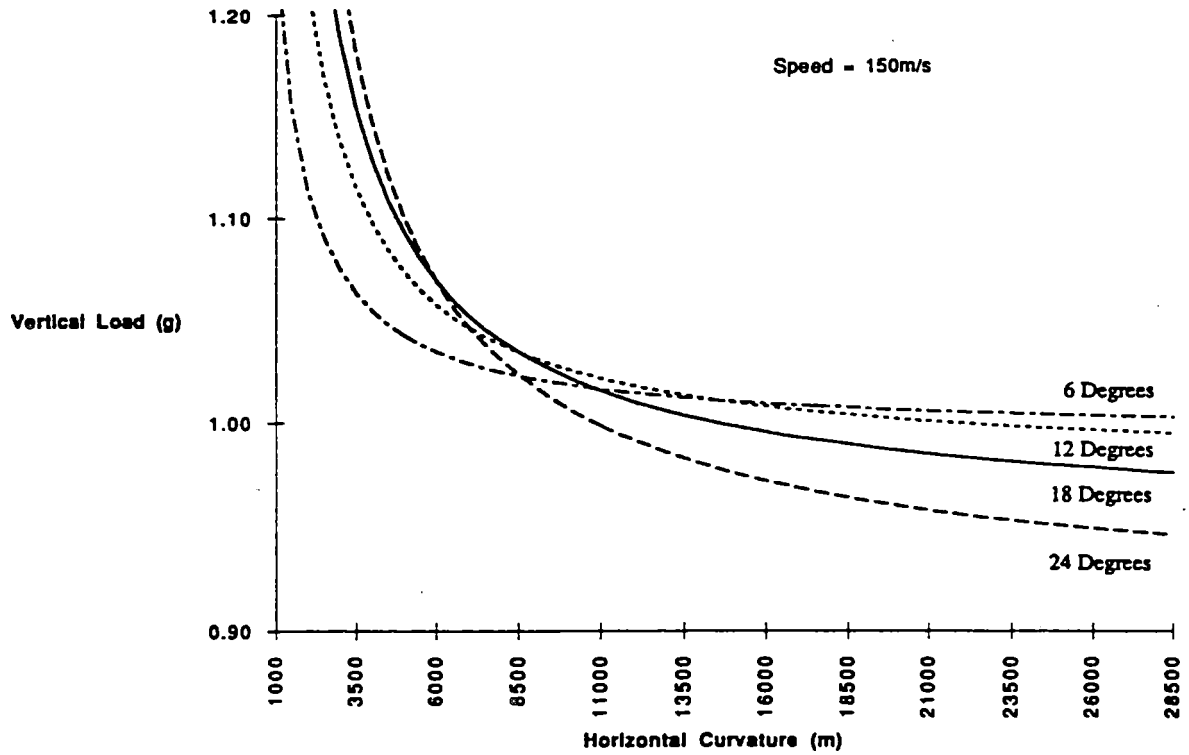

Figure 3.3.3.2-8 Acceptable Radii Values for Vertical Comfort

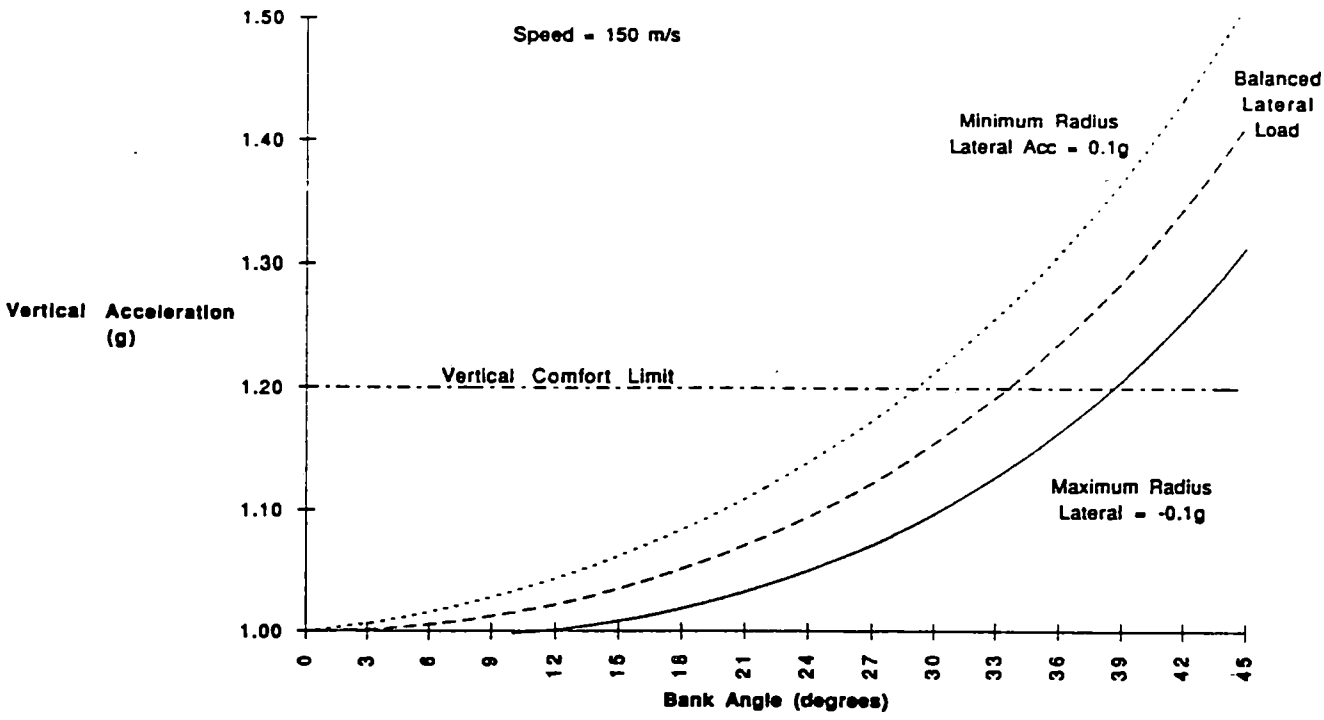

Figure 3.3.3.2-9 Acceptable Banking Values for Vertical Comfort

3.3.3.3 Grade

Figure 3.3.3.3-1 shows the decomposition of forces for a simple grade (∂) with no vertical curvature. The only force acting in the z direction is the force of gravity which only changes 0.005g for the maximum gradient allowed (10 percent or approximately 6 degrees). Maximum vehicle speed does not change due to the grade because vehicle power has been assumed to be unconstrained. There is no geometric force which limits the vehicle speed by an upward or downward grade. What does change is the allowable longitudinal acceleration. The term gsin(∂) acts either positively or negatively based on the direction of the motion. Therefore, vehicle-powered, longitudinal acceleration may be increased when ascending a grade to reach or maintain the maximum limit, and may be decreased when descending to remain within longitudinal comfort limits.

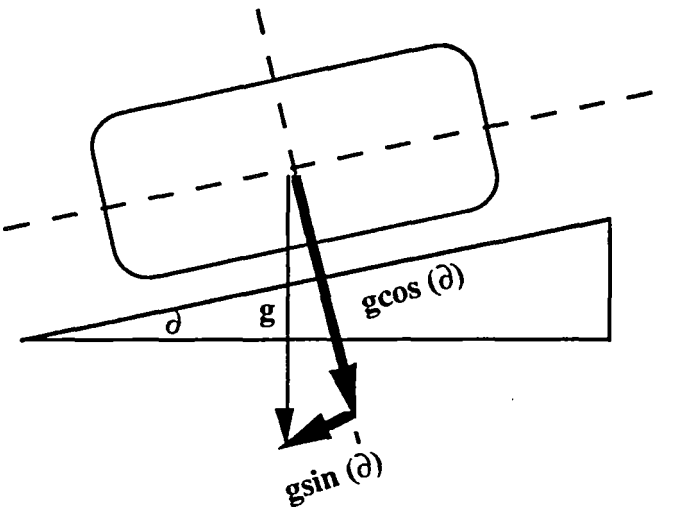

Figure 3.3.3.3-1 Vertical Influence Of Grade

3.3.3.4 Vertical Curvature

Cresting a hill or summit produces a negative vertical acceleration force, while traversing a valley or sag produces a positive vertical acceleration force. These two cases have different comfort limits assigned to them due to passenger responses to acceleration forces (see subsection 3.2.5). Figure 3.3.3.4-1 and 3.3.3.4-2 show the vertical forces as a result of these two cases.

Banking cannot be used to offset the effects of vertical curvature. The minimum vertical radius to allow a 150 m/s vehicle speed without exceeding comfort limits is 45,918 meters for a summit and 11,480 meters for a sag. The Transrapid 07 vehicle has minimum vertical radii of 38,580 and 19,290 meters, for summits and sags, respectively, at 500km/hr (134 m/s). This works out to a vertical acceleration range from 0.95g to 1.1g.

Y: $\Sigma a_y = 0$ Z: $\Sigma a_v = g - \frac{v^2}{r_v} = 1.0 - 0.05 = .95g$

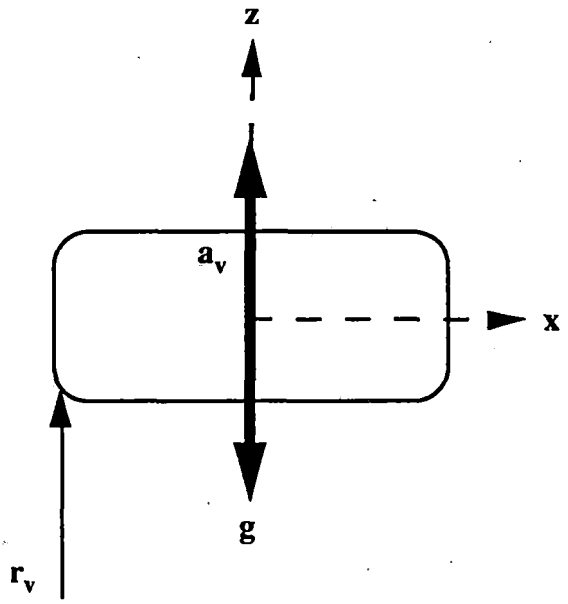

Figure 3.3.3.4-1 Crest of Hill

Y: $\Sigma a_y = 0$ Z: $\Sigma a_v = g + \frac{v^2}{r_v} = 1.0 + 0.20 = 1.2g$

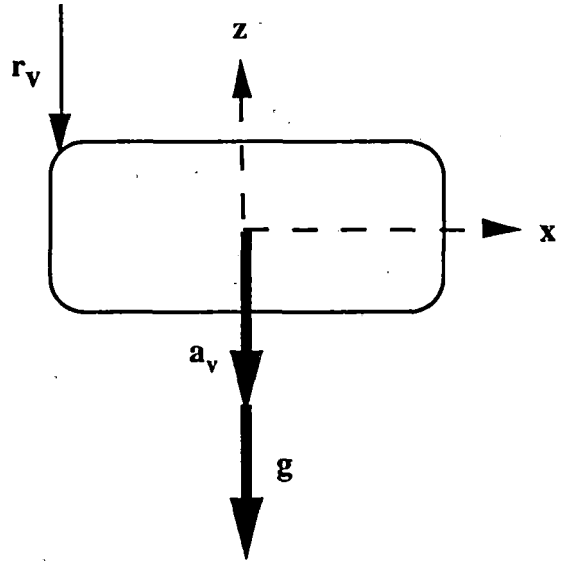

Figure 3.3.3.4-2 Bottom of Valley

When the elements of grade and vertical curvature are combined, there is a net effect on the maximum operating speeds of the vehicle. Figures 3.3.3.4-3 and 3.3.3.4-4 depict the vehicle at different points along the vertical curvature. The longitudinal component of gravity resists the vehicle when climbing a grade and assists the vehicle when descending.

Y: $\sum a_y = 0$ Z: $\sum a_z = -\frac{v^2}{r_v} + g\cos(\partial) = 0.95g$

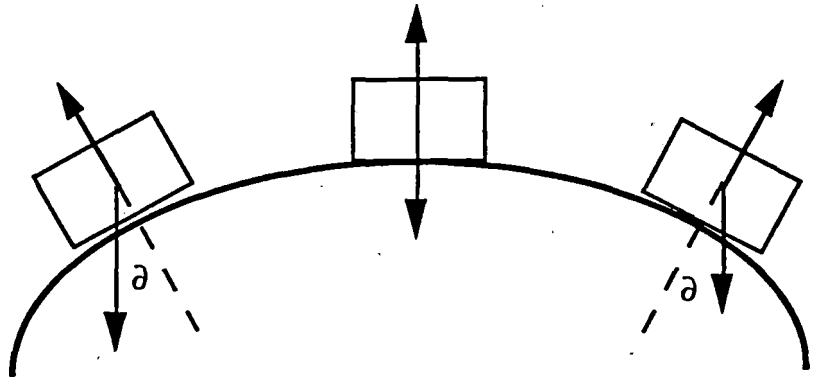

Figure 3.3.3.4-3 Grade And Vertical Summit

Y: $\sum a_y = 0$ Z: $\sum a_z = \frac{v^2}{r_v} + g\cos(\partial) = 1.20g$

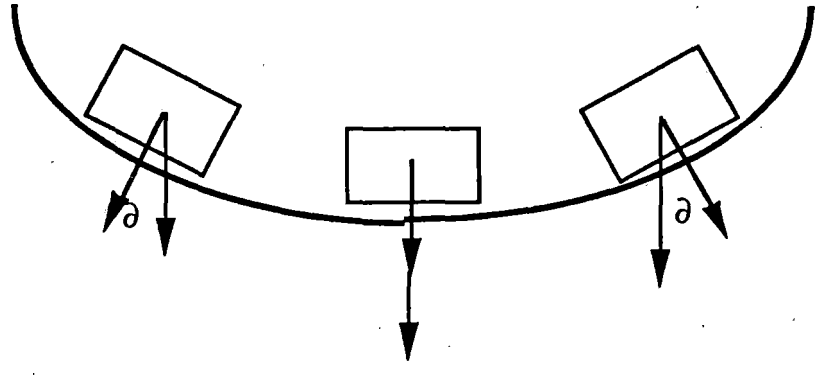

Figure 3.3.3.4-4 Grade and Vertical Sag

Table 3.3.3.4-1 expresses the change of speed as a result of vertical radius and grade. In the case of summits, maximum speeds decrease in the presence of grade. At a 10 percent grade the maximum speed is reduced approximately 5 percent. For sags, speed is allowed to increase 1.5 percent. Longitudinal acceleration experiences similar effects as seen in subsection 3.3.3.3. It is important to realize that the changes in maximum speed are a result of the net effect of vertical loads due to grade and vertical curvature and not associated with the increase or decrease of longitudinal acceleration.

Table 3.3.3.4-1 Allowable Vehicle Speeds (m/s) for Grade and Vertical Curves

Summits	5000 m	10000 m	20000 m	30000 m	45000 m
0% Grade	49.50	70.00	98.99	121.24	148.49
5% Grade	48.87	69.12	97.75	119.72	146.62
10% Grade	46.96	66.41	93.92	115.03	140.88
Sags	**2000 m**	**4000 m**	**6000 m**	**8000 m**	**11000 m**
0% Grade	62.61	88.54	108.44	125.22	146.83
5% Grade	62.81	88.82	108.78	125.61	147.29
10% Grade	63.39	89.64	109.79	126.77	148.66

3.3.3.5 Other Alignment Characteristics

Other guideway characteristics, namely rate of change of bank angle (roll) and horizontal curvature, do not enter into the calculations for maximum vehicle speeds. These characteristics represent the rates of change for the guideway characteristics in the speed equations and are applied over some guideway distance. The effects of these parameters will be reflected in the trip-time calculation of subsection 3.5.

3.3.4 Overlapping or Dual Curvature

There will be situations in guideway alignment where both horizontal and vertical curvature exist. It is clear that there is a cross-contribution of acceleration forces through the application of banking. It is suggested that if strict adherence to the existing right-of-way is required for maglev systems, additional research will be required to fully assess the usefulness of dual curvature. However, no allowance for dual curvature has been made in this study.

3.3.5 Maximum Speed Tables

Tables of maximum vehicle speeds due to guideway characteristics are given in Appendix C. Speed Table 1 reports speeds as a function of horizontal curvature for the four specified bank angles. Radii increments are every 150 meters, and speeds are reported as low as 10 m/s. Grade changes were evaluated for every 0.5 percent. However, since grade did not impact maximum speed, tables reflect only the case of no grade. Speed Table 2 reports horizontal radii ranges that bound vertical comfort limits as a function of speed. Speed increments are every 2 m/s. Speed Table 3 reports the maximum vehicle speed (for both summits and sags) as a function of vertical curvature.

3.4 SEGMENT SPEED PROFILES

3.4.1 Introduction

This section presents segment speed profiles for three specified corridors: New York City-Syracuse, Detroit-Chicago, Los Angeles-San Francisco. The speed profiles were used to evaluate the maximum allowable speed along a segment of guideway as constrained by terrain characteristics, guideway geometry, and the recommended comfort limits.

A route analysis program was developed to calculate and plot segment speed profiles for one highway and railroad route per corridor. Station endpoints and intermediate stops are specified. Plots of speed profiles are provided along with discussions on distinct route areas in which speed is severely restricted due to tight curves in the right-of-way.

All intersections (i.e., crossings, rivers, interchanges, etc.) encountered by the guideway have been recorded. Non-default span lengths are identified and reported in order to estimate the number of additional structures that must be built for a potential route. Spans are categorized by length.

The following assumptions are used in the analysis of segment speed profiles:

1) The maximum allowable speed is 150 m/s.
2) The maximum speed for all curved segments is based on a 12 degree bank angle.
3) Grade and vertical curvature variations can be minimized through the use of support columns as high as 12 meters.
4) Maglev vehicles are assumed to be running along the centerline of the existing highway and parallel to the existing railroad.
5) Standard maglev span length is set at 25 meters.

3.4.2 Methodology

Information regarding guideway alignment characteristics, namely values for segment length, radius, and elevations was collected from 7.5-minute topographic maps. Quadrangle maps were used to divide routes into segments based on similar geographic alignment. Segment lengths and radii were then measured, and elevations were manually extracted from the maps. Alignment information derived from the topographic maps was entered into a computer model designed to calculate maximum vehicle speeds based on the equations developed in subsection 3.3.3.

Segment speeds are limited by the horizontal and vertical geometries of the guideway. The speed for any given segment is defined as the minimum of the allowable speeds due to horizontal and vertical curvature, respectively and maximum guideway superelevation.

Horizontal radii for curved segments were extracted from the quadrangle maps using instruments designed to measure radii. It was assumed that appropriate spiral lengths and roll rates are fit into the curved alignment and do not impact the trip time and average speed estimates.

Vertical radius values could not be taken directly from the topographic maps. Therefore, values were obtained through an estimation method using elevation data obtained from the maps to approximate grade changes and knowledge of minimum vertical curve radii used in highway and railroad construction. Minimum vertical curve radii for highways are based on line-of-sight distances needed to safely stop vehicles. Railroads limit vertical curvature to 0.05 to 0.10 percent change in grade per 100 feet. An algorithm was developed to increase the vertical radius along the existing right-of-way through the modulation of columns (up to 12 meters). This increase is needed to limit vertical loads associated with high-speed operation.

Guideway intersections and span length requirements were also collected from the quadrangle maps. The number and type of guideway intersections were entered into a database and tabulated to establish span length requirements.

3.4.3 Speed Profiles

Speed profiles for a rail and highway route in each of the three specified corridors are provided on subsequent pages in graph format. Maximum speed of route segments are reported for station-to-station travel and assume comfort-limited spirals and 12 degrees of guideway superelevation to reduce lateral loads.

The three corridors studied were New York City-Syracuse, Detroit-Chicago, and Los Angeles-San Francisco. Intermediate station stops for the New York corridor are Albany and Utica. Stops along the Detroit-Chicago corridor are at Ann Arbor and Kalamazoo. For California, different station stops were identified for the rail and highway routes to allow for equivalencies in station-to-station distances. The highway route along Route 5 has stops at Buttonwillow and Santa Nella. The railroad stops are at Bakersfield and Merced.

Estimates for trip time and average speed were calculated for each corridor route. These estimates are lower bounds for trip time and upper bounds for average speed because infinite vehicle acceleration was assumed. Trip times and average speed values reflect the entire corridor route, and no time was added for station stops. Subsection 3.5 will introduce realistic longitudinal acceleration and deceleration consistent with the comfort limits developed in Subsection 3.2.

3.4.3.1 New York Highway

The New York State Thruway was chosen for the trip from New York City to Syracuse. Travel started at the Tappan Zee Bridge. Station stops were placed at interchanges along the Thruway, and the line ended at I-481 just east of Syracuse.

The speed profile revealed that sharp curves exist along the route and that there are no straight segments of sufficient length to achieve sustained high speeds. The minimum speed experienced was 38.1 m/s while traveling along the Mohawk River between Albany and Utica.

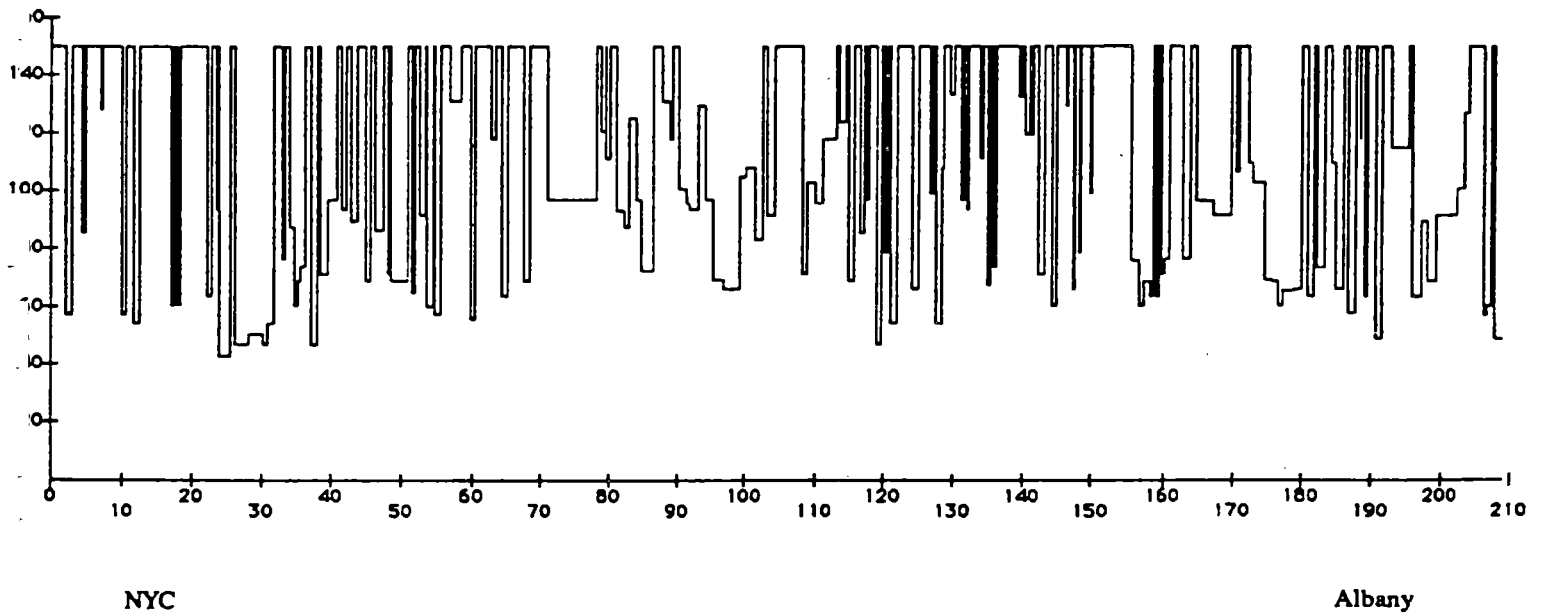

Figure 3.4.3.1-1 NY Highway Tappan Zee Bridge to Albany

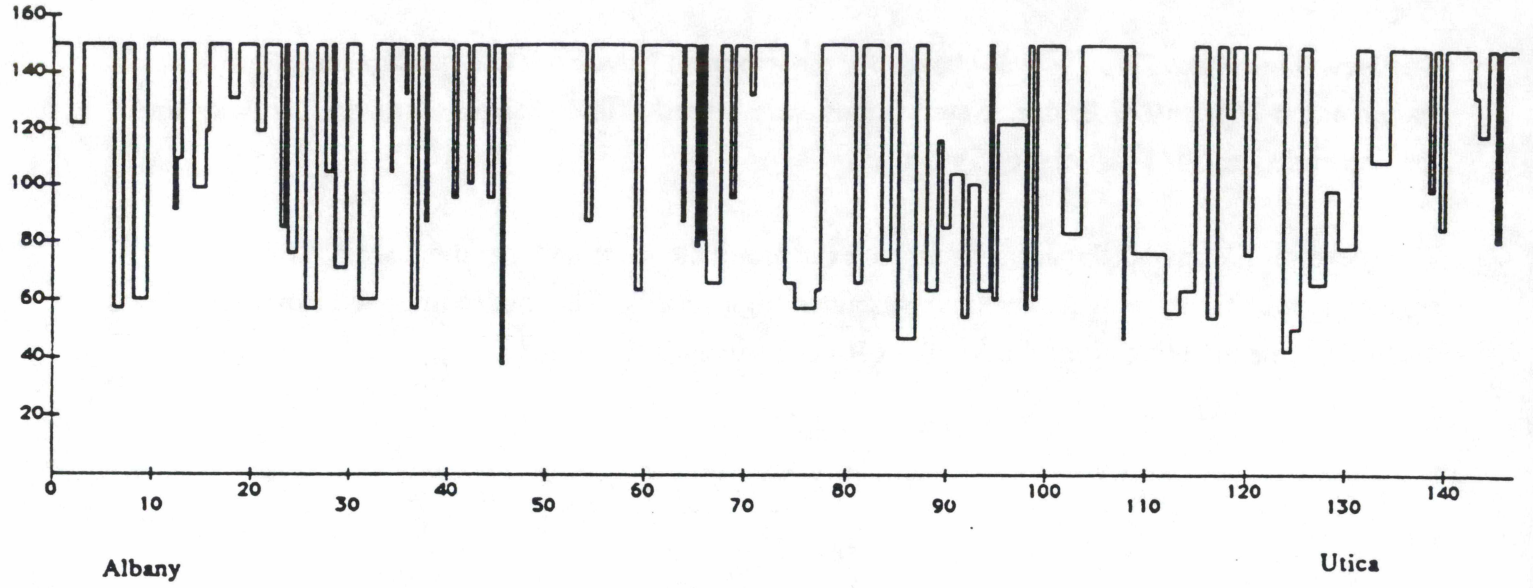

Figure 3.4.3.1-2 NY Highway Albany to Utica

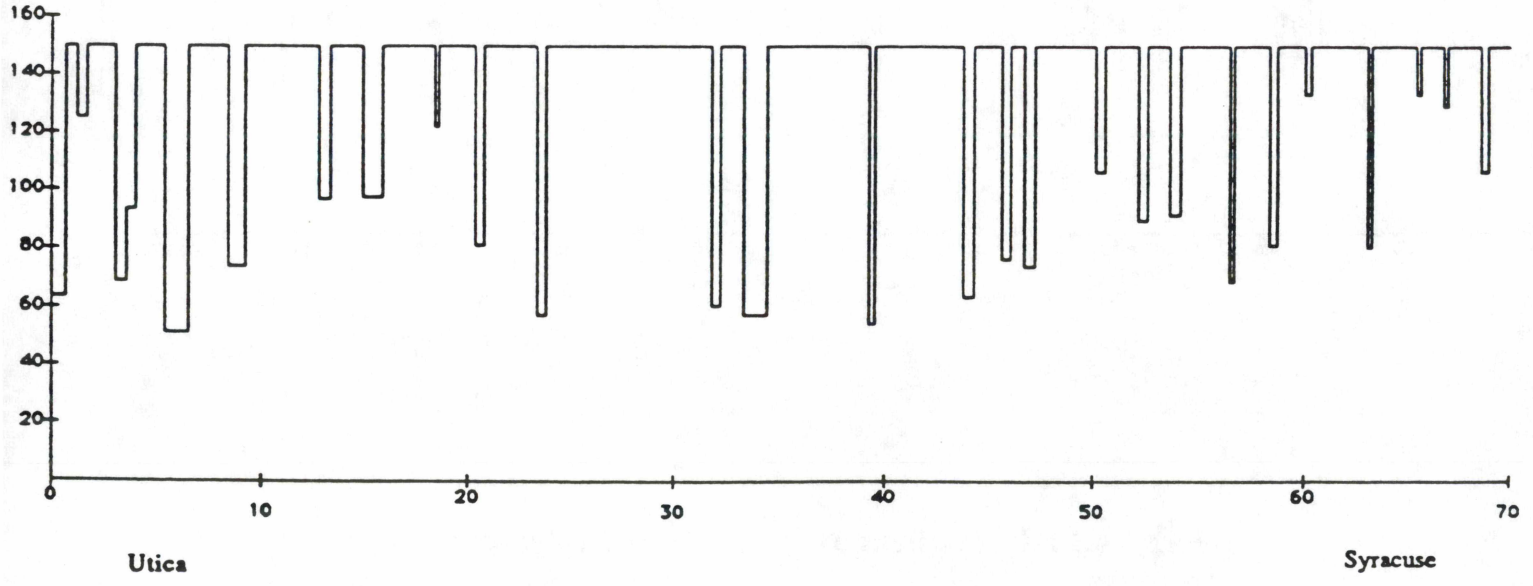

Figure 3.4.3.1-3 NY Highway Utica to Syracuse

3.4.3.2 New York Railroad

The current Conrail line from the Yonkers station to DeWitt yards in Syracuse served as the guideway for the New York railroad route. This line follows the Hudson River north to Albany, then picks up the Mohawk River west through Utica to Syracuse.

Following the meandering of the rivers produced a jagged speed profile. The absolute minimum speed along the route was 27.0 m/s. However, at the proposed Albany stop there is a series of curves which would keep the maglev vehicle in the 30 to 50 m/s range. There is also a single sharp curve inside the city limits at Little Falls which also would force the maglev vehicle to slow to less than 30 m/s.

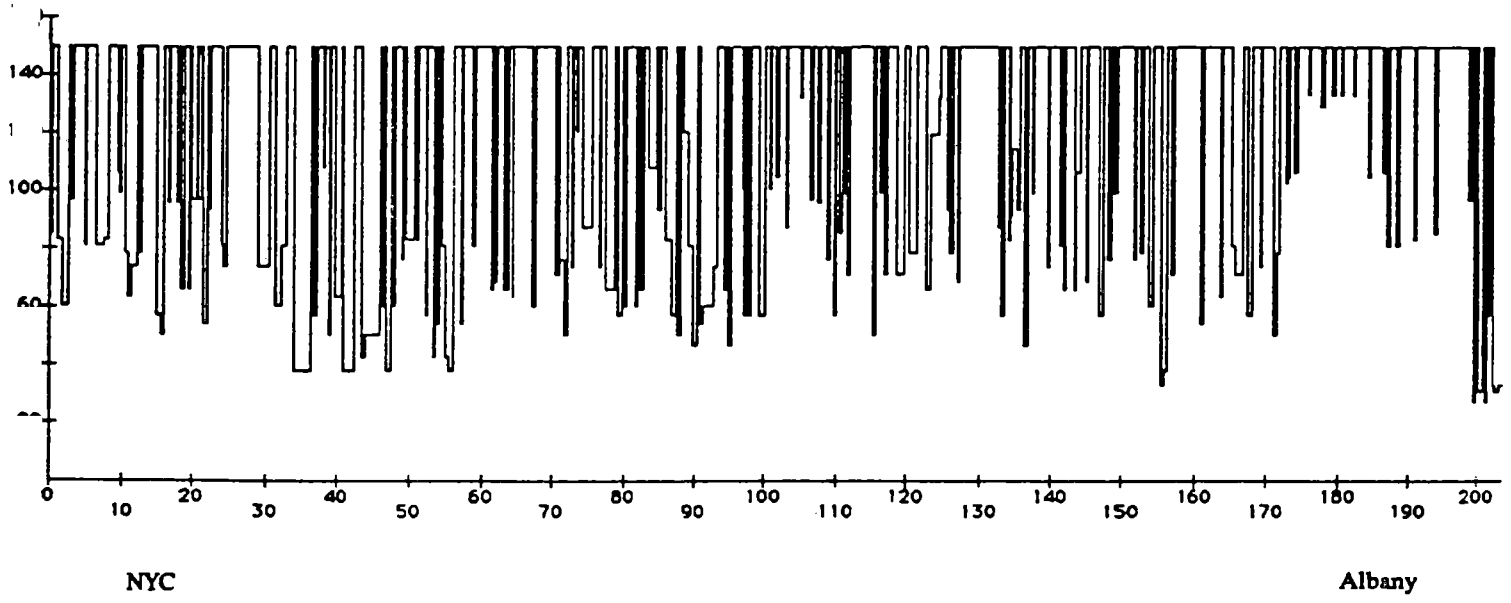

Figure 3.4.3.2-1 NY Railroad Yonkers to Albany

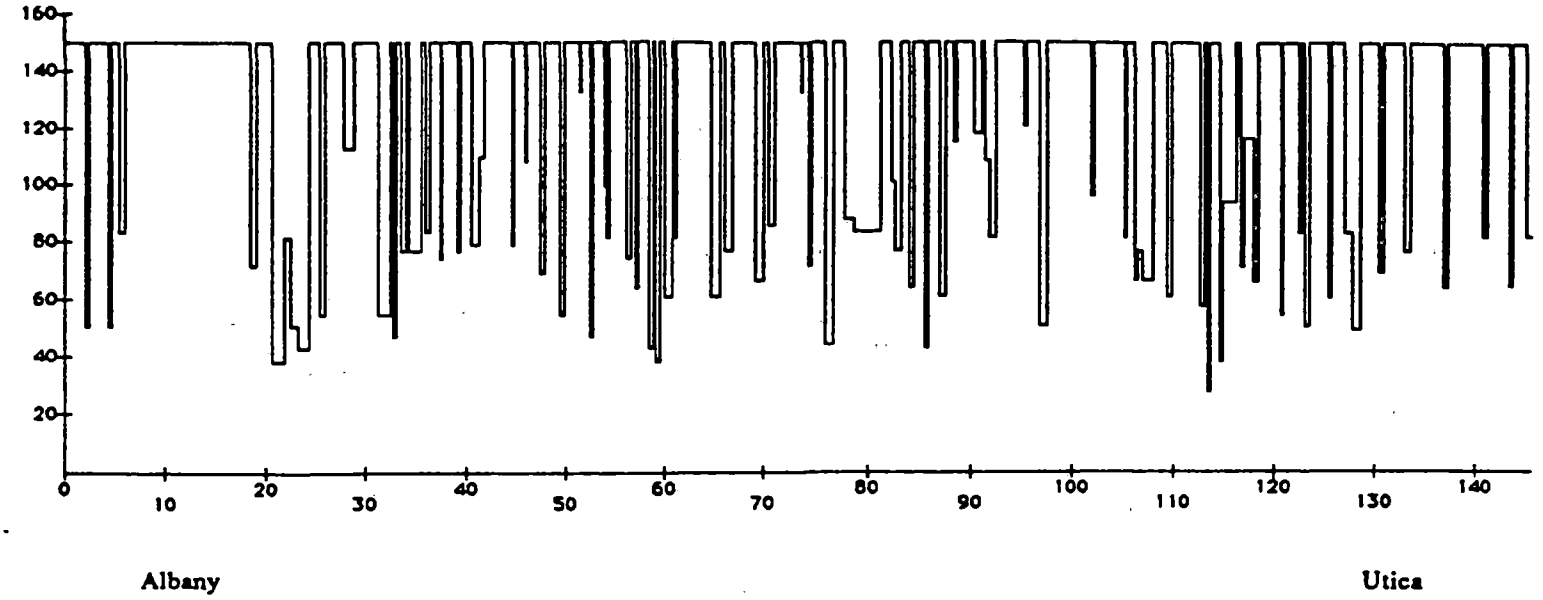

Figure 3.4.3.2-2 NY Railroad Albany to Utica

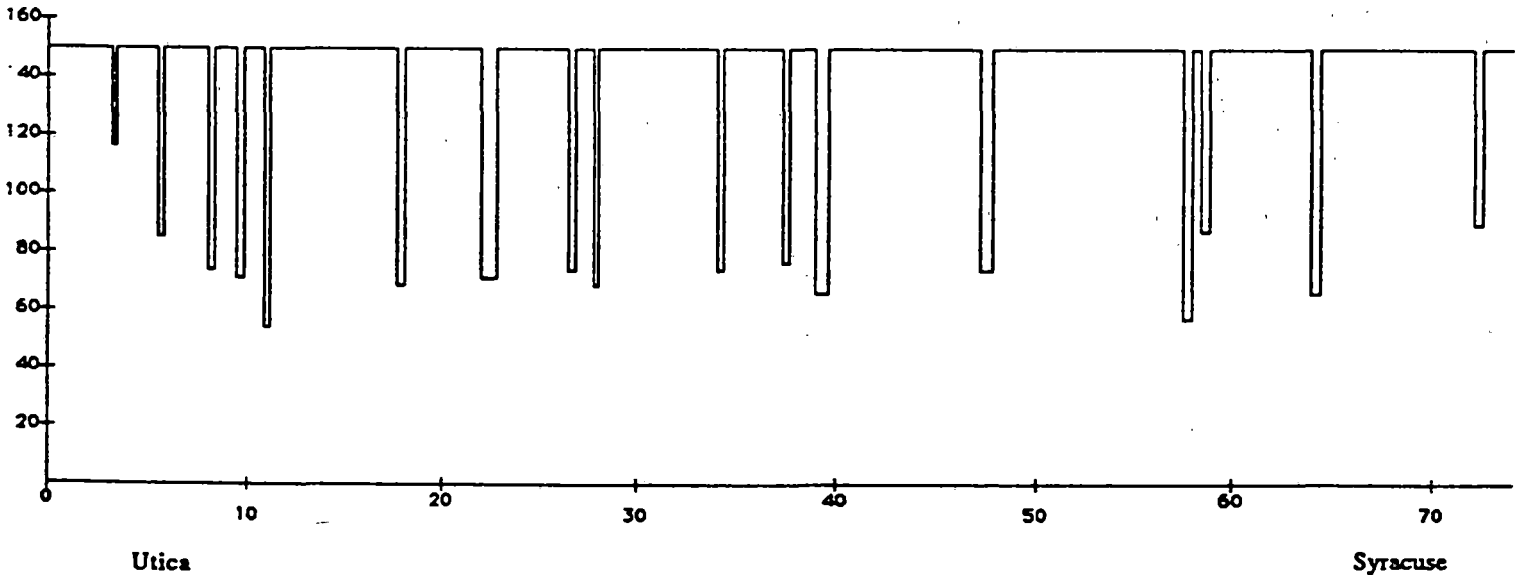

Figure 3.4.3.2-3 NY Railroad Utica to Syracuse

3.4.3.3 Detroit-Chicago Highway

The highway used for this route was mainly I-94 which runs from downtown Detroit to downtown Chicago. The considerable amount of inner city travel is not reflected in the speed profiles because the only restriction placed on the vehicle speed was geometric considerations. Restrictions due to noise and surrounding environment were not considered in this analysis.

There is one particular instance where the maglev vehicle was forced to slow to minimal speeds. The vehicle needed to shift from I-94 to I-90 in Gary, Indiana. There was no easy transition from one interstate to another; the highway exits were clover leafs. Since the maglev vehicle was assumed to be on the centerline and the right-of-way area was unknown, a conservative estimate was made for the radius, which resulted in a maximum speed of 15.4 m/s.

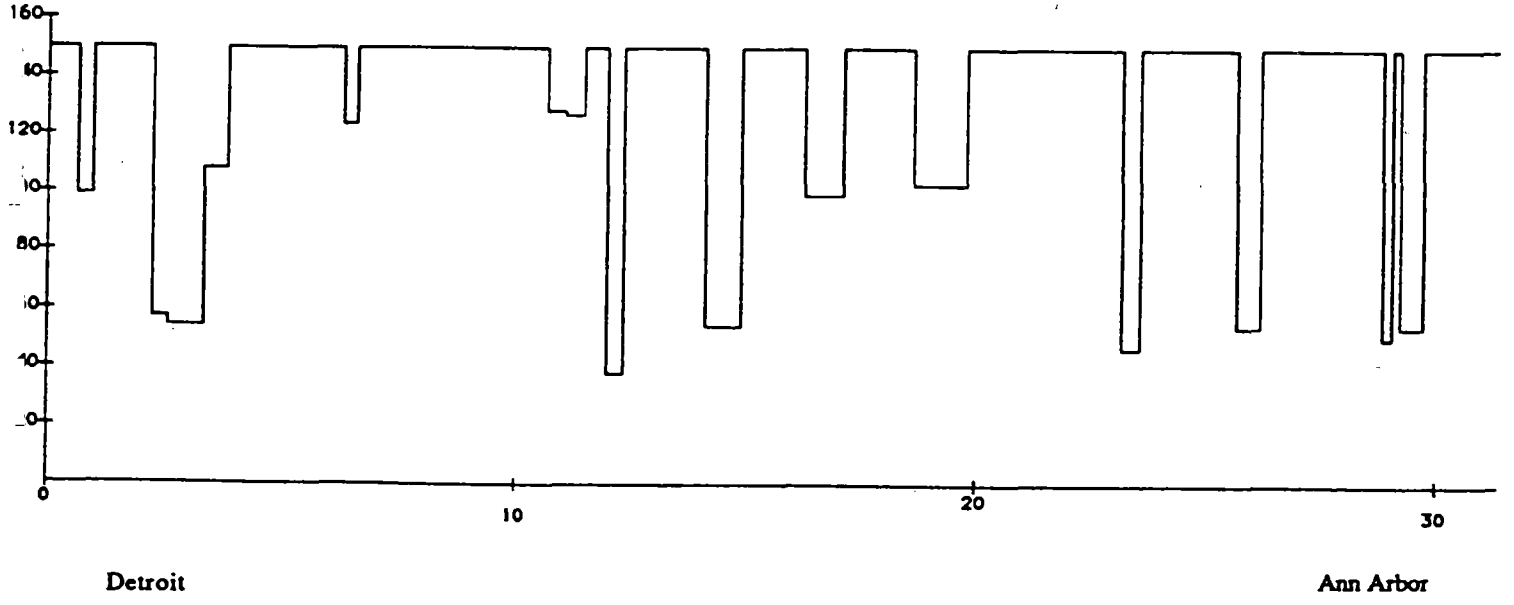

Figure 3.4.3.3-1 DET-CHI Highway Detroit to Ann Arbor

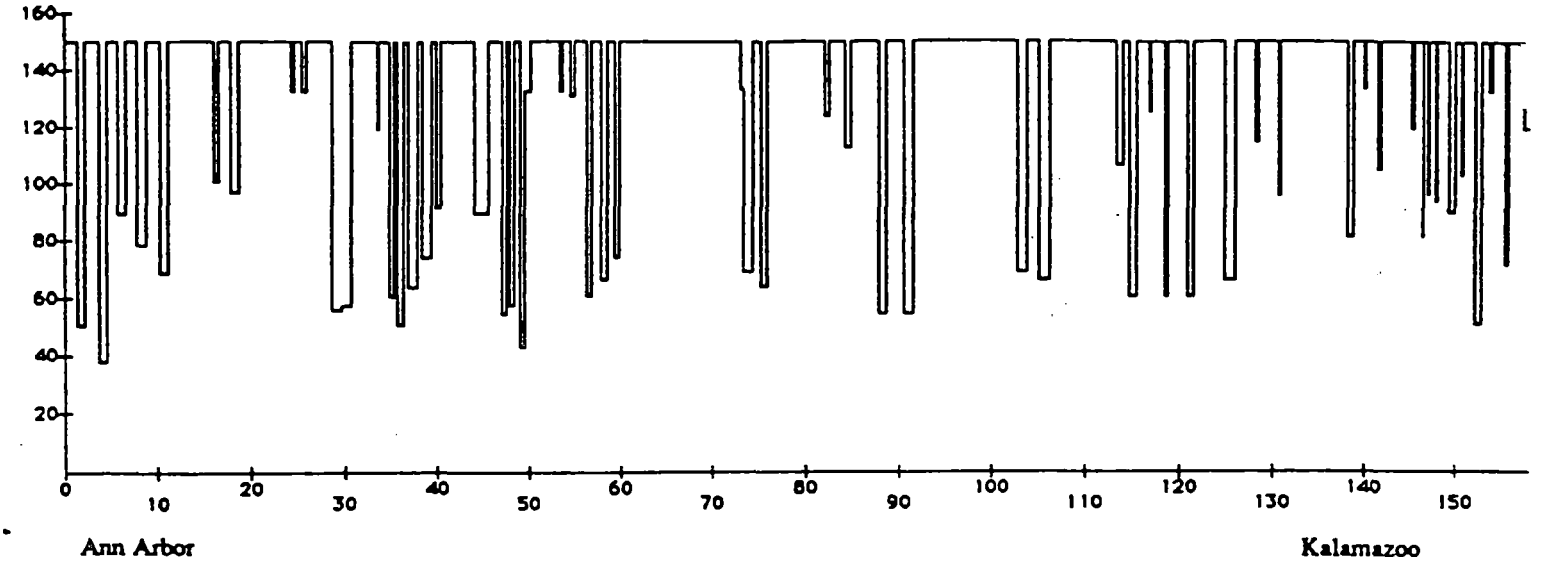

Figure 3.4.3.3-2 DET-CHI Highway Ann Arbor to Kalamazoo

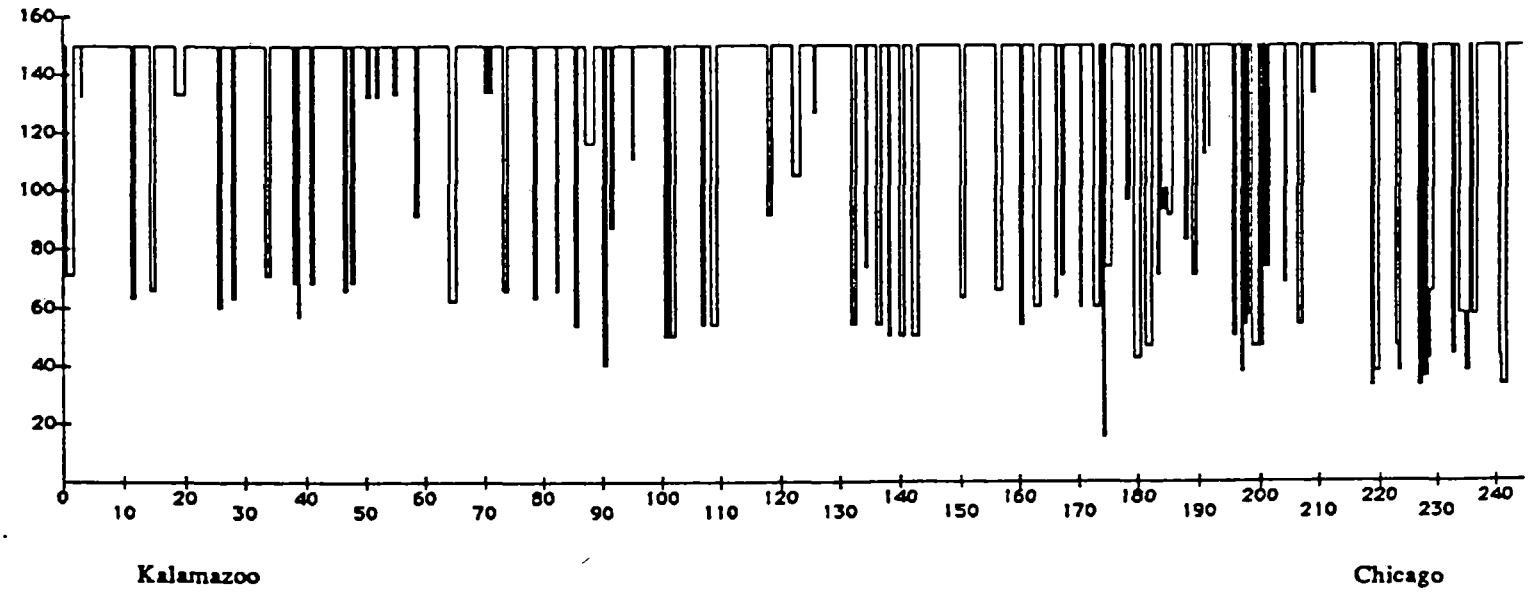

Figure 3.4.3.3-3 DET-CHI Highway Kalamazoo to Chicago

3.4.3.4 Detroit-Chicago Railroad

The current Conrail line provided service for this guideway route. This route was characterized by a few, long straight sections (20km to 40km posts and 260km to 295km posts) and some very rough areas of track (40km to 70km post). The long straights are in the rural areas of Michigan. The short radii occur when the rail line follows the Huron River near the city of Ann Arbor, where the maglev vehicle reached a maximum speed of 30.9 m/s.

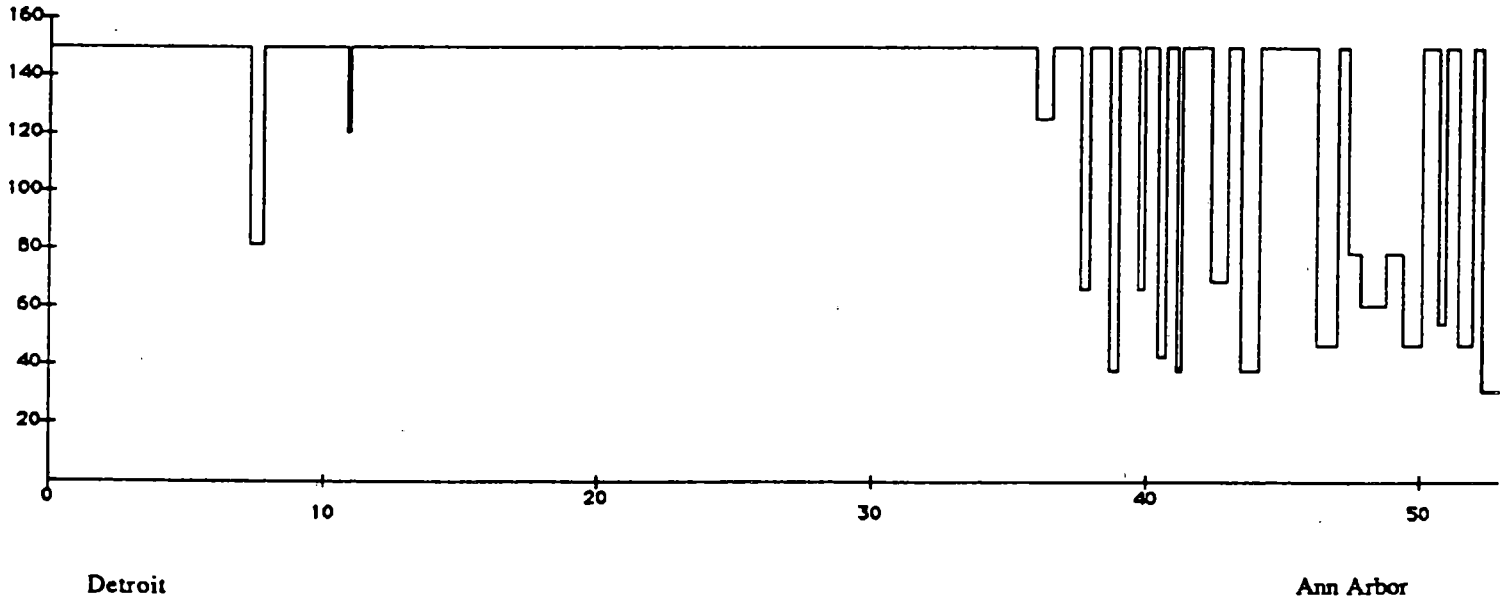

Figure 3.4.3.4-1 DET-CHI Railroad Detroit to Ann Arbor

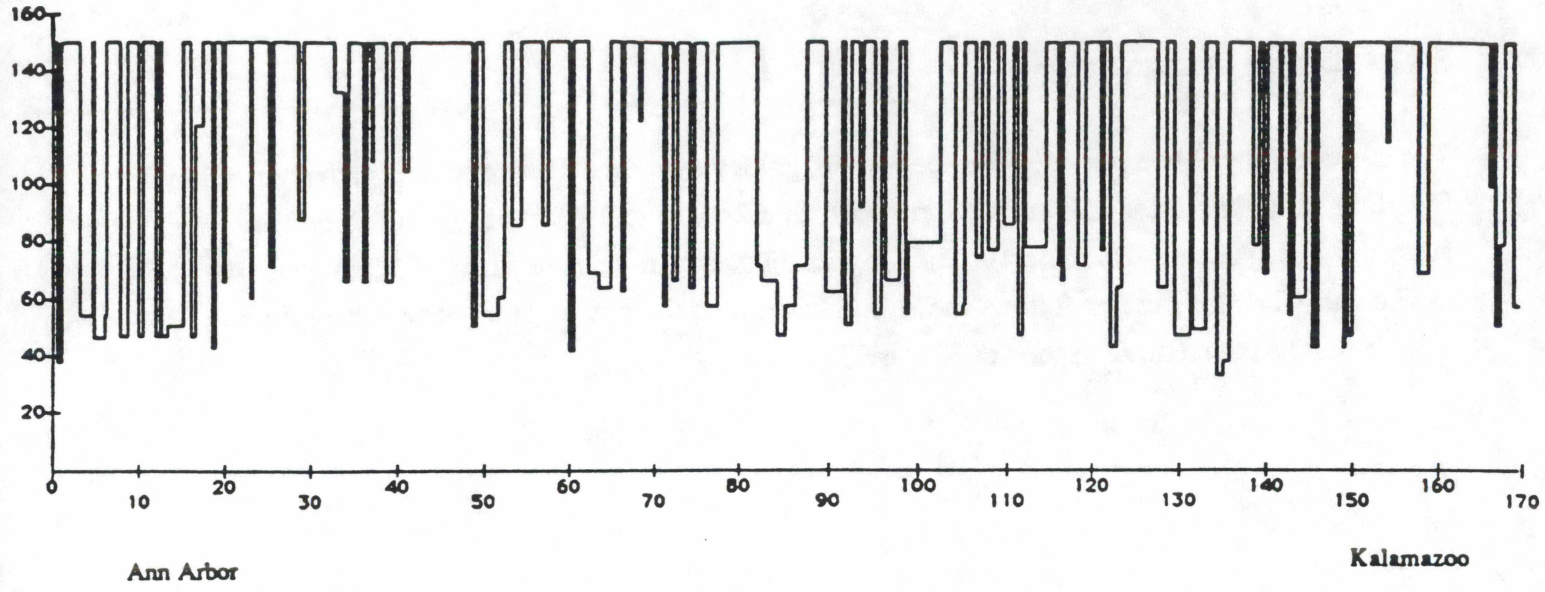

Figure 3.4.3.4-2 DET-CHI Railroad Ann Arbor to Kalamazoo

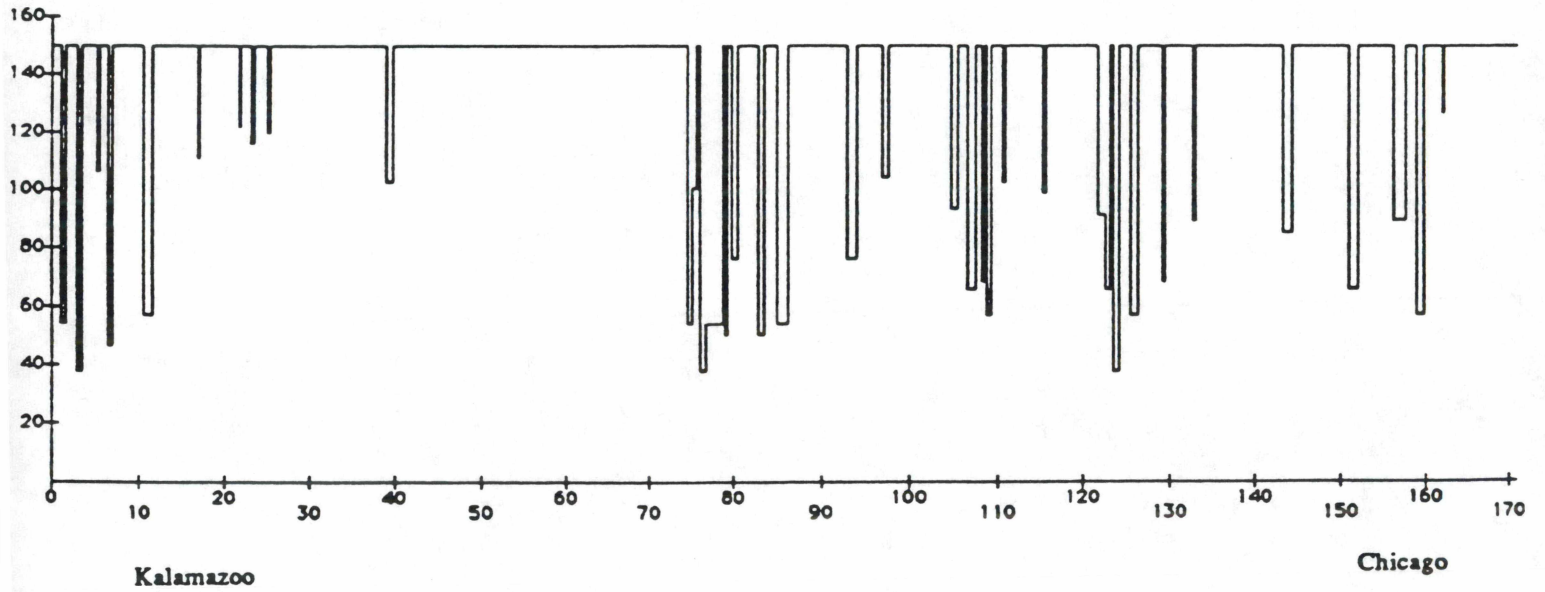

Figure 3.4.3.4-3 DET-CHI Railroad Kalamazoo to Chicago

3.4.3.5 California Highway

Route 5 was used as the highway route for Los Angeles to San Francisco. The trip begins by passing through the Tehachapi mountains. Vehicle speeds are slow due to the rough terrain through the mountain passes. Minimum speed through the area is 32.8 m/s. After the mountains the route levels, and speed improves dramatically. The profile shows only a few segments that are non-straights for nearly 400 kilometers. Approaching San Francisco, a small stretch of curved segments is encountered near Dublin. A tight canyon passing restricts vehicle speed, which resulted in an absolute minimum speed for the route, 26.7 m/s.

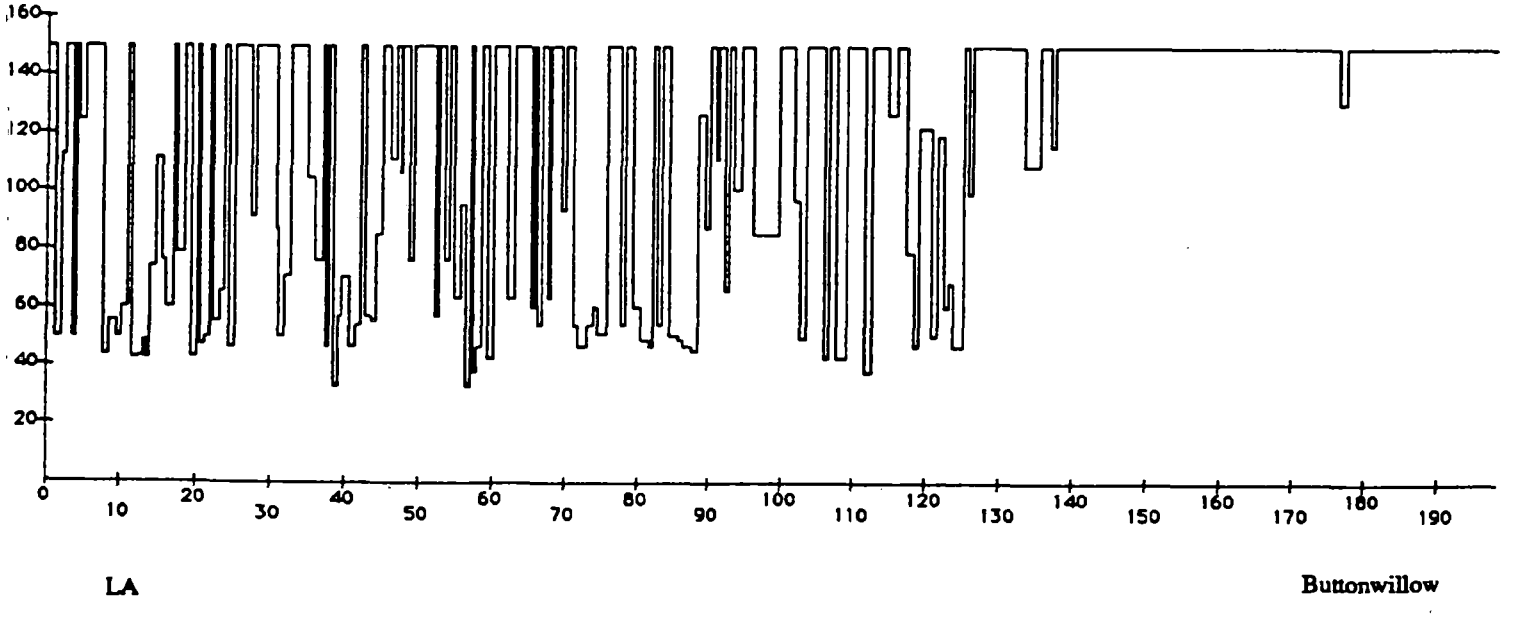

Figure 3.4.3.5-1 CAL Highway Los Angeles to Buttonwillow

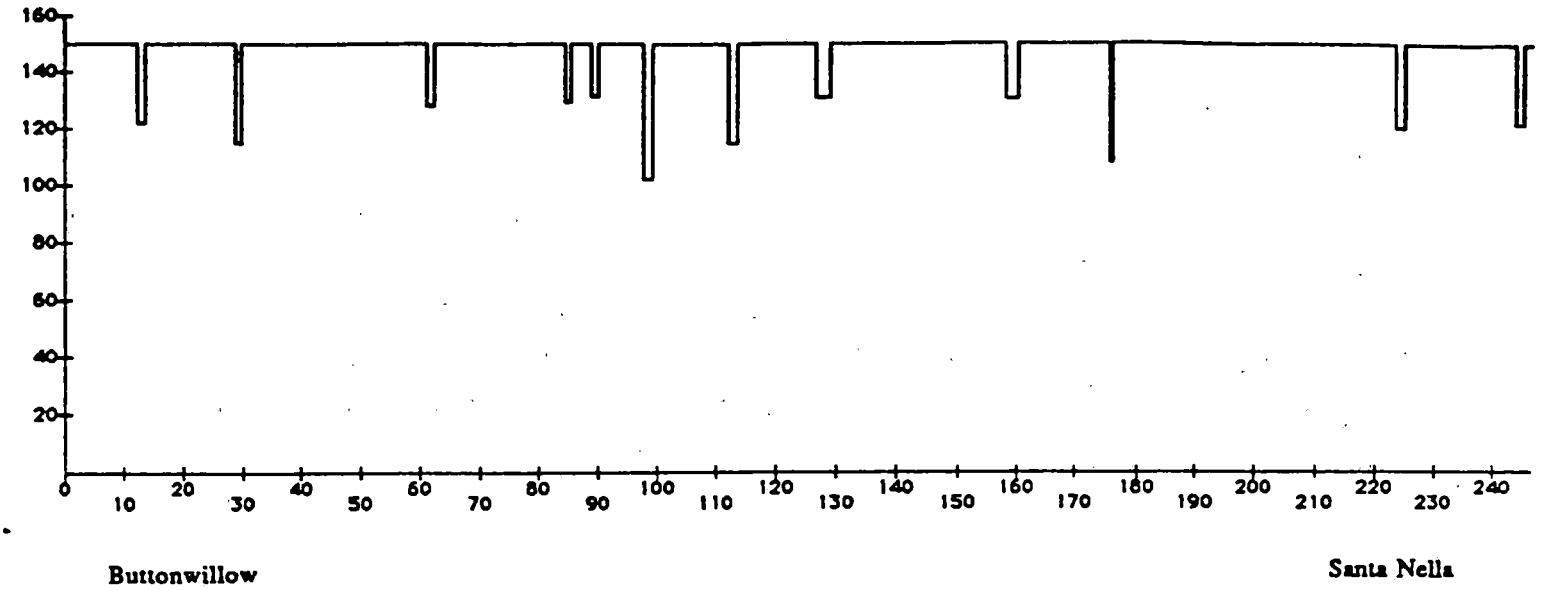

Figure 3.4.3.5-2 CAL Highway Buttonwillow to Santa Nella

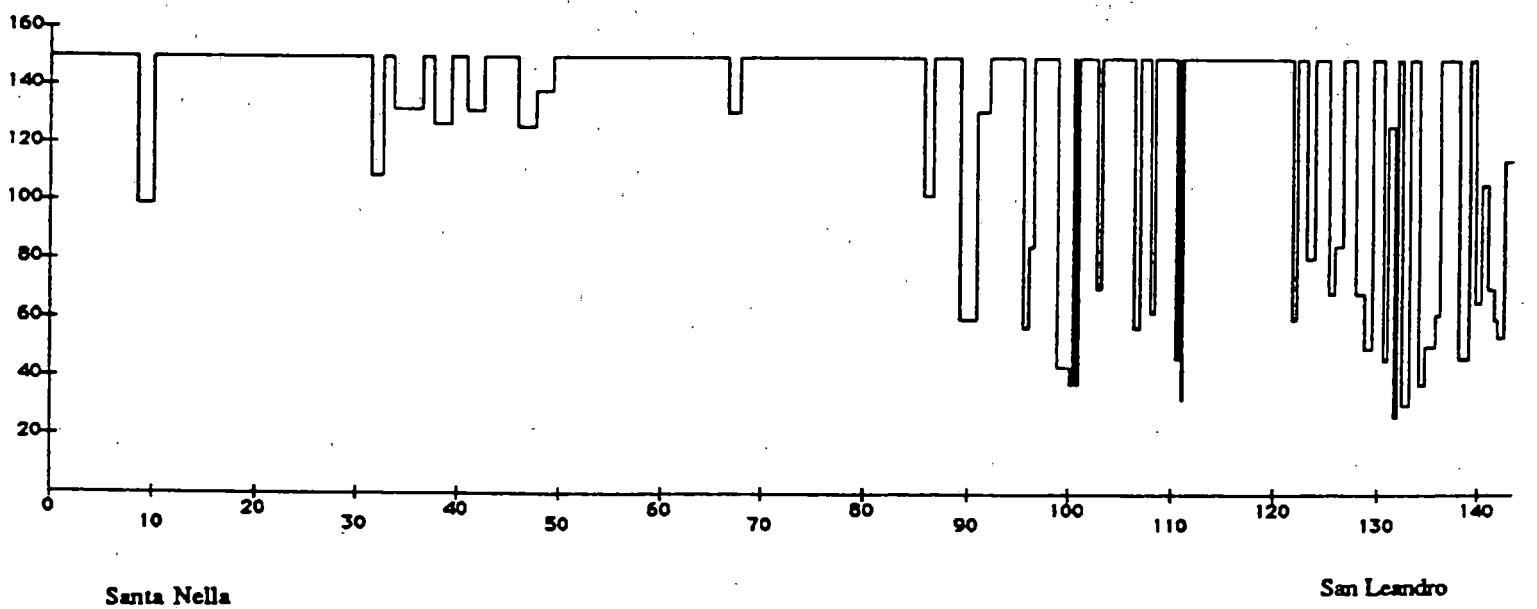

Figure 3.4.3.5-3 CAL Highway Santa Nella to San Leandro

3.4.3.6 California Railroad

The California railroad route is over 725 kilometers. This is 125 kilometers more than the highway route. The route specified goes through the mountains northeast of Los Angeles and then heads west back to Bakersfield. The trip through the mountain is extremely slow, as the profile reveals. The first set of slow speed segments are during the passing of the San Gabriel mountains. Speeds through the mountains ranged from 15 m/s to near 50 m/s. The second mountain range (Tehachapi) is shorter in duration but more limiting of vehicle speed. Maximum speeds again falls near 15 m/s.

Once out of the mountains the route levels out for a substantial distance. Over the next 350 kilometers there are only a few segments where curves are present. Right-of-way excursions could easily be made to maintain 150 m/s maximum speed.

A final mountain range is encountered in northern California which forces the maglev vehicle to travel farther north than the highway and approach the end station (at Richmond) from the northeast. The profile along this area has some tight segments while following the Carquinez Strait and San Pablo Bay.

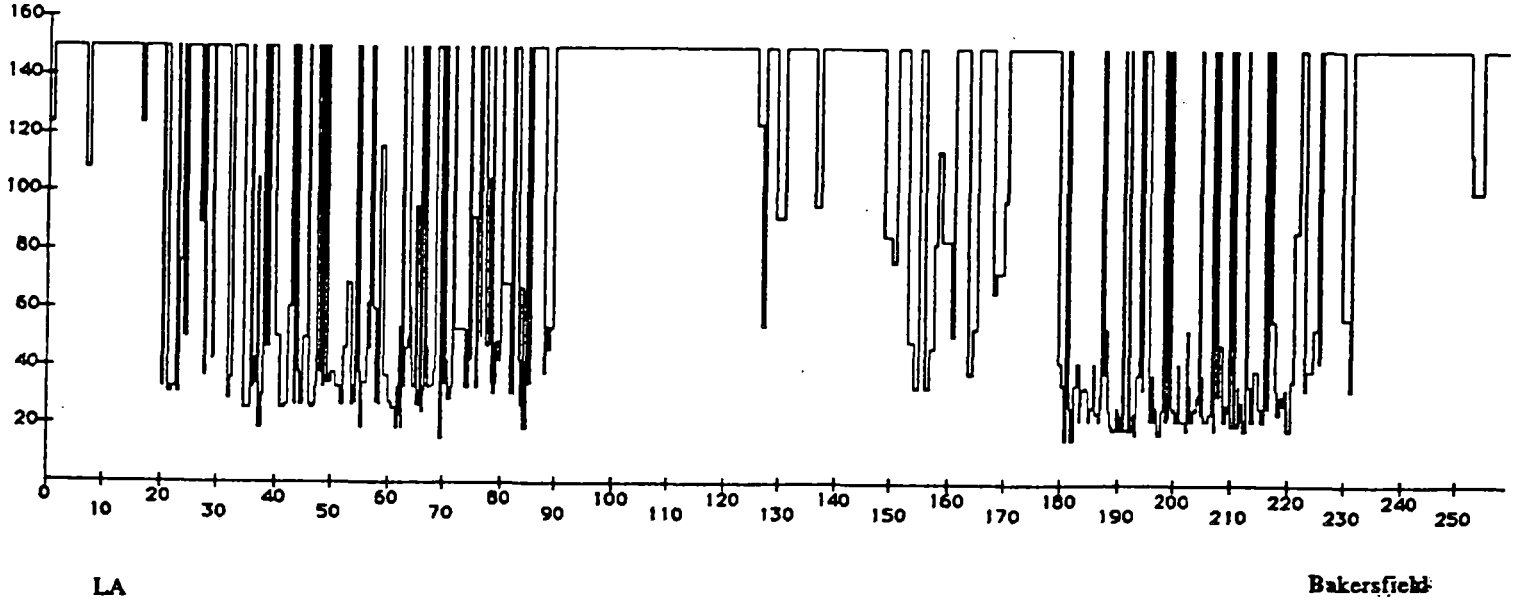

Figure 3.4.3.6-1 CAL Railroad Los Angeles to Bakersfield

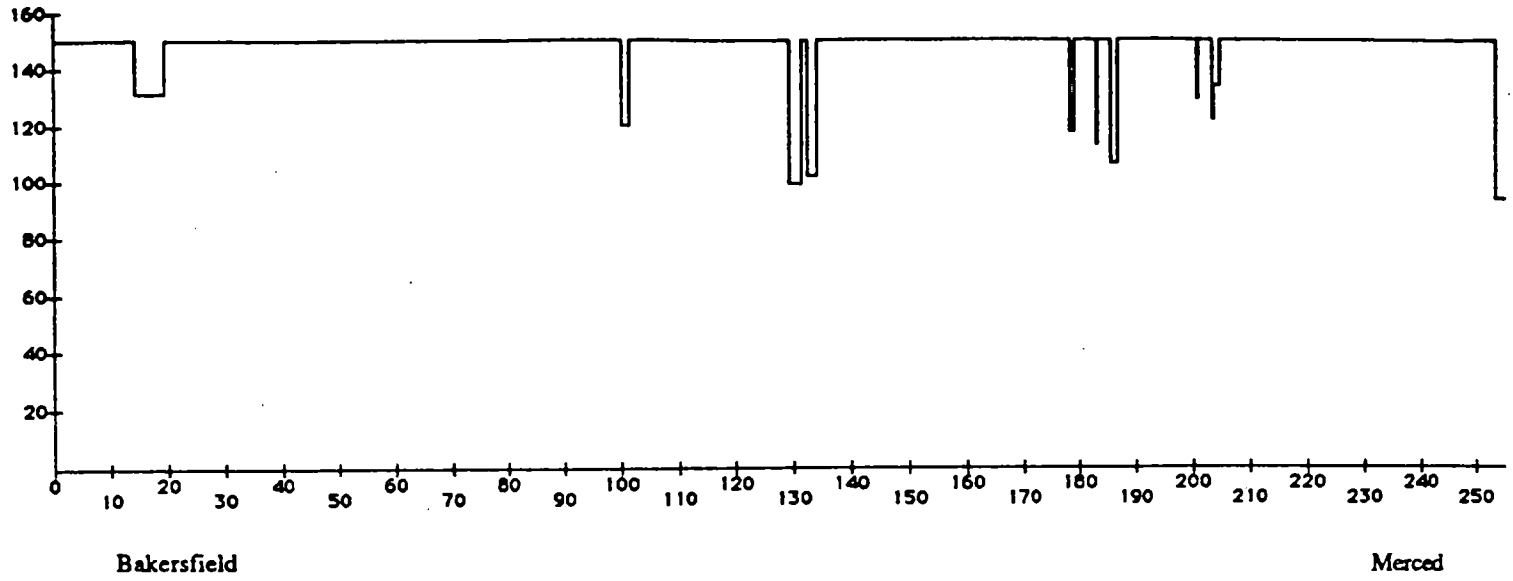

Figure 3.4.3.6-2 CAL Railroad Bakersfield to Merced

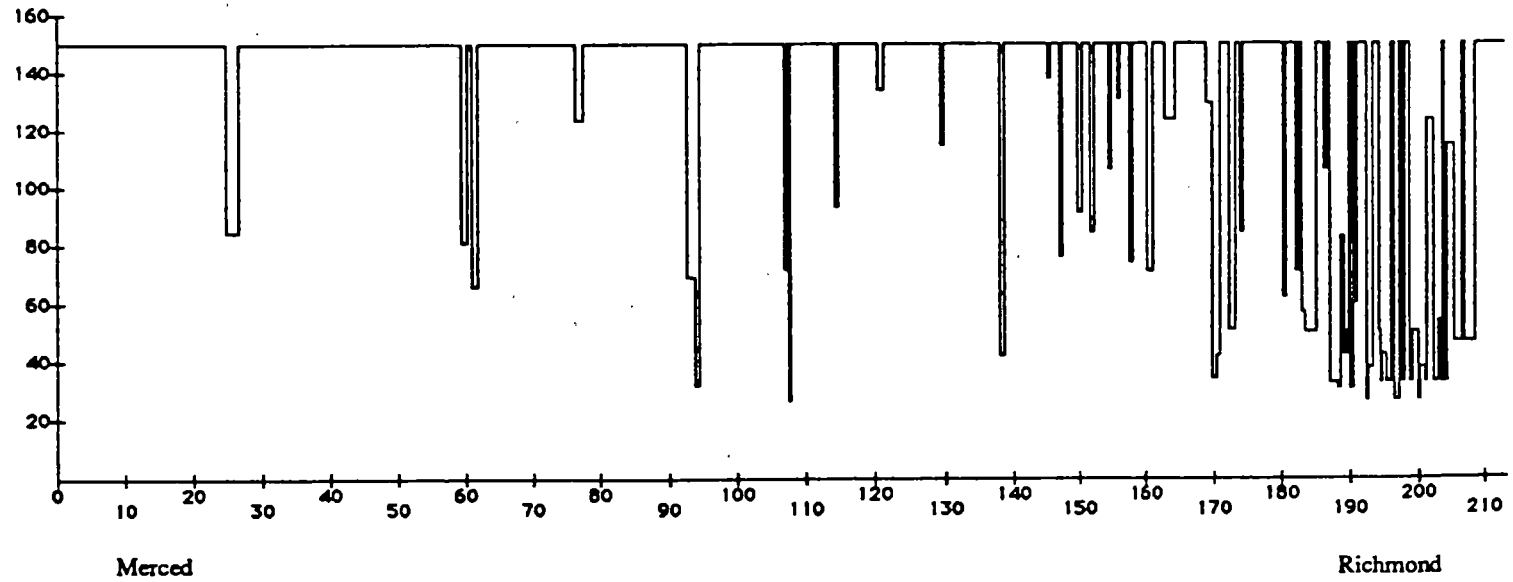

Figure 3.4.3.6-3 CAL Railroad Merced to Richmond

3.4.4 Spiral Analysis

Spiral transition curves are used to control lateral and vertical forces as vehicles move from straight segments to curves or vice versa. It is difficult for some existing highway and rail alignments to accommodate high speed maglev environments using relatively long spirals. This is most evident in areas of rolling, undulating terrain where many existing curve radii are less than 2500m, tangent lengths average less than 1000m, and several curves may exist sequentially without interspersed tangent segment alignments. The need for spirals in the design of maglev guideways will raise many questions on existing right-of-way usage. Most of the interstate highways were not designed with spirals. Railroad spiral transitions were built into track designs but for slower speeds and less superelevation than needed for maglev use.

Speed and bank angle requirements necessary to allow substantial right-of-way usage and to preserve comfort must be determined and specified. Comfort factors that most influence spiral geometries include unbalanced accelerations, acceleration change rates (jerk), and vehicle roll rates. At higher speeds the guideway length needed to transition into or out of a curve may be several hundred meters. An analysis of spiral transitions for different vehicle speeds and elements of passenger comfort is described in the following paragraphs. Higher speeds through tight radius curves made possible by increased superelevation will require long spirals determined roll rate constraints. This will force the guideway to extend outside the existing right-of-way in some instances. Land will need to be acquired and additional structures built to meet geometric requirements increasing the per mile cost of the guideway.

Both clothoid (used by Transrapid for vertical transitions) and sinusoid (used by Transrapid for lateral transitions) spiral transitions are considered in the analysis. Clothoid spirals are more suited for right-of-way use because of their shorter length. Sinusoidal transitions would require more distance, meaning more area outside the right-of-way and longer span lengths (leaving and re-entering right-of-way), but would result in a smoother overall ride. Further examination of maximum roll rate and vertical jerk tolerable to passengers is necessary. It is possible that the advantages of smooth jerk onsets in the sinusoid case will allow a higher roll rate limits. Higher limits reduce spiral lengths. Ride quality simulation using people in full motion simulators is needed before United States maglev developers, operators, and passengers can be comfortable adopting new aggressive passenger comfort limits.

3.4.4.1 Alignment Attributes of Existing Rights-of-Way

The curvature attributes of the existing New York Thruway alignment between the Tappan Zee Bridge, north of New York City, and Syracuse is illustrated in Figure 3.4.4.1-1 The data was obtained from United States Geological Survey (USGS)1:24,000 scale topographic maps. Of 402 alignment segments, 56 percent (222) are curves. Examination of the data revealed that 81 percent (179 curves) were less than 5000m in radius and 15 percent (34 curves) have internal angles greater than 40 degrees and radii less than 1250m. Application of spiral alignments to suit passenger comfort and high speed operation deviates most from the existing alignment centerline for curves combining high internal angles and shorter radius attributes.

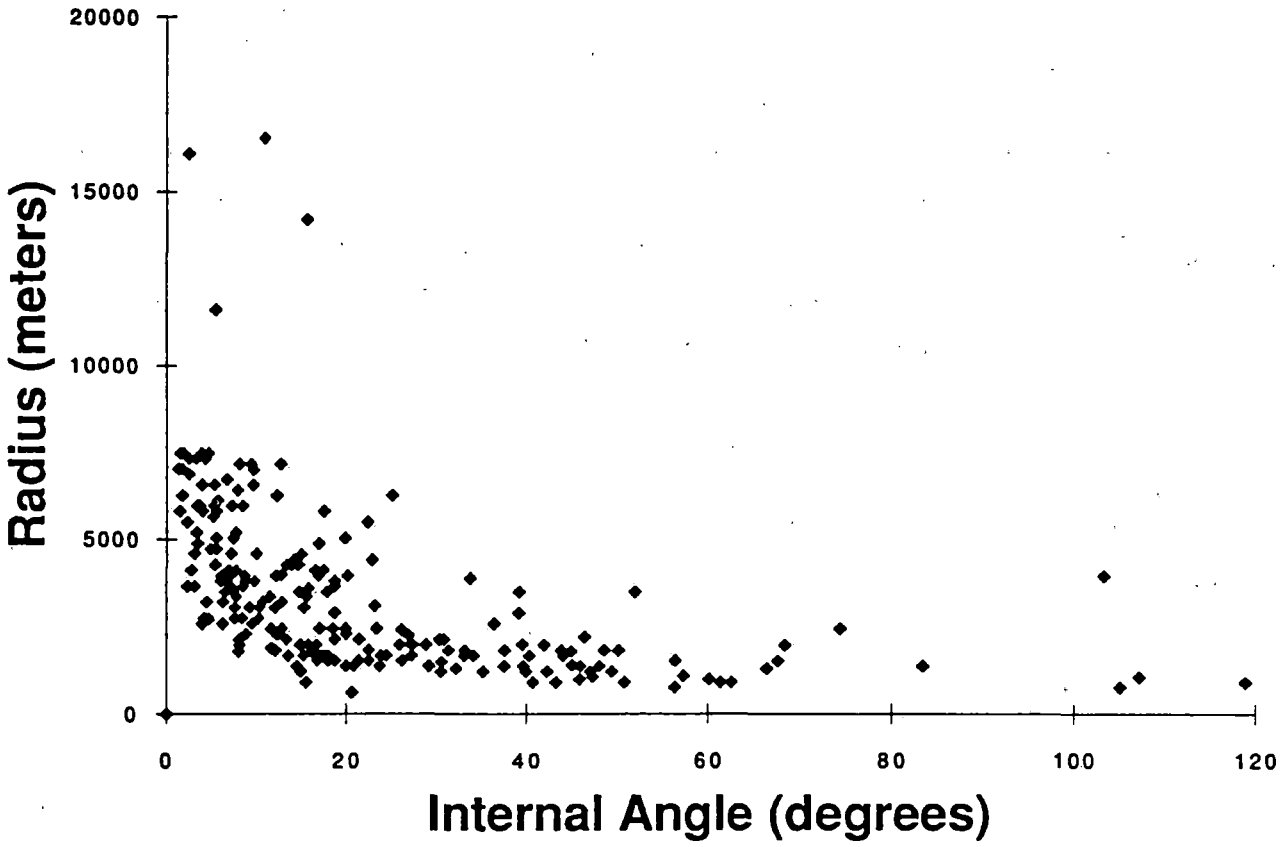

Figure 3.4.4.1-1 Curvature Attributes on the New York Thruway

Figure 3.4.4.1-1 does not indicate the distribution of these curves along the route or the presence and length of adjacent tangent alignments which are necessary for spirals to begin and end in order to preserve near centerline alignments. The distribution of curves is important because consecutive

curves, particularly those reversing direction, offer no adjacent tangent from which to begin a deviation-limiting spiral. Between the 26 and 32 kilometer posts, four reversing curves with radii between 1220m and 915m and internal angles of 119, 107, 41 and 47 degrees occur in immediate succession. .Clearly, a unique spiral solution will be required in this area.

3.4.4.2 Clothoid and Sinusoidal Transitions

The difference between clothoid and sinusoidal transitions is that the clothoid exhibits a constant change in acceleration throughout the spiral length. The jerk is a constant that has a value less than or equal to the maximum jerk comfort limit. In contrast to the step change in the clothoid jerk function, the acceleration changes more gradually at the beginning and end of a sinusoidal transition and the maximum jerk is reached only at mid-transition. The sinusoid transition is more comfortable, however the length of the spiral is twice that of the clothoid for the same jerk limit. These differences are illustrated in Figure 3.4.4.2-1.

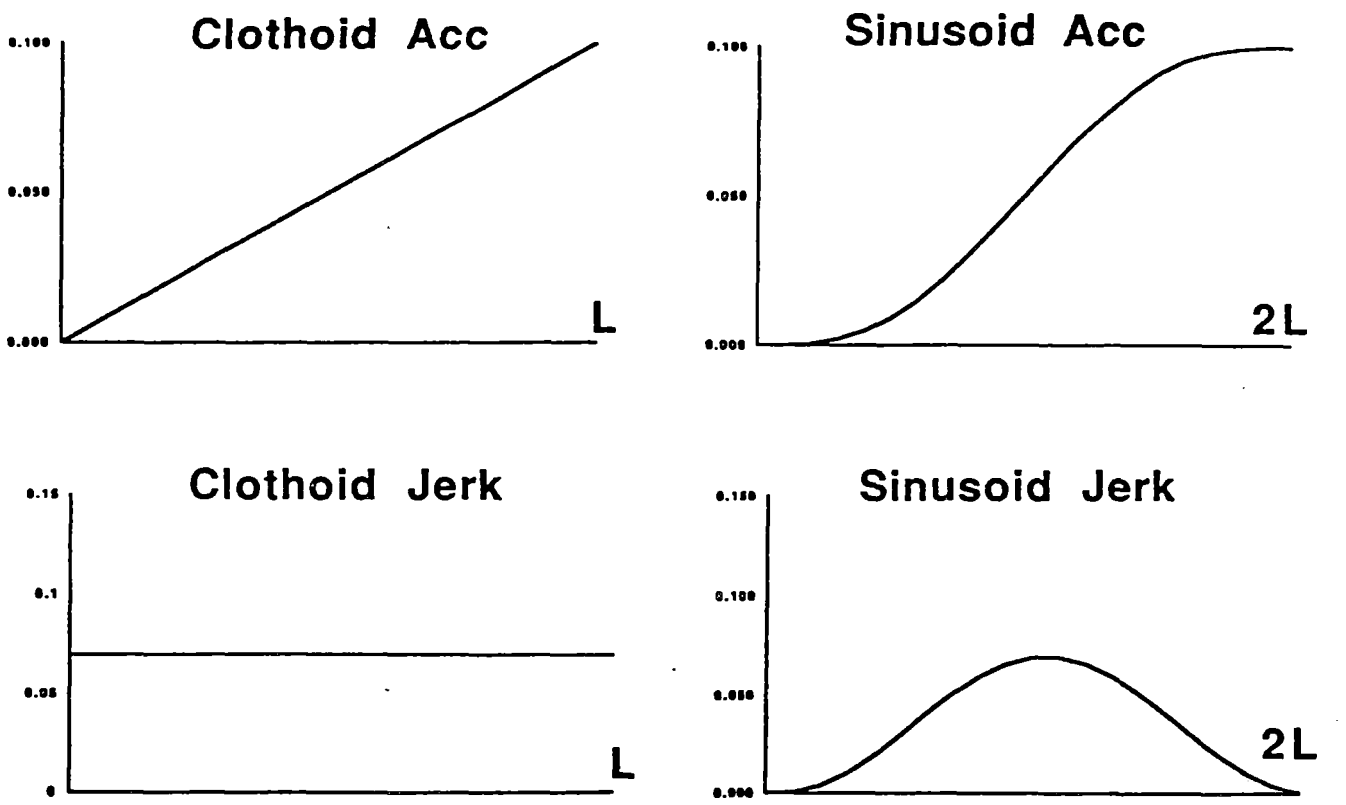

Figure 3.4.4.2-1 Clothoid and Sinusoid Transition Functions

The advantage of the sinusoid is that the onset of jerk is a smooth function, with no discontinuities, and is generally more pleasing to passengers. The gradual onset of jerk allows passengers to prepare for the subsequent unbalanced lateral load and, perhaps, to tolerate larger lateral jerk and unbalanced lateral load limits. Ride quality testing is required to assess the actual tolerable limits. However, the sinusoid spiral length is twice that of the clothoid spiral for a transition to a given radius which increases land requirements for the guideway alignment. Table 3.4.4-1 shows the spiral length equations, for which the jerk constraint is not exceeded, and shows an example for which the radius of curvature is the minimum allowed with acceptable unbalanced lateral acceleration.

Table 3.4.4.2-1 Clothoid and Sinusoid Spiral Length Calculations

Clothoid	**Sinusoid**
$L = v^2/R * v/r_y$	$L = v^2/R * 2*v/r_y$
where:	where:
L = spiral length = **214m**	L = spiral length = **428m**
v = vehicle speed = 150 m/s	v = vehicle speed = 150 m/s
R = horizontal radius = 23000 m	R = horizontal radius = 23000 m
r_y = lateral jerk = 0.07 g/ s	r_y = lateral jerk = 0.07 g/ s

These spiral length equations assume no superelevation (see paragraph 3.4.4.3 for superelevation effects) and, consequently, no balancing lateral load contributed by gravity. Although these lengths are relatively short, the 23,000 meter minimum radius is unacceptable when considering accommodation by existing right-of-way alignments where curves of 2,000 meters and less are common. Superelevation is necessary to reduce curve radii for compatibility of maglev guideway alignments with existing rights-of-way and to maintain lateral comfort within the recommended tolerances.

3.4.4.3 Superelevation and Roll Rate Effects on Lateral Transitions

Controlling unbalanced lateral loads through guideway superelevation and spiral transitions is necessary to develop a maglev alignment within the existing rights-of-way and to simultaneously maintain ride comfort. If vehicle speed and guideway geometrics are coordinated perfectly, a balanced lateral load can be maintained. Equations developed to coordinate bank angle changes with the onset of centripetal acceleration to produce a balanced lateral load throughout a sinusoidal transition curve are described below. Results for the clothoid transition spiral are analogous, with the advantage of half the length required by the sinusoid, and are not developed here in detail.

Variables are as defined in Table 3.4.4-1. Additionally, g= acceleration of gravity, r_Z = vertical jerk, b = superelevation, Lrr = spiral length defined by roll rate, Ljv = spiral length defined by vertical acceleration and jerk, and S/L is a fraction ($0 \leq S \leq L$) of proportion for displacement along the spiral length L. For S=0, the spiral is just beginning, the bank angle is flat and there is no lateral acceleration due to curvature. For S=L, the spiral has ended, the constant radius curve has begun, the bank angle is constant, and unbalanced lateral load is maintained within tolerance.

Lateral load is balanced by the following relation:

$$(v*v/R) * (S/L - 1/(2*p) * SIN(2*p*S/L)) * COS(b) - g * SIN(b) = 0$$

Balanced lateral load is maintained by coordinated superelevation changes:

$$BETA(S/L) = ARCTAN (v*v/(R*g) * (S/L - 1/2/p * SIN(2*p*S/L))) * 180/p$$

A specific alignment is analyzed by setting values for two of the three principal variables (v, R, and b) and solving for the third. Figures 3.4.4.1-1 and 3.4.4.1-2 illustrate BETA(S/L) for v=150m/s. Note that S/L is dimensionless and indicates the displacement along the spiral. BETA(S/L) shows the changes in superelevation necessary to balance lateral load.

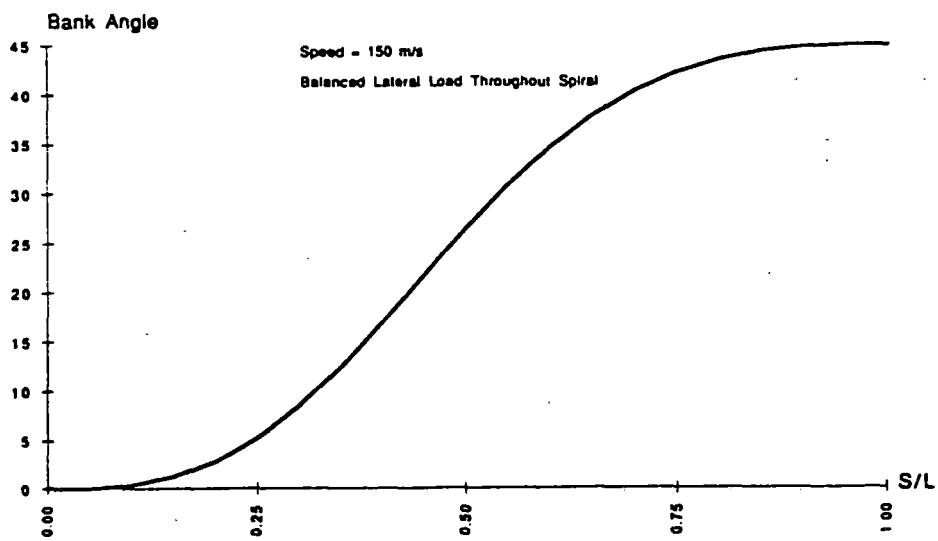

Figure 3.4.4.3-1 Bank Angle Balances Lateral Load During Sinusoidal Transition

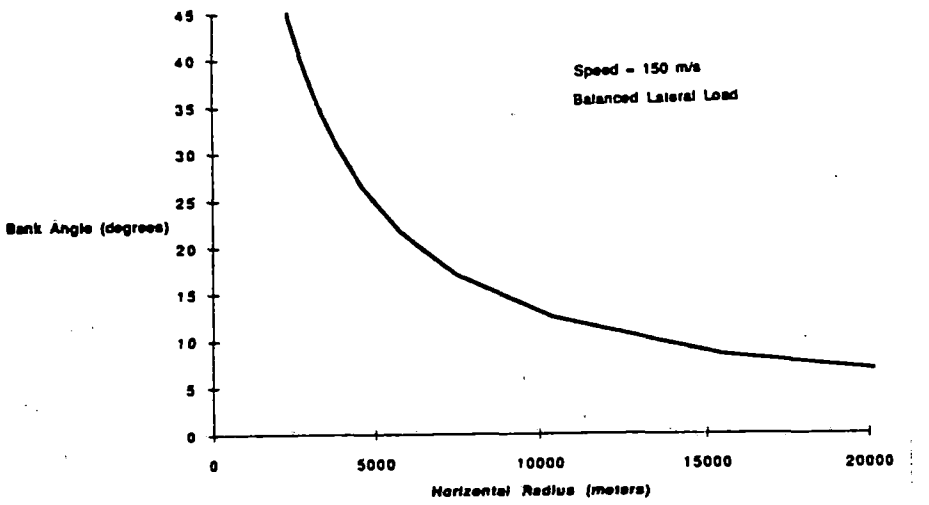

Figure 3.4.4.3-2 Bank Angle Compensates Exactly for Curvature at Constant Speed

Note that this coordinated spiral maintains a balanced lateral load independent of the length of the spiral. Spiral length is now a function of the roll rate and the unbalanced vertical acceleration and jerk constraints. Roll rate is the derivative of the BETA function above with respect to time:

$$RR = v*v/(R*g) * v/Lrr * FRR$$

where FRR =

$$(1-COS\ (2*p*S/L)) / (1+ ((v*v/(R*g))*(S/L - 1/(2*p)*SIN(2*p*S/L)))**2)*180/p$$

The length of the spiral, constrained by maximum roll rate, can be calculated by using:

$$Lrr = (v*v/(R*g)) * (v / RRmax) * FRRmax$$

The spiral must still be examined for adherence to the vertical acceleration and jerk limits. The equation for unbalanced vertical acceleration is given below:

$$1.2 * g >= v*v/R * (S/L) * SIN (BETA(S/L) * p/180) + g * COS(BETA(S/L)* p/180)$$

The vertical jerk is obtained from the derivative of the right hand side of the above equation:

$$Jvert = (v*v / R) * (v / Ljv) * FJV$$

where FJV =

$$(1-COS(S/L * 2 * p)) * SIN (BETA(S/L) * p/180)$$

The spiral length constrained by vertical acceleration and jerk is found by:

$$Ljv = (v * v / R) * (v/ Jvert\text{-}max) * FJVmax$$

Figures 3.4.4.1-3 and 3.4.4.1-4 illustrate the relationship between vertically constrained and roll-rate constrained sinusoidal spirals. For the given superelevation, curvature radius, and vehicle speed, the length constrained by roll rate will satisfy the geometric comfort constraints: lateral loads are balanced, roll rate peaks do not exceed the specified maximum, and vertical jerk is held to one half the comfort limit.

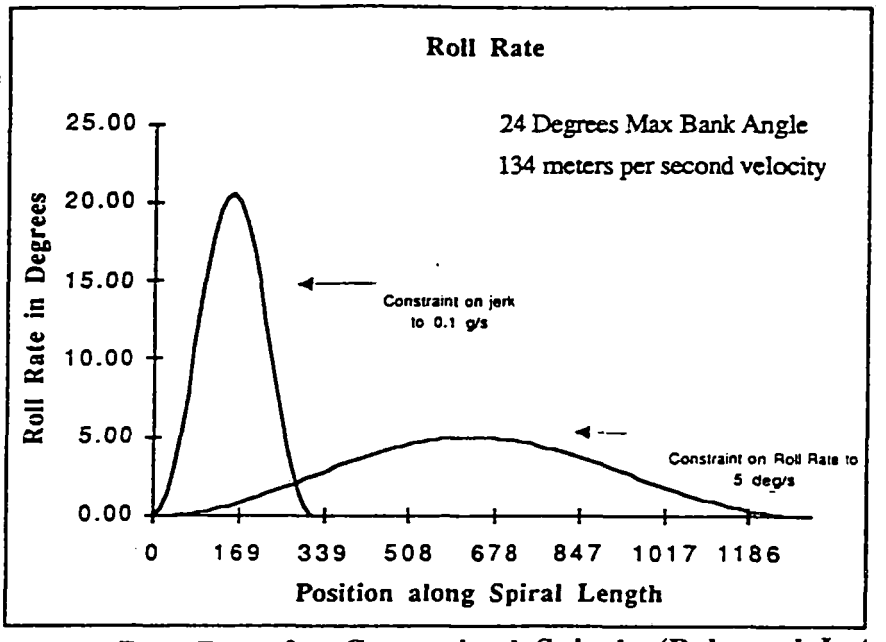

Figure 3.4.4.3-3 Roll Rate for Constrained Spirals (Balanced Lateral Loads)

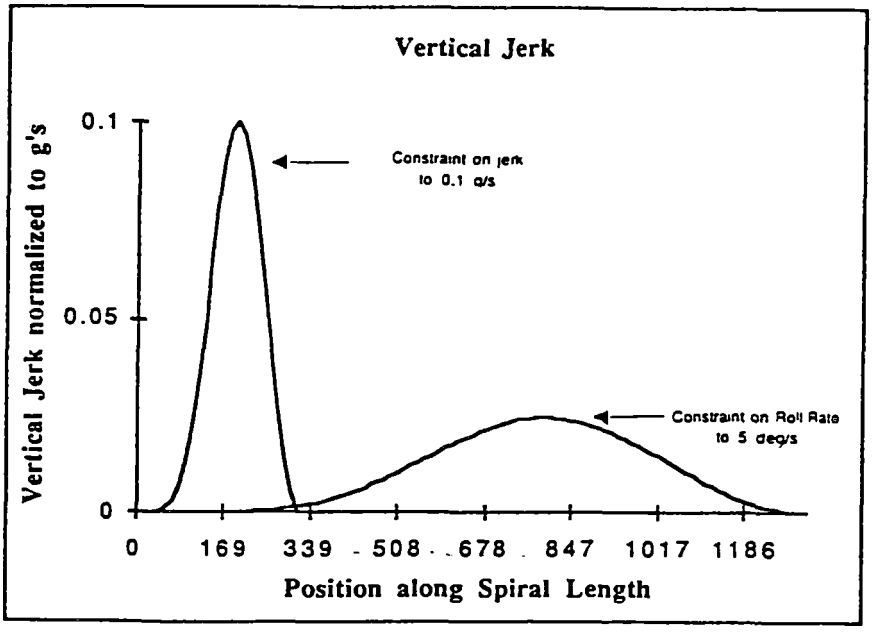

Figure 3.4.4.3-4 Vertical Jerk for Constrained Spirals (Balanced Lateral Loads

3.4.4.4 Application of High Speed Spiral Transitions

High speed maglev operations using existing rights-of-way will require significantly more superelevation than used in currently common transportation modes. This is necessary to balance lateral loads while maintaining high vehicle speeds in the relatively short radius curves found within existing rights-of-way. Alignment spirals are necessary to make the transition in horizontal curvature as well as in superelevation. It is shown in the previous paragraphs that transition in horizontal curvature is limited by lateral acceleration and jerk constraints, but that the overall character of the spiral is limited more severely by the transition in superelevation as constrained by vehicle roll rate.

Designing spiral alignments involves considering a number of solutions that include options to deviate to the inside or the outside of the existing centerline. Figure 3.4.4.4-1 illustrates the inside solution that is analyzed here. The outside solutions involve successive application of spirals in a reverse curve configuration for a given tangent-curve-tangent alignment. In practice, desired vehicle speed, terrain, and land use will influence spiral selection.

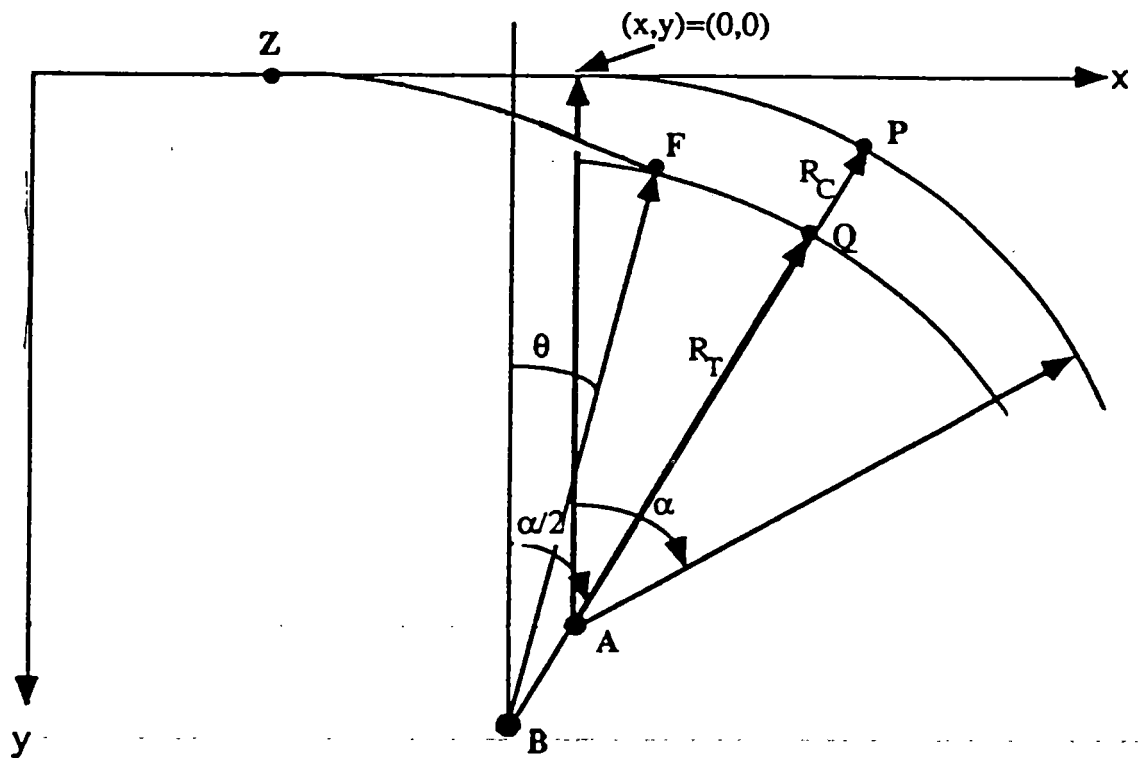

Figure 3.4.4.4-1 Inside Spiral Alignment Characteristics

Table 3.4.4.4-1 compares the spiral attributes for a particular horizontal curve with a 1000m radius and a 30 degree internal angle. The spiral angle is the angle subtended by the spiral portion of the curve. Some "solutions" are not applicable because the angle subtended by the spiral, θ, is too large for the internal half angle, $\alpha/2$ (15 degrees). The distance off the existing centerline is measured along the angle bisector where the plan curve and the curve comprised of spirals are farthest apart. The tangent used refers to the distance back along the adjacent tangent from the plan curve onset that the spiral begins. Maintaining or increasing the target 75 m/s (the maximum speed on the original plan curve using 1000m radius and 30 degree superelevation) with little deviation from the centerline, and achieving a subtended angle equal to the internal half angle is desired.

Table 3.4.4.4-1 Inside Spiral Characteristics for a 1000m Radius, 30 Degree Curve

Action	Case Number	Min. Spiral Radius (meters)	Bank Angle (deg.)	Roll Rate (deg. / sec)	Speed (m/s)	Tangent Used (meters)	Spiral Angle θ (deg.)	Distance off Centerline (meters)
Increase Radius	1	1000	30	5	75	470.6	26.8	16.6
	2	2000	30	5	106	932.7	18.9	52
	3	**3000**	30	5	**130**	**1349.4**	**15.5**	**87.3**
Decrease Bank Angle & Increase Radius	4	1000	24	5	66	327.0	18.6	8.1
	5	**1540**	**24**	5	**82**	**550.2**	15.0	**27.1**
	6	2000	24	5	93	729.9	14.4	31.6
Constant Radius & Vary Bank Angle	7	1000	12	5	46	111.3	6.4	0.9
	8	1000	18	5	56	207.5	11.8	3.3
	9	1000	**21**	5	**61**	**263.3**	15.0	**5.3**
Hold Speed	10	**1250**	**22.5**	5	**71**	**396.6**	15.0	**15.4**
Increase Roll Rate	11	1000	30	**10**	75	234.7	13.4	**4.2**

Referring to Table 3.4.4.4-1, cases 1-3 illustrate the effect of increasing the minimum spiral radius while holding bank angle and roll rate constant. Speed increases at the cost of increased tangent usage and distance from the centerline. The angle subtended by the spiral does not fall within half the internal angle and the cases 1-3 are not solutions to the given alignment, although existing curve with greater than 31 degree internal angles could be solved with case 3.

In cases 4-6, the bank angle is reduced to 24 degrees, lowering the allowed vehicle speed, and yielding a solution, case 5, in which the vehicle speed is higher than the 75 m/s target, but the tangent used and the deviation from the centerline are significant. Cases 7-9 demonstrate that the centerline deviation can be appreciably small by holding the radius constant and increasing the bank angle. Cases 7-9 are all potential solutions although each results in a speed less than the 75 m/s target.

Case 10 illustrates a solution that approximately holds the vehicle speed to that allowed in the 1000m, 30 degree original plan and does not deviate from the centerline excessively. Case 11 shows quite clearly that doubling the allowed roll rate to 10 degrees yields a solution closely aligned with the original centerline. Assessment of passenger responses to these roll rates is warranted given the potential payoff in avoided land acquisition costs.

3.4.5 Span Lengths

Information was collected on the number of structures encountered by the guideway over a given route. Structures were placed into the following groups with justification for the recommendation of alternative structures:

1) Underpasses - Alternative structures may or may not be needed depending on the type and width of the crossing structure.
2) Overpasses - Used same criteria as underpasses.
3) Powerlines - Included telephone line crossings. Alternative structures were reported only if multiple lines forced span length to exceed the 25-meter default value.
4) Pipelines - The number of pipeline crossings was recorded, but in no cases were alternative structures needed.
5) Bridges - The presence of bridges usually indicated the crossing of a body of water or cavity. Bridges always required an alternative span length structure.
6) Tunnels - It was impossible to place maglev adjacent to existing right-of-way for a tunnel. Therefore, a requirement was specified for a new tunnel. This tunnel is classified as an alternative span.
7) Railroad Crossings - For railroads passing over (through) roads or other rail lines, it was assumed that the 25-meter default span was sufficient and no alternative structures were needed.

The default span length is set at 25 meters. This value is consistent with the span lengths at the Emsland Transrapid Test Facility in Germany. Non-default length are categorized by length. The following groups are used:

1) Default (25 meters)
2) 26 - 100 meters
3) 101 - 200 meters
4) 201 - 300 meters
5) Greater than 300 meters

The span length results are given as a matrix in Tables 3.4.5-1 to 6. The total number of alternative structures needed for each route and their length is given.

Table 3.4.5-1 Tappan Zee Bridge-Syracuse Highway Span Requirements

	Default	26-100m	101-200m	201-300m	> 300m	Total
Underpasses	123	1	1	0	0	125
Overpasses	50	18	2	0	0	70
Powerlines	10	0	0	0	0	10
Pipelines	1	0	0	0	0	1
Bridges	0	2	10	2	1	15
Tunnels	0	0	0	0	0	0
Total	184	21	13	2	1	221

Table 3.4.5-2 Yonkers-Syracuse Railroad Span Requirements

	Default	26-100m	101-200m	201-300m	> 300m	Total
Underpasses	63	16	0	0	0	79
Overpasses	12	4	0	0	0	16
Crossings	58	0	0	0	0	58
Powerlines	9	0	0	0	0	9
Pipelines	0	0	0	0	0	0
Bridges	0	5	1	1	1	8
Tunnels	0	4	3	0	0	7
Total	133	29	4	1	1	168

Table 3.4.5-3 Chicago-Detroit Highway Span Requirements

	Default	26-100m	101-200m	201-300m	> 300m	Total
Underpasses	159	5	3	0	0	167
Overpasses	61	6	10	0	0	77
Powerlines	19	0	0	0	0	19
Pipelines	4	0	0	0	0	4
Bridges	0	2	3	1	4	10
Tunnels	0	0	0	0	1	1
Total	243	13	16	1	5	278

Table 3.4.5-4 Chicago-Detroit Railroad Span Requirements

	Default	26-100m	101-200m	201-300m	> 300m	Total
Underpasses	26	7	0	0	0	33
Overpasses	12	13	2	0	0	27
Crossings	181	0	0	0	0	181
Powerlines	10	0	0	0	0	10
Pipelines	7	0	0	0	0	7
Bridges	0	1	3	0	0	4
Tunnels	0	0	0	0	0	0
Total	236	21	5	0	0	262

Table 3.4.5-5 Los Angeles-San Leandro Highway Span Requirements

	Default	26-100m	101-200m	201-300m	> 300m	Total
Underpasses	87	31	1	1	0	120
Overpasses	78	15	1	0	0	94
Powerlines	25	0	0	0	0	25
Pipelines	15	0	0	0	0	15
Bridges	0	0	1	2	0	3
Tunnels	0	0	0	0	0	0
Total	205	46	3	3	0	257

Table 3.4.5-6 Los Angeles-Richmond Railroad Span Requirements

	Default	26-100m	101-200m	201-300m	> 300m	Total
Underpasses	43	25	0	0	0	68
Overpasses	28	14	0	0	0	42
Crossings	241	0	0	0	0	241
Powerlines	31	0	0	0	0	31
Pipelines	4	0	0	0	0	4
Bridges	0	4	3	3	0	10
Tunnels	0	4	9	1	2	16
Total	347	47	12	4	2	412

3.5 ESTIMATED TRIP TIMES

3.5.1 Introduction

This section expands on the route analysis completed in subsection 3.4 for the three specified corridors. Equations for vehicle acceleration and deceleration are added to the route analysis to calculate vehicle speed characteristics and trip times. The value of 0.16g is used for vehicle acceleration and deceleration as identified in Table 3.2.5-1.

Trip-time runs were calculated using the railroad and highway routes for the three corridors (New York City-Albany-Syracuse, Detroit-Chicago, Los Angeles-San Francisco) based on three maximum speeds, 110 m/s, 134 m/s, and 150 m/s. Plots of station-to-station travel for each of the three maximum speeds (54 plots in all) are given in Appendix D along with route information for each of the trip-time runs made. Data were collected for alignment, time, and speed characteristics. Also included in Appendix D is a speed report specifying vehicle speed at 300-meter intervals along the route.

The following assumptions are used in the analysis of acceleration and deceleration profiles:

1) The set of maximum vehicle speeds is 110 m/s, 134 m/s, and 150 m/s.
2) The maximum bank angle is 12 degrees.
3) The lateral acceleration is set at 0.1g. The range for vertical acceleration is 0.95g to 1.2g
4) Grade and vertical curvature variations are minimized through the use of column heights as high as 12 meters.
5) Maglev vehicles are assumed to be running along the centerline of the existing highway and parallel to the existing railroad. Deviations from the existing right-of-way are not allowed in this case.
6) Trip times and average speeds for this subsection are calculated using the value of 0.16g (1.568 m/s^2) for vehicle acceleration and deceleration. The effects of longitudinal jerk on trip time and vehicle speeds are not considered in the trip-time calculations.
7) Route alignments are made up of curves and straights along the centerline of the highway and railroad alignments. No ROW departures are made in this portion of the analysis. Considerations for spiral transitions (i.e., roll rate, lateral and vertical jerk) are part of the alignment designated as curves.
8) Station dwell time is set at 2 minutes.

3.5.2 Methodology

Using the kinematic equations for straight-line motion, an algorithm was developed for vehicle acceleration and deceleration. The algorithm establishes baseline trip times for routes along the three detailed corridors. Speeds, positions, and travel time are calculated along the route and are constrained by the comfort parameters established in subsection 3.2.

3.5.3 Trip Times and Average Speeds

Table 3.5.3-1 lists the trip time and average speed for each of the three maximum speeds. Trip-time results reflect speeds restricted by the guideway geometry, allowable acceleration, and deceleration. The trip time includes a 2-minute dwell time for each of two station stops along the routes.

Table 3.5.3-1 Corridor Trip Times and Average Speeds

Route	Max Speed = 150 (m/s)	Max Speed = 134 (m/s)	Max Speed = 110 (m/s)
New York - Syracuse			
*Highway (425.8 km)	1hr 29 min / 79.82 m/s	1hr 29min / 79.79 m/s	1hr 30 min / 79.00 m/s
*Railroad (423.7 km)	1hr 34 min / 75.05 m/s	1hr 34 min / 74.95 m/s	1hr 35 min / 74.39 m/s
Detroit - Chicago			
Highway (433.7 km)	1hr 32 min / 78.92 m/s	1hr 32 min / 78.74 m/s	1hr 34 min / 76.97 m/s
Railroad (411.0 km)	1hr 23 min / 82.24 m/s	1hr 25 min / 81.11 m/s	1hr 28 min / 77.83 m/s
LA - SF			
Highway (587.5 km)	1hr 39 min / 99.18 m/s	1hr 43 min / 94.92 m/s	1hr 53 min / 86.33 m/s
Railroad (726.4 km)	2hr 32 min / 79.39 m/s	2hr 37 min / 77.03 m/s	2hr 49 min / 71.86 m/s

* New York highway route starts at the Tappan Zee Bridge. The railroad route begins at the Yonkers station

Trip time calculations are also reported in Table 3.5.3-2 for the opposite directions to compare baseline trip times.

Table 3.5.3-2 Opposite Direction Trip Times and Average Speeds

Route	Max Speed = 150 (m/s)	Max Speed = 134 (m/s)	Max Speed = 110 (m/s)
New York - Syracuse			
*Highway (425.8 km)	1hr 29 min / 79.85 m/s	1hr 29 min / 79.83 m/s	1hr 30 min / 79.02 m/s
*Railroad (423.7 km)	1hr 35 min / 74.66 m/s	1hr 35 min / 74.55 m/s	1hr 36 min / 73.96 m/s
Detroit - Chicago			
Highway (433.7 km)	1hr 32 min / 78.76 m/s	1hr 32 min / 78.65 m/s	1hr 34 min / 77.03 m/s
Railroad (411.0 km)	1hr 23 min / 82.25 m/s	1hr 25 min / 81.15 m/s	1hr 28 min / 77.85 m/s
LA - SF			
Highway (587.5 km)	1hr 39 min / 99.03 m/s	1hr 43 min / 94.80 m/s	1hr 53 min / 86.17 m/s
Railroad (726.4 km)	2hr 33 min / 79.26 m/s	2hr 37 min / 77.06 m/s	2hr 49 min / 71.86 m/s

* New York highway route starts at the Tappan Zee Bridge. The railroad route begins at the Yonkers station

Tables 3.5.3-1 and 3.5.3-2 show very little difference in trip times between the three maximum speeds. This occurs because the design speed of the existing rights-of-way is not suitable for the high operating speeds of maglev. Even along the California highway and railroad, where long stretches of straight right-of-way occur, the overall trip-time savings between 110 and 150 m/s is only 15 minutes.

Strict adherence to the right-of-way will severely reduce the high-speed potential of maglev systems unless other measures are taken to reduce the trip time. Increasing the average speed can be done by increasing maximum bank angle or increasing longitudinal acceleration . Trip time can be saved by smoothing route alignments and shortening distances through right-of-way excursions. These considerations will need to be addressed to determine how much of the existing right-of-way is actually usable and what can be done to help achieve the highest possible system performance based on the alignment.

3.5.4 Vehicle Speed Profiles

An example of a vehicle speed profile based on comfort-constrained acceleration and deceleration is given in Figures 3.5.4-1 through 3.5.4-3. The example profile displays the station-to-station travel for the New York corridor for a maximum speed of 150 m/s and reflect a 2-minute dwell time at each intermediate stop.

NY Railroad 150 m/s
Avg Speed = 75.05 m/s Trip Time = 1hr 34 min

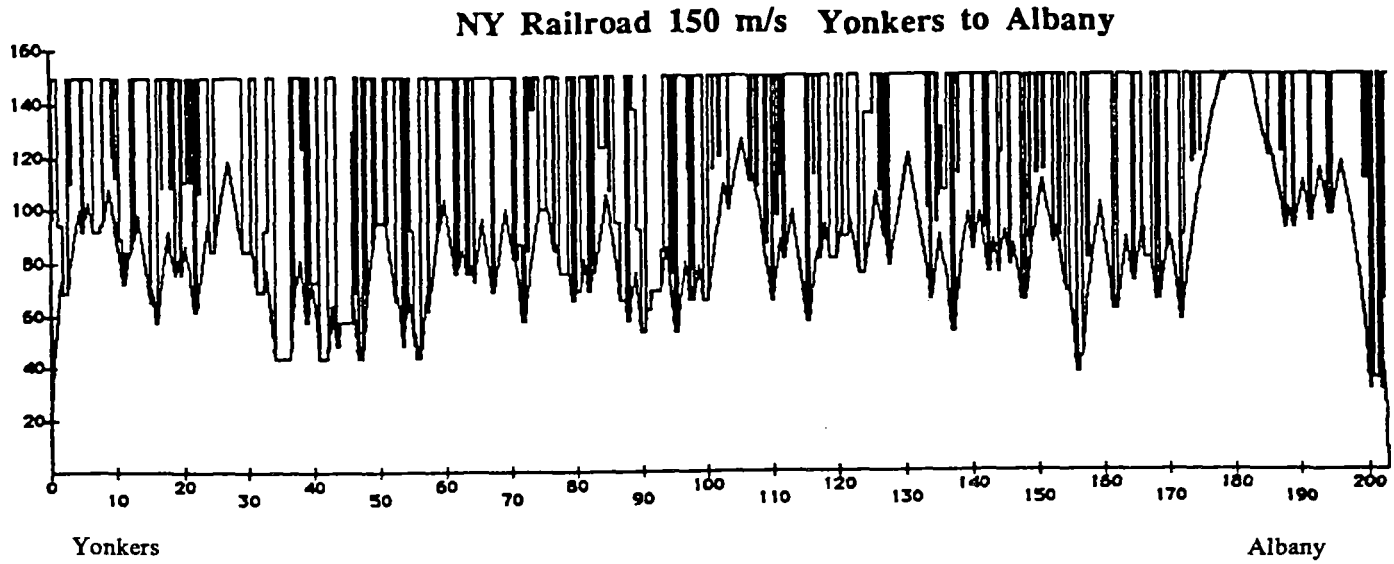

Figure 3.5.4.1-1 NY Railroad 150 m/s Yonkers to Albany

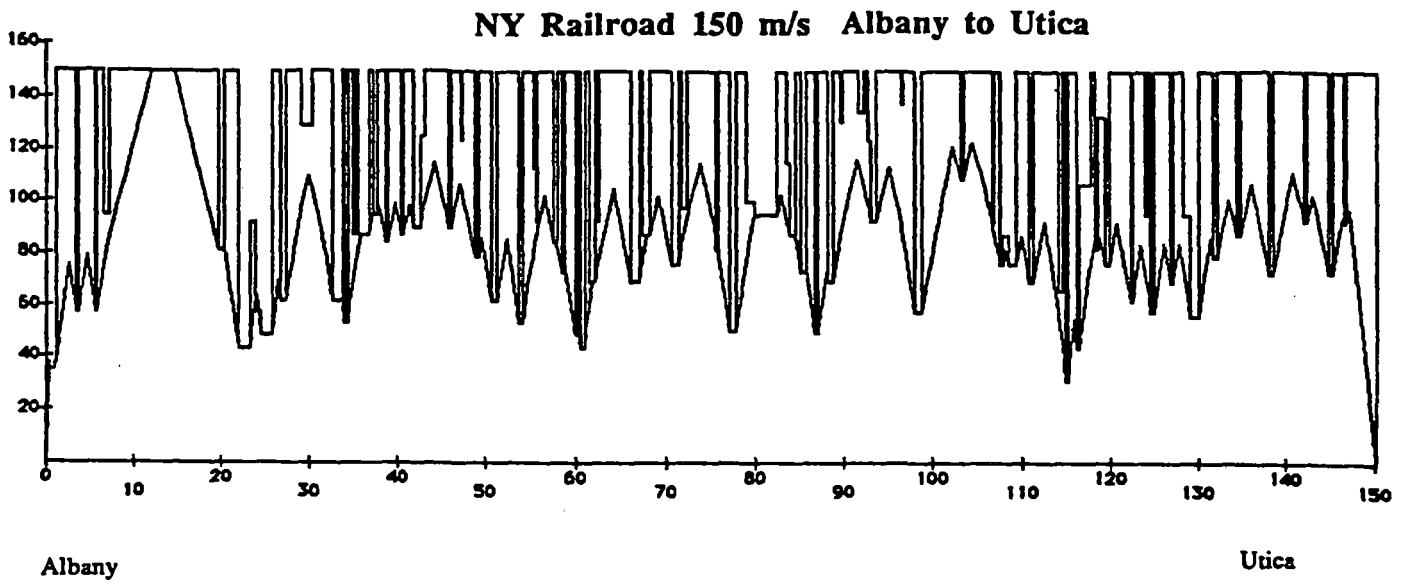

Figure 3.5.4.1-2 NY Highway 150 m/s Albany to Utica

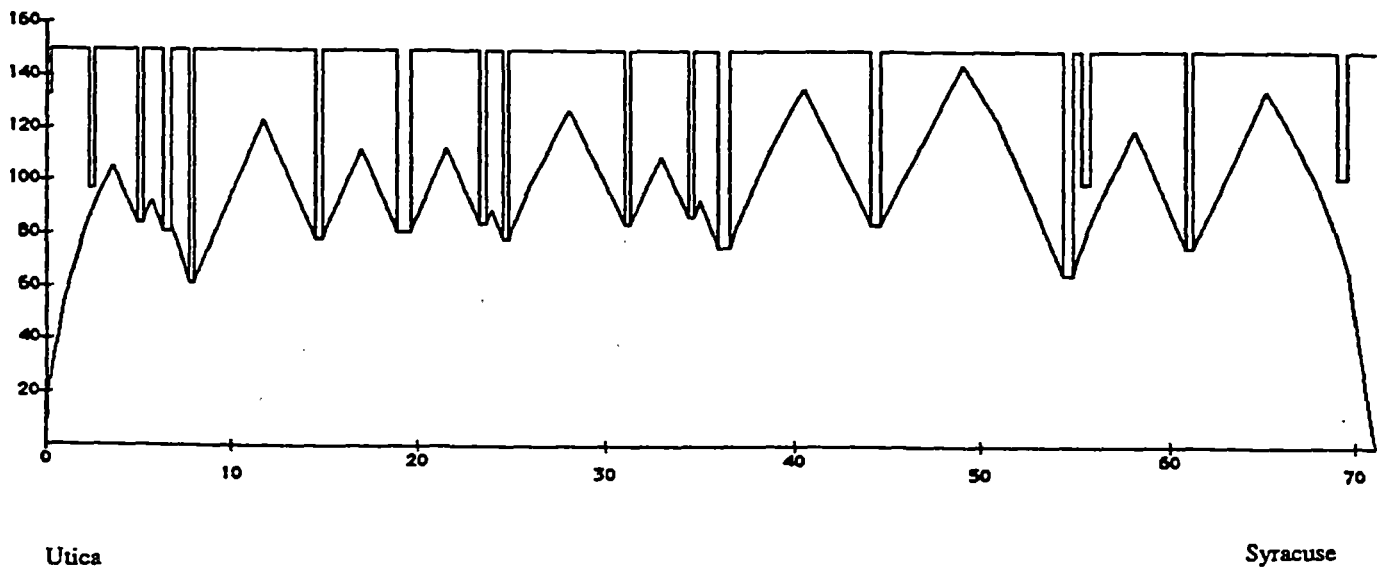

Figure 3.5.4.1-3 NY Highway 150 m/s Utica to Syracuse

3.5.5 Effects of Longitudinal Jerk

The vehicle speed profiles are shown assuming infinite longitudinal jerk. This assumption allows the vehicle to instantaneously reach maximum acceleration limits. Inclusion of finite longitudinal jerk into the calculation of the vehicle speed profile requires the vehicle to gradually accelerate to the maximum operating acceleration, 0.16g. The gradual change results in shorter intervals in which the vehicle operates at higher speeds and a reduction of the average speed for the route.

Figure 3.5.5-1 illustrates the cumulative effect of estimating trip times and average speed for different levels of analysis. The square curve represents the speed constrained by guideway geometry. A vehicle that could maintain maximum speed on all portions of the guideway would require instantaneous speed change. The inverted V-curve (dashed line) combines guideway geometry with the maximum operating acceleration for the vehicle, and assumes instantaneous acceleration and infinite jerk. The smoothed curve shows vehicle speed change constrained by finite jerk and provides a more realistic result for trip time and vehicle speed.

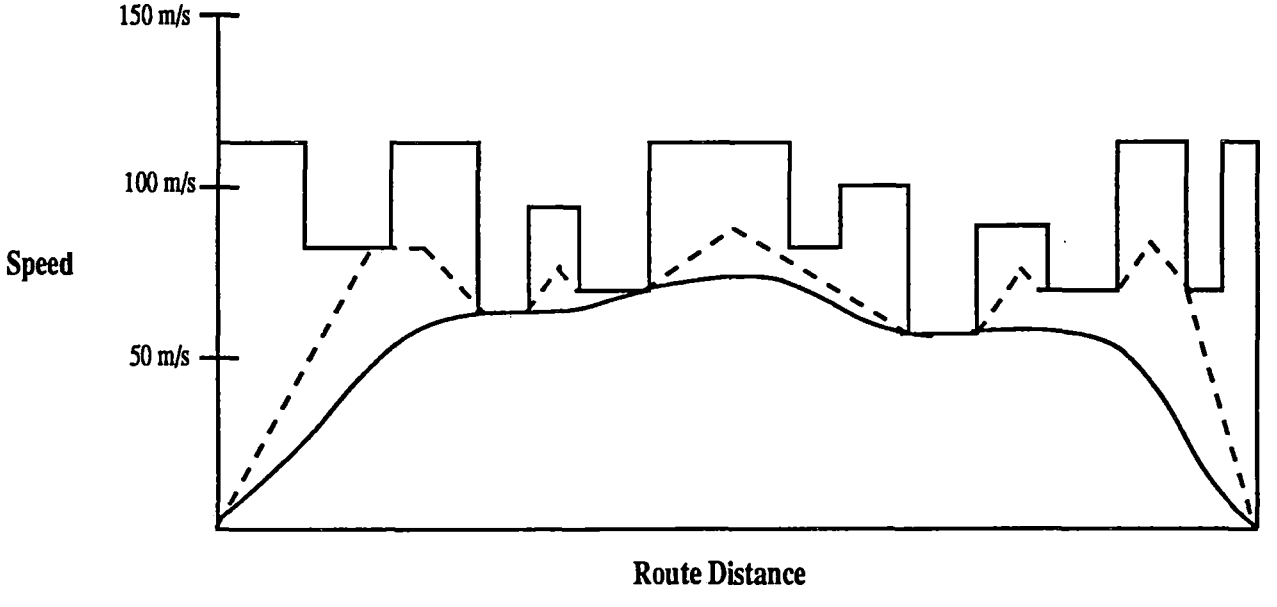

Figure 3.5.5-1 Vehicle Profile Including Jerk

3.5.5.1 Longitudinal Jerk Parameters

The three parameters of interest when determining the effect of longitudinal jerk on route trip times are speed, distance, and time. The changes in speed and time necessary to reach maximum acceleration are independent of the starting speed of the vehicle. Figure 3.5.5.1-1 shows that regardless of the starting speed, the speed at which you reach maximum acceleration and the time it takes to do so are constant and determined by the ratio of the acceleration and jerk limits, A_x and r_x, respectively. However, the distance traveled to reach maximum acceleration values varies with the starting speed. At higher initial speeds, longitudinal transition distances become large with respect to route segment lengths. This additional distance could prohibit vehicle speeds from accelerating into the higher speed peaks of the geometry-constrained profile.

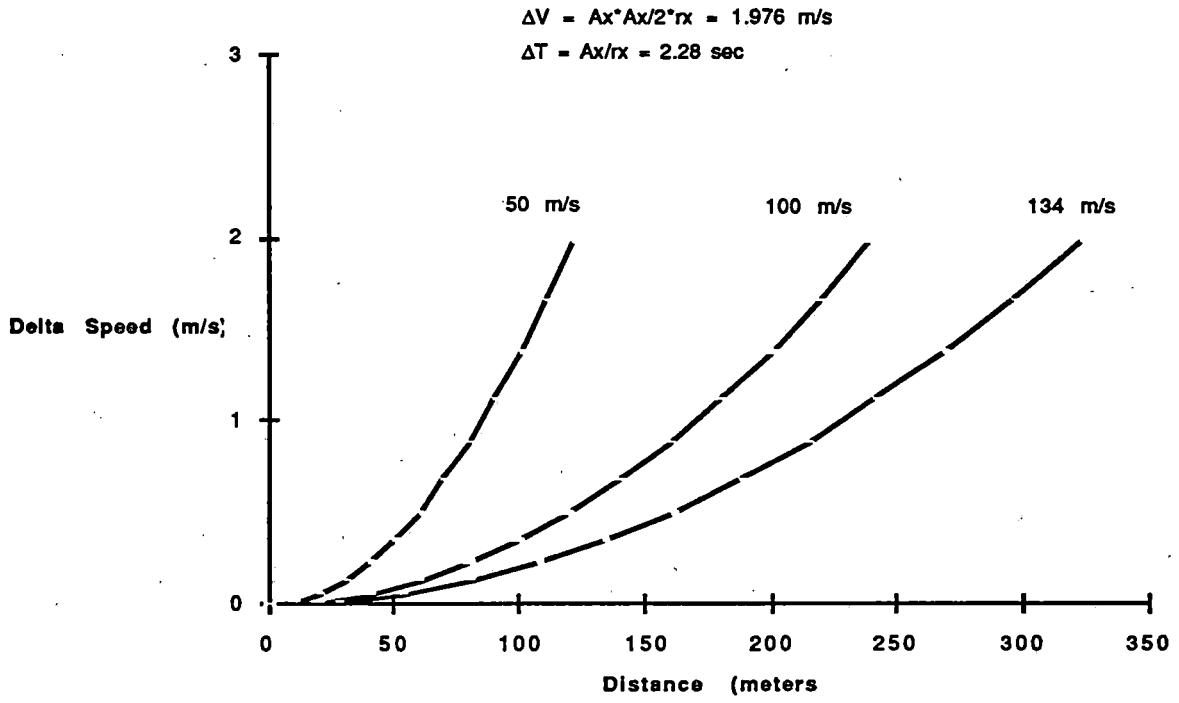

Figure 3.5.5.1-1 Delta Speed and Time Versus Distance

3.5.5.2 Effect on Trip Time

Analysis performed using a constant rate of change of acceleration (clothoidal function) revealed that longitudinal jerk would result in less than a 5-percent increase in the route trip times reported in Tables 3.5.3-1 and 3.5.3-2. Figure 3.5.5.2-1 shows an example for the difference in the vehicle

speed profile between instantaneous maximum acceleration (using 0.16g) and a jerk-limited transition (using 0.07g/s).

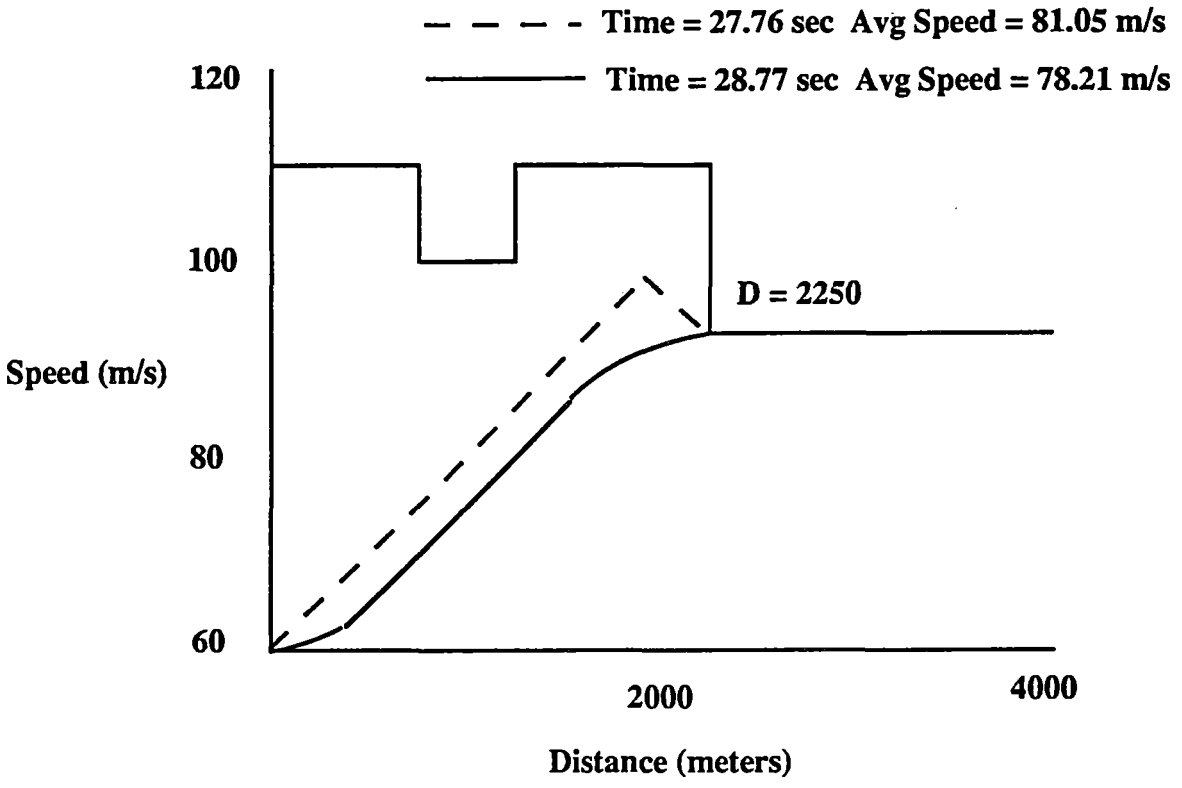

Figure 3.5.5.2-1 Jerk Limited Speed and Delta Time

The instantaneous case takes less time and has a higher average speed over the same distance. Additional time and distance are needed by the jerk-limited case to reach the same speed. Higher operating speeds will have minimal jerk effects due to the longer distances being traveled.

3.5.5.3 Sinusoid Acceleration Function

It is possible to use a sinusoidal function for the rate of change of longitudinal acceleration. The use of a sinusoidal function gives a smoother ride (i.e., lower jerk values), but distances and time to reach the maximum allowable acceleration are double that of the linear case. If a route is expected to have several areas of acceleration and deceleration in its speed profile, using a sinusoid rate of change could have a negative effect on trip times. However, passengers may react more favorably to gradual changes if accelerations are frequent. Further study is needed to examine the tradeoffs between ride comfort and competitive trip times.

3.6 ROUTE ALIGNMENT ALTERNATIVES

3.6.1 Introduction

Corridor trip times can be improved by departing from the right-of-way to improve guideway alignment. Judicious departures, from the centerline route alignments used in subsections 3.4 and 3.5, can be performed by identifying areas which most limit vehicle speed and determining if an excursion from the right-of-way is feasible. Costs associated with excursions include land acquisition, entry-exit bridges, and clearing new right-of-way for the proposed route. Construction cost savings are accrued if the excursion shortens the length of the route enough to overcome the cost of entry-exit bridges. The benefits of route excursions stem from a shorter trip time which may improve the competitiveness of the maglev transportation mode.

3.6.2 Methodology

Right-of-way departures were identified through the analysis of 7.5-minute topographic maps. Areas for improvement included increasing radii to create less constraining horizontal curve alignments. All excursions are checked to assure that the guideway could conform to the 10 percent maximum grade limitation of maglev systems using 12 meter column heights. No analyses were made for cut-and-fill considerations. Right-of-way excursions were not allowed in densely populated areas where there is excessive interference with existing structures (houses, buildings, stations, etc.), areas containing potential safety hazards, or areas where grades are steeper than maglev limitations allow.

3.6.3 Improved Trip Times

Using alignment information gathered for the judicious departure routes, trip-time calculations are made to determine the time saved by leaving the right-of-way. Table 3.6.3-1 shows the individual results and differences obtained from the route analysis program for several excursions made along each route. A maximum vehicle speed of 150 m/s, maximum bank angle of 12 degrees, and 2-minute station dwell time are assumed in the analysis. Excursions, ranked by trip time saved per kilometer outside of the right-of-way, and acreage requirements are reported in Appendix E.

Table 3.6.3-1 Alternate Route Comparison

	Route Distance	Trip Time	Average Speed
*NYC-SYR Highway			
Centerline Route	425.8 km	1:29 hrs	79.82 m/s
Alternate Route	416.8 km	1:25 hrs	82.04 m/s
Difference	-9.0 km	-4 min	+2.22 m/s
*NYC-SYR Railroad			
Centerline Route	423.7 km	1:34 hrs	75.05 m/s
Alternate Route	420.7 km	1:29 hrs	78.20 m/s
Difference	-3.0 km	-5 min	+3.15 m/s
DET-CHI Highway			
Centerline Route	433.6 km	1:32 hrs	78.91 m/s
Alternate Route	433.1 km	1:26 hrs	83.33 m/s
Difference	-0.5 km	-6 min	+4.42 m/s
DET-CHI Railroad			
Centerline Route	411.0 km	1:23 hrs	82.24 m/s
Alternate Route	408.0 km	1:18 hrs	87.15 m/s
Difference	-3.0 km	-5 min	+4.91 m/s
LA-SF Highway			
Centerline Route	587.5 km	1:39 hrs	99.17 m/s
Alternate Route	583.4 km	1:32 hrs	105.59 m/s
Difference	-4.1 km	-7 min	+6.42 m/s
LA-SF Railroad			
Centerline Route	726.4 km	2:32 hrs	79.39 m/s
Alternate Route	704.3 km	2:10 hrs	90.22 m/s
Difference	-22.1 km	-22 min	+10.83 m/s

* New York highway route starts at the Tappan Zee Bridge. The railroad route begins at the Yonkers station

3.6.4 The Value of Excursions

Departure from the right-of-way incurs both costs and benefits. Costs include land acquisition, building condemnation, entry-exit bridges from the original centerline route, and geotechnical survey of the area outside the right-of-way. The primary benefit is trip-time reduction which will improve maglev competitiveness, especially against short-haul air travel, and increase ridership revenues. Excursions are rated by trip-time reduction per kilometer outside the right-of-way. This metric reflects both the land acquisition and guideway construction costs of making an improvement.

The trip times recorded for the three detailed corridors in subsection 3.5.3 are compared to the median airline trip times to determine the competitiveness of potential maglev routes within the right-of-way, and how trip times could be improved through excursions. (Note: Airline times were obtained from the Official Airline Guide, March 1992). For all routes, airline travel is faster than the centerline maglev route. Alignment improvements are specifically directed at reducing the gap between modal trip times. Table 3.6.4-1 gives the data on how maglev routes would compare against rival short-haul commuter flights and what percentage competitive improvement (PCI) was made through the excursion routes. The PCI is calculated by dividing the time saved through making judicious excursions by the total time difference between airline flight time and centerline maglev routes. This percentage can be used to reflect the revenue enhancement potential of making the excursion.

Table 3.6.4-1 Maglev-Airline Competitive Analysis

Route	Maglev Centerline Route (hr:min)	Maglev Excursion Route (hr:min)	Airline Flight Time (hr:min)	Percentage Competitive Improvement
*NY-Syr Highway	1:29	1:25	1:14	26.7 %
*NY-Syr Railroad	1:34	1:29	1:14	25.0 %
Det-Chi Highway	1:32	1:26	1:17	40.0 %
Det-Chi Railroad	1:23	1:18	1:17	83.3 %
LA-SF Highway	1:39	1:32	1:30	77.8 %
LA-SF Railroad	2:32	2:10	1:30	35.5 %

* New York highway route starts at the Tappan Zee Bridge. The railroad route begins at the Yonkers station

Maglev centerline and excursion routes have the same starting and stopping locations. These locations are specified in subsection 3.4 and are located outside city limits, but not at the airport. Maglev routes contained two required station stops which added 4 minutes to the actual travel time. Airline flight times reflect departure-to-arrival times and do not include additional time spent for access/egress between the terminal and downtown urban areas. The analysis performed for PCI is only a representative comparison of corridor trip times.

The trip-time improvements gained through judicious departures from the right-of-way were attained through conservative departure criteria (see subsection 3.6.2). More aggressive criteria may be necessary to achieve a competitive position on some routes.

There are two ways to achieve trip-time reduction through excursions. First, trip time will decrease if the length of the route is shortened. Using right-of-way departures to shorten

meandering sections of highways and railroads will result in a straighter alignment and higher average speed along the route. Independent routes not constrained to follow the right-of-way could be aligned more directly from station to station by taking advantage of Maglev technology advances (i.e., grade climbing, elevated guideway, etc). Second, trip time will decrease if the average speed of the route is increased. Departures specifically designed to cut corners on existing curves or avoid them will allow the vehicle to maintain higher operating speeds. Once the guideway is built, the length and geometry are set. Improvements in trip time can only be made by increasing vehicle speed which will be done by increasing the maximum allowable banking through the use of tilting vehicles or increasing the maximum acceleration and deceleration limits of the system.

An analysis was done to determine the value of the excursions performed for the alternative routes, and to find the criteria for evaluating right-of-way excursions along potential routes. Comparisons of the centerline, alternate, and Great Circle routes can determine the optimum ratio of speed increase to length decrease needed to make maglev competitive with short-haul flights and approach maximum system performance. Table 3.6.4-2 has equivalency ratios to reduce trip time by 1 minute for each of the six detailed routes.

Table 3.6.4-2 Speed Increases and Length Reductions for 1 Minute Saved

Route	Average Speed Increase for 1 Minute Saved	Length Reduction for 1 Minute Saved
NY-Syr Highway	0.87 m/s	4735 meters
NY-Syr Railroad	1.00 m/s	4934 meters
Det-Chi Highway	1.01 m/s	5951 meters
Det-Chi Railroad	0.52 m/s	4763 meters
LA-SF Highway	0.91 m/s	4789 meters
LA-SF Railroad	0.81 m/s	4503 meters

3.6.5 Span Lengths for Excursion Routes

Span length requirements were collected for the alternative routes. The criteria used for determining span lengths is the same as was used in subsection 3.4.5. For alternative routes a span is needed to cross over the highway when departing and re-entering the right-of-way since the centerline is assumed for the highway case. These spans are usually larger than the 25-meter default value because of the angle created between the guideway and highway. Span length results are given in meters in Tables 3.6.5-1 through 3.6.5-6.

Table 3.6.5-1 Span Lengths (m) for TZ Bridge-SYR Alternative Highway Route

	Default	26-100 (m)	101-200 (m)	201-300 (m)	> 300 (m)	Total
Underpasses	123	1	1	0	0	125
Overpasses	60	51	3	0	0	114
Powerlines	10	0	0	0	0	10
Pipelines	1	0	0	0	0	1
Bridges	0	2	12	2	2	18
Tunnels	0	0	0	0	0	0
Total	194	54	16	2	2	268

Table 3.6.5-2 Span Lengths (m) for Yonkers-SYR Alternative Railroad Route

	Default	26-100 (m)	101-200 (m)	201-300 (m)	> 300 (m)	Total
Underpasses	62	16	0	0	0	78
Overpasses	14	28	1	0	0	43
Crossings	57	0	0	0	0	57
Powerlines	9	0	0	0	0	9
Pipelines	0	0	0	0	0	0
Bridges	0	5	1	1	2	9
Tunnels	0	3	3	0	0	6
Total	142	52	5	1	2	202

Table 3.6.5-3 Span Lengths (m) for DET-CHI Alternative Highway Route

	Default	26-100 (m)	101-200 (m)	201-300 (m)	> 300 (m)	Total
Underpasses	157	5	3	0	0	165
Overpasses	68	48	11	0	0	127
Powerlines	19	0	0	0	0	19
Pipelines	4	0	0	0	0	4
Bridges	0	3	3	1	5	12
Tunnels	0	0	0	0	1	1
Total	248	56	17	1	6	328

Table 3.6.5-4 Span Lengths (m) for DET-CHI Alternative Railroad Route

	Default	26-100 (m)	101-200 (m)	201-300 (m)	> 300 (m)	Total
Underpasses	25	7	0	0	0	32
Overpasses	18	26	2	1	1	48
Crossings	179	0	0	0	0	179
Powerlines	10	0	0	0	0	10
Pipelines	7	0	0	0	0	7
Bridges	0	2	3	0	1	6
Tunnels	0	0	0	0	0	0
Total	239	35	5	1	2	282

Table 3.6.5-5 Span Lengths (m) for LA-San Leandro Alternative Highway Route

	Default	26-100 (m)	101-200 (m)	201-300 (m)	> 300 (m)	Total
Underpasses	86	30	1	1	0	118
Overpasses	83	40	45	10	0	178
Powerlines	27	0	0	0	0	27
Pipelines	15	0	0	0	0	15
Bridges	0	0	1	2	0	3
Tunnels	0	0	0	0	0	0
Total	211	70	47	13	0	341

Table 3.6.5-6 Span Lengths (m) for LA-Richmond Alternative Railroad Route

	Default	26-100 (m)	101-200 (m)	201-300 (m)	> 300 (m)	Total
Underpasses	40	25	0	0	0	65
Overpasses	43	42	6	1	1	93
Crossings	224	0	0	0	0	224
Powerlines	33	0	0	0	0	33
Pipelines	4	0	0	0	0	4
Bridges	0	6	3	3	0	12
Tunnels	0	4	9	1	2	16
Total	344	77	18	5	3	437

3.6.6 Independent Routes

Route descriptions for the independent routes on the three detailed corridors are given along with route trip times, average speeds, and non-default span requirements. Alignment selection for independent routes used existing highway and rail rights-of-way to exit and enter urban areas near station stops. This rule was established because of the high cost of land acquisition in downtown areas. Once outside urban areas maglev guideways were free to leave the right-of-way and seek gentler alignments.

3.6.6.1 Tappan Zee Bridge to Syracuse Independent Route

The New York independent route starts at the Tappan Zee Bridge and heads north following the centerline of the New York Thruway. At Suffern, the guideway leaves the centerline and travels along the Thruway. To accommodate the large radius curves associated with the maglev guideway the route passes over the Thruway several times on its trip towards Albany. In Albany, a station stop is made just south of city limits. The route then heads west along the Thruway and switches to a westerly heading along route 20 past Carlisle. The route heads northwest past Van Hornesville and Clayville and joins the railroad. The route follows the railroad north to the station

stop in Utica. The route follows route 5 out of Utica and travels parallel to it to the final station in Syracuse.

Table 3.6.6-1 Tappan Zee Bridge - Syracuse Independent Route Information

	h:mm-m/s-%	26-100 (m)	101-200 (m)	201-300 (m)	> 300 (m)
Trip Time	0:59				
Average Speed	112.88 m/s				
ROW Utilization	6.8%				
Non-Default Spans		30	2	1	2

3.6.6.2 Detroit - Chicago Independent Route

The route starts in Dearborn and follows the Norfolk and Western railroad out of Detroit. The route breaks off the railroad, runs past the Detroit airport, and travels south of Ford Lake to the first station stop in Ann Arbor. The route continues west north of Gilletts Lake along I-94 to the second station at Kalamazoo. The route continues west, then southwest, past Benton Harbor and south of Michigan City. In Gary, Indiana the route follows the Conrail line and travels along the railroad to the final station in Chicago.

Table 3.6.6-2 Detroit - Chicago Independent Route Information

	h:mm-m/s-%	26-100m	101-200m	201-300m	> 300m
Trip Time	0:53				
Average Speed	124.28 m/s				
ROW Utilization	13.2%				
Non-Default Spans		18	1	1	1

3.6.6.3 Los Angeles - San Francisco Independent Route

The route starts in Elsyian Park and travels the I-5 centerline out of the urban area. Once outside Los Angeles the route exits the right-of-way and follows a path similar to I-5 with larger radius curves through the mountain passes. After traversing through the mountains the route runs parallel to I-5 and heads northwest and stops at Buttonwillow and Santa Nella stations just off the I-5 roadway. The route continues northwest after Santa Nella but cuts across I-5 and travels through Corral Hollow and passes south of Livermore before picking up the I-580 centerline to the final station in San Leandro.

Table 3.6.6-3 Los Angeles - San Francisco Independent Route Information

	h:mm-m/s-%	26-100m	101-200m	201-300m	> 300m
Trip Time	1:22				
Average Speed	117.99 m/s				
ROW Utilization	8.9%				
Non-Default Spans		20	4	0	0

3.6.7 Judicious Use of the Right-of-Way

The alignments of the existing highway and railroad networks are generally contained in areas where the systems could handle the surrounding terrain. These areas are known as transportation corridors and are generally adjacent to population centers. These corridors were considered the shortest path routes based on the technology available at the time of implementation. However, the technology breakthroughs for Maglev in speed, superelevation, grade climbing, and elevated structures will allow Maglev to tackle some of the rough terrain presently avoided by the current transportation systems.

The selection of independent route alignments were generally along these transportation corridors with two notable exceptions. In New York, the highway and railroad networks travel from Albany west via the Mohawk River to service the cities of Schenectady, Amsterdam, and Utica. The potential Maglev line was only required to service Utica, so a true independent section was designed through the mountains as a more direct route to Utica. Maglev's grade climbing ability and elevated structures used to minimize grade and vertical curvatures made this alignment possible. In California, a more direct alignment was achieved between Santa Nella and San Francisco by using the 12-meter column heights to modulate grade in the Diablo mountain range. The result of both deviations from existing transportation corridors was a shortened route length, a straighter alignment, and a reduced trip time.

3.7 ADDITIONAL CORRIDOR ANALYSIS

3.7.1 Introduction

The results of the previous subsections provide trip times and vehicle speeds for the three detailed corridors. An estimation method is developed to approximate trip times to extend the previous results along 20 additional corridors specified by the government to represent maglev routes. Trip-time approximations are made for centerline, excursion, and independent routes. Estimates are also made for structural span and land requirements.

3.7.2 Methodology

The additional 20 corridors specified for analysis are listed in Table 2-2. Route alignment information was needed for the corridors to perform analyses for vehicle speeds and trip times. The sheer volume of maps needed to analyze the 20 corridors made it infeasible to use the 7.5-minute maps used for subsection 3.4. Therefore, a methodology was developed to automate the process of gathering route alignment information using scanned 1:250,000 scale topographic map images and overlaying them onto an electronic terrain database.

Route alignments and corridor trip times for the three detailed corridors were redone at the 1:250,000-scale to provide a baseline comparison between the two methodologies. From the images, highway and railroad centerline routes were identified and digitized using the map images to create route segments containing information on length, radius, and elevations. Alignment files were created and run through the route analysis program to calculate a trip time (TT_{250CL}) and route length (RL_{250CL}) for each centerline route. These alignments were divided into shorter routes defined by the alignments between station stops. Sixteen of these shorter routes were used to perform a regression analysis which produced equations for estimation of travel times and route lengths at the 1:24,000 scale. The results of the regression are listed below.

$$TT_{24CL} = 1.12*TT_{250CL} + 0.2$$
$$RL_{24CL} = 1.01*RL_{250CL} + 0.6$$

where TT_{24CL} = the estimated centerline trip time (in minutes) at 1:24,000 scale
TT_{250CL} = the trip time calculated using centerline alignment at the 1:250,000 scale
RL_{24CL} = the estimated centerline route length (in kilometers) at 1:24,000 scale
RL_{250CL} = the route length calculated using centerline at the 1:250,000 scale

Route lengths correlated very well between the two scales, differing on the order of one percent. This result verifies that differences in trip time between the two scales were related to the average speed along the route which is directly correlated to the measurements of individual segments. Trip-time analysis revealed a 12 percent difference between the 1:24,000 and 1:250,000 scales. This difference can be attributed to the fact that a certain amount of information on individual segments was lost with the smaller scale maps. This is especially true for curves along the route which are aggregated at the smaller scale. The result is smoother alignment definition for routes and ultimately a shorter trip-time result from the route analysis program.

Similar analyses was performed for the judicious excursion and independent routes. In the case of judicious excursions from the existing right-of-way, many departures at the 1:24,000 scale were identified as a series of segments that could be avoided through leaving the right-of-way. This excursion criteria has a similar effect on guideway alignment as the smaller scale aggregation. A regression analysis established the following equations.

$$TT_{24Exc} = 1.04*TT_{250CL} + 0.4$$
$$RL_{24Exc} = 0.99*RL_{250CL} + 3.2$$

where TT_{24Exc} = the estimated excursion route trip time (in minutes) at the 1:24,000 scale
TT_{250CL} = the trip time calculated using centerline alignment at the 1:250,000 scale
RL_{24Exc} = the estimated excursion route length (in kilometers) at the 1:24,000 scale
RL_{250CL} = the route length calculated using centerline at the 1:250,000 scale

Independent routes are characterized by the straightening of alignments to take advantage of the high-speed operation of Maglev technology. Route alignments digitized at the 1:250,000 are good estimates for independent routes because short-radius curves (and consecutive curves) would be avoided in the independent route case because of their speed-limiting effects. Therefore, the independent route trip times reflect trip times calculated using 1:250,000 digitized data.

3.7.3 Results for Additional Corridors

3.7.3.1 Centerline, Excursion, and Independent Trip Time Results

Table 3.7.3.1-1 lists the estimated trip times for the additional corridors based on the estimation equations in subsection 3.7.2. Intermediate station stops were used for these corridors only as noted in Table 2-2. This analysis used only a maximum speed of 150 m/s because the detailed analysis showed small trip-time differentials with respect to different maximum speeds.

Table 3.7.3.1-1 Estimated Trip Times for Additional Corridors

Corridor	Highway Centerline Trip Time (h:mm/km)	Highway Excursion Trip Time (h:mm/km)	Railroad Centerline Trip Time (h:mm/km)	Railroad Excursion Trip Time (h:mm/km)	Independent Route Trip Time (h:mm/km)
	TT&RL24CL	TT&RL24Exc	TT&RL24CL	TT&RL24Exc	TT&RL250I
Northeast					
Boston to Hartford	0:31 / 145.0	0:30 / 144.8	0:50 / 192.5	0:47 / 191.3	0:19 / 142.7
Hartford to New York City	0:44 / 176.3	0:41 / 175.5	0:44 / 184.4	0:41 / 183.4	0:25 / 170.0
NewYorkCity to Philadelphia	0:36 / 176.7	0:34 / 175.8	0:33 / 162.7	0:31 / 162.1	0:26 / 175.8
Philadelphia to Wilmington	0:10 / 52.1	0:10 / 53.7	0:11 / 42.0	0:10 / 43.8	0:07 / 41.3
Wilmington to Baltimore	0:23 / 123.8	0:22 / 124.0	0:22 / 108.7	0:20 / 109.1	0:12 / 95.9
Baltimore to Washington	0:14 / 55.0	0:14 / 56.5	0:14 / 59.2	0:12 / 60.6	0:10 / 62.9
Syracuse-Rochester-Buffalo	0:39 / 221.8	0:37 / 220.0	0:48 / 229.9	0:45 / 227.9	0:32 / 220.7
Buffalo to Niagara Falls	0:10 / 34.9	0:09 / 36.9	0:10 / 39.0	0:09 / 40.8	0:06 / 40.3
Mid-West					
Chicago to Milwaukee	0:32 / 143.0	0:31 / 142.8	0:28 / 144.0	0:26 / 143.8	0:17 / 134.6
Milwaukee to Madison	0:25 / 121.8	0:23 / 122.0	0:22 / 127.9	0:20 / 127.9	0:20 / 121.9
Southwest					
Dallas to Houston	1:05 / 381.0	1:01 / 376.0	1:16 / 383.0	1:10 / 378.1	0:43 / 366.8
Dallas to Waco	0:25 / 142.8	0:23 / 142.6	0:31 / 148.8	0:30 / 148.4	0:17 / 143.7
Waco to Austin	0:28 / 158.3	0:26 / 157.7	0:38 / 184.8	0:36 / 183.8	0:19 / 151.4
Austin to San Antonio	0:22 / 127.6	0:21 / 127.7	0:25 / 128.1	0:23 / 128.2	0:14 / 111.6
Houston to Austin	0:51 / 257.8	0:47 / 255.3	1:02 / 268.6	0:58 / 265.9	0:27 / 230.0
West					
Los Angeles to Las Vegas	1:21 / 449.9	1:15 / 443.6	1:14 / 331.2	1:09 / 327.2	0:50 / 411.7
Los Angeles to San Diego	0:39 / 186.1	0:36 / 185.0	0:38 / 198.7	0:36 / 197.3	0:26 / 187.9
Seattle-Tacoma-Oympia-Portland	0:58 / 288.8	0:53 / 285.7	1:22 / 313.2	1:16 / 309.6	0:46 / 271.6
Southeast					
Miami-WPalmB-FtLaud-Orlando	1:02 / 357.6	0:58 / 353.2	1:11 / 390.5	1:07 / 385.3	0:42 / 324.4
Orlando to Tampa	0:22 / 131.2	0:20 / 131.2	0:27 / 148.1	0:25 / 147.8	0:14 / 125.4

3.7.3.2 Results for Estimated Land Requirements and Span Lengths

Estimates of land requirement for excursion routes is provided in Table 3.7.3.2-1. The 20 corridors are divided into groups based on terrain types: rough, medium, and flat. This method is used because a correlation was found between the 'roughness' of terrain and the amount of judicious excursions performed. Terrain roughness was measured by the average grade and bend angle along the route. The three detailed corridors were again used as sample data divided into sections based on station stops. A factor was derived for each terrain type (4%-Flat, 7%-Medium, and 10%-Rough) to represent the percentage of the judicious excursion performed along a given

route as a function of the route length. This total excursion length is then multiplied by the default right-of-way width (18.3 meters) to determine the total area of guideway needed outside the existing right-of-way.

Determining additional land requirements for Maglev corridors is very site dependent. Considerations need to be made not only for the terrain but physical and environmental constraints as well. For example, the New York railroad route between Yonkers and Albany had many tight radius curves in the alignment. However, the railroad was built between the mountainside and the Hudson River, and land was not readily available for excursions.

Table 3.7.3.2-1 Estimated Land Requirements for Excursion Routes

Corridor	Terrain Type	Estimated Land for Highway (m^2)	Estimated Land for Railroad (m^2)
Northeast			
Boston to Hartford	Medium	183200	243400
Hartford to New York City	Medium	222900	233100
New York City to Philadelphia	Medium	223300	205600
Philadelphia to Wilmington	Medium	65300	52500
Wilmington to Baltimore	Medium	156300	137000
Baltimore to Washington	Medium	69000	74300
Syracuse-Rochester-Buffalo	Medium	280500	290800
Buffalo to Niagara Falls	Medium	43600	48700
Mid-West			
Chicago to Milwaukee	Flat	103200	103900
Milwaukee to Madison	Medium	153700	161400
Southwest			
Dallas to Houston	Flat	275700	277200
Dallas to Waco	Flat	103000	107400
Waco to Austin	Flat	114300	133500
Austin to San Antonio	Flat	92000	92400
Houston to Austin	Flat	186400	194200
West			
Los Angeles to Las Vegas	Rough	814086	598972
Los Angeles to San Diego	Medium	191500	251200
Seattle-Tacoma-Oympia-Portland	Rough	522207	566462
Southeast			
Miami-W.Palm Beach-Ft Laud-Orlando	Flat	258800	282600
Orlando to Tampa	Flat	94700	106900

Estimates for non-default span lengths (lengths greater than 25 meters) are tabulated from topographic maps and given for highway, railroad, and independent routes in Tables 3.7.3.2-2 to 3.7.3.2-4. Tunnel requirements are included in the tabulation of non-default structures.

Table 3.7.3.2-2 Estimated Non-Default Span Lengths (m) for Highway Routes

Corridor	26-100	101-200	201-300	> 300	Total
Northeast					
Boston to Hartford	13	0	0	0	13
Hartford to New York City	6	0	0	0	6
New York City to Philadelphia	7	0	0	0	7
Philadelphia to Wilmington	3	0	0	1	4
Wilmington to Baltimore	9	1	0	0	10
Baltimore to Washington	1	0	0	0	1
Syracuse-Rochester-Buffalo	15	0	0	0	15
Buffalo to Niagara Falls	5	0	0	0	5
Mid-West					
Chicago to Milwaukee	7	0	0	0	7
Milwaukee to Madison	4	0	0	0	4
Southwest					
Dallas to Houston	10	1	0	0	11
Dallas to Waco	5	0	0	0	5
Waco to Austin	7	0	0	0	7
Austin to San Antonio	4	0	0	0	4
Houston to Austin	5	0	0	0	5
West					
Los Angeles to Las Vegas	23	1	0	0	24
Los Angeles to San Diego	18	0	0	0	18
Seattle-Tacoma-Oympia-Portland	20	2	0	1	23
Southeast					
Miami-WPalmB-FtLaud-Orlando	13	0	0	0	13
Orlando to Tampa	2	0	0	0	2

Table 3.7.3.2-3 Estimated Non-Default Span Lengths (m) for Railroad Routes

Corridor	26-100	101-200	201-300	> 300	Total
Northeast					
Boston to Hartford	6	2	0	1	9
Hartford to New York City	15	0	0	0	15
New York City to Philadelphia	9	1	0	1	11
Philadelphia to Wilmington	4	1	1	0	6
Wilmington to Baltimore	8	0	0	2	10
Baltimore to Washington	5	0	0	0	5
Syracuse-Rochester-Buffalo	13	0	0	0	13
Buffalo to Niagara Falls	4	0	1	1	6
Mid-West					
Chicago to Milwaukee	7	0	0	0	7
Milwaukee to Madison	3	0	0	0	3
Southwest					
Dallas to Houston	13	0	0	0	13
Dallas to Waco	5	0	0	0	5
Waco to Austin	3	0	0	0	3
Austin to San Antonio	7	0	0	0	7
Houston to Austin	6	0	0	0	6
West					
Los Angeles to Las Vegas	8	0	0	0	8
Los Angeles to San Diego	15	0	0	0	15
Seattle-Tacoma-Oympia-Portland	14	0	0	0	14
Southeast					
Miami-WPalmB-FtLaud-Orlando	6	0	0	0	6
Orlando to Tampa	6	0	0	0	6

Table 3.7.3.2-4 Estimated Non-Default Span Lengths (m) for Independent Routes

Corridor	26-100	101-200	201-300	> 300	Total
Northeast					
Boston to Hartford	11	0	0	0	11
Hartford to New York City	10	2	0	0	12
New York City to Philadelphia	21	0	0	2	23
Philadelphia to Wilmington	6	0	0	1	7
Wilmington to Baltimore	7	0	0	1	8
Baltimore to Washington	6	0	0	1	7
Syracuse-Rochester-Buffalo	7	0	0	0	7
Buffalo to Niagara Falls	3	0	0	0	3
Mid-West					
Chicago to Milwaukee	7	0	0	0	7
Milwaukee to Madison	7	0	0	0	7
Southwest					
Dallas to Houston	11	1	0	0	12
Dallas to Waco	2	0	0	0	2
Waco to Austin	6	0	0	0	6
Austin to San Antonio	3	0	0	0	3
Houston to Austin	4	0	0	0	4
West					
Los Angeles to Las Vegas	9	0	0	0	9
Los Angeles to San Diego	12	0	0	0	12
Seattle-Tacoma-Oympia-Portland	25	1	0	1	27
Southeast					
Miami-WPalmB-FtLaud-Orlando	11	0	0	0	11
Orlando to Tampa	7	0	0	0	7

3.8 SPAN LENGTHS

3.8.1 Introduction

Under normal guideway conditions spacing between guideway pillars will measure approximately 25 meters. However, circumstances will occur when the default span configuration cannot be used. For these occasions, alternative structures must be identified and chosen based on cost and structural criteria.

3.8.2 Methodology

Engineering analyses of guideway structures were reviewed, including bridge design research and maglev design research. Recommended alternatives to cases where the default span length must be exceeded were developed based on the analysis of cost and structural elements. The following assumptions were used in the analysis.

1) The structures are examined for dual guideway, with a pillar height of 12 meters.
2) Vehicles will travel at a maximum speed of 150 meters per second.
3) Normal guideway spans will be 25 meters.
4) Minimal site impact will be required. Vegetation will be cleared within the right-of-way.
5) No ground-level maintenance will be required. All maintenance to the guideways will be accomplished from the top of the guideways.
6) Guideway support structures will be designed to minimize damage occurring from seismic activity.
7) Per mile guideway costs do not include mechanical or electrical portions of the guideway.
7) Soil conditions permit the use of cast-in-place concrete foundations.
8) The guideway support structure refers to the foundation and pier system under the guideway spans. The superstructure refers to the span and structures above the foundation and piers.
9) An assumed width of 3.7 meters is used for single guideway.
10) Cost estimates are done in 1992 dollars.

3.8.3 Default Span Length

The most suitable and economical type of structure for the default span is a rigid-beam structure. The supporting structure for a rigid-beam guideway structure is either grounded in footers or pilings. In wetland areas, pilings can be driven down to load-bearing geological foundations. These pilings are topped with concrete pile caps to support the pillars and guideway. In dryer, upland areas, reinforced concrete spread footers are installed as foundations for the cast-in-place pillars and guideway. Both the concrete pile caps and spread footers are buried slightly below the surface of the water or land to allow surface water sheet flow and wildlife to pass unobstructed beneath the guideway. Figure 3.8.3-1 shows an example of the default span system.

upland areas, reinforced concrete spread footers are installed as foundations for the cast-in-place pillars and guideway. Both the concrete pile caps and spread footers are buried slightly below the surface of the water or land to allow surface water sheet flow and wildlife to pass unobstructed beneath the guideway.

Figure 3.8.3-1 shows an example of the default span system.

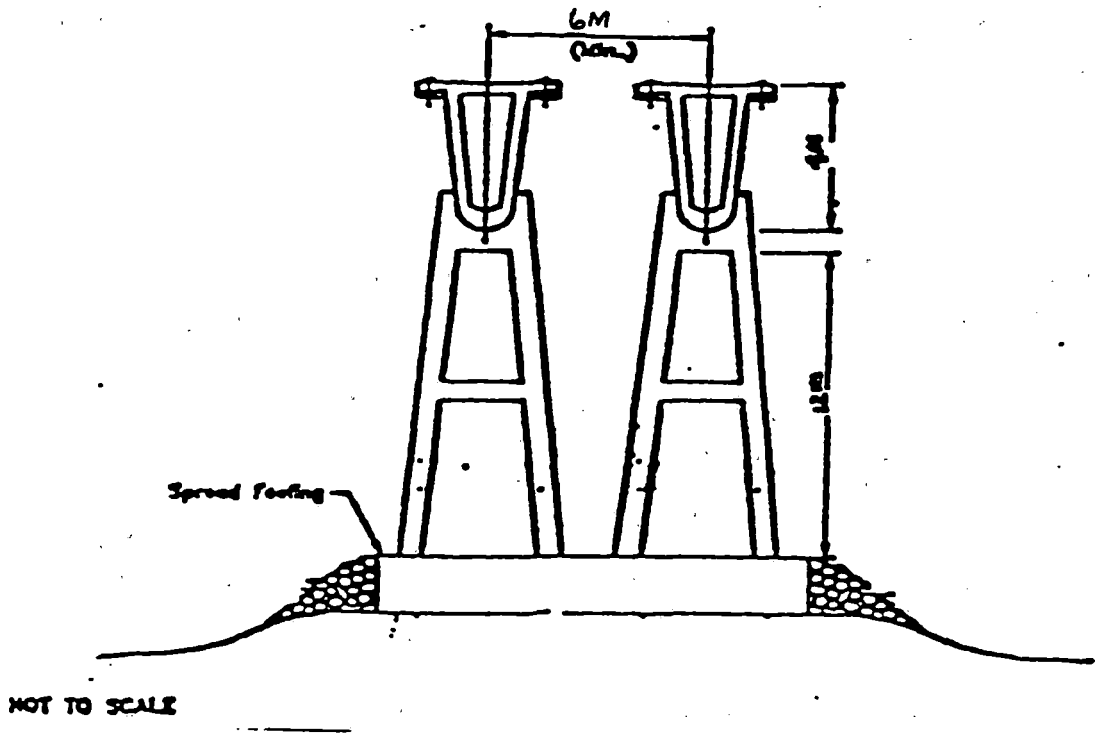

Figure 3.8.3-1 Default Span System

Three parameters were identified as affecting the substructure design and cost: the degree of restraint (connection) between the beam and pier, the configuration of the pier column, and the configuration of the foundation. A rigid connection between the superstructure and supporting structure was chosen because it behaves as a single unit, which enhances the stability of the structure and provides better resistance against wind and earthquake loads.

The cost estimate is based on a 12 meter high pier, supporting a normal 25-meter default span. A circular cast-in-place pier is used because it is the least expensive type of pier. The trapezoidal pier is usually the configuration of choice because it is considered more aesthetically pleasing, however, labor and form costs of the circular pier are lower than that of the trapezoidal pier. The cast-in-place pier is chosen because transportation and erection costs are 30% less than the pre-cast pier. Costs are based on estimated quantities and unit prices. Unit prices were derived by considering factors such as materials, labor rates, equipment, transportation, and crane costs.

It has been assumed that soil conditions permit the use of a cast-in-place concrete foundation. This foundation type is commonly used for good soil conditions. If soil conditions are poor, a pile foundation may be required. The additional cost of employing a pile foundation may increase the cost by 35% per pier, due to additional concrete costs and dewatering requirements.

Research shows that construction costs increase with increasing span length. As the span length increases, the cost of the superstructure, which represents 70% of the total structural cost, increases considerably faster than the potential cost savings for the pier and foundation on a linear meter basis. Analysis shows that the optimum span distance for the default structure is 25 meters. Table 3.8.3-1 has estimated costs (reference 11) for the default structure at $12.5 M per guideway mile, or $7,760 per meter of span length.

Table 3.8.3-1 Cost Estimate for Default Span Length (1992 Dollars)

Description	Dollars / Kilometer	Dollars / Mile
Footing	418,500	725,000
Form/Pour Concrete Columns	8,660	15,000
Install Bearings	158,040	273,600
Prestressed Concrete Guideway	5,830,000	10,100,000
Other costs	791,700	1,371,500
Total Cost / Unit Length Guideway	7,207,300	12,485,100

Footing costs include the costs of clearing land, earth and structural excavation, and pouring of the concrete footing. Prestressed concrete guideway costs include the cost of materials and construction of the guideway, jack/shim for alignment, installation of the glide steel pads and vertical guide plates, and final testing and calibration. Prestressed concrete guideway costs do not include power and propulsion elements. Other construction costs include dewatering, vegetation control, surveying, the mobilization and demobilization of equipment. Mechanical and electrical guideway components are not included in the estimate.

3.8.4 Alternative Span Structures

Where guideways cross interchanges, rivers, and other topographical structures, alternatives are needed to augment the basic 25 meter span length. A number of different bridge types were considered:

Rigid-Beam Bridges

Rigid-beam bridges, shown in Figure 3.8.4-1, are the most common bridge type built in the United States. On short-span to medium-span bridges (6 meters to 30 meters), it is the simplest and most economical structure to build. Typically, I-shaped steel beams are laid across the abutments on suitable supports, and the beams are decked with a reinforced concrete slab about 20 cm thick. Structures can be lengthened to 60 meters by using a 2-span continuous girder, however, the span distance between pillars is still 6 meters to 30 meters.

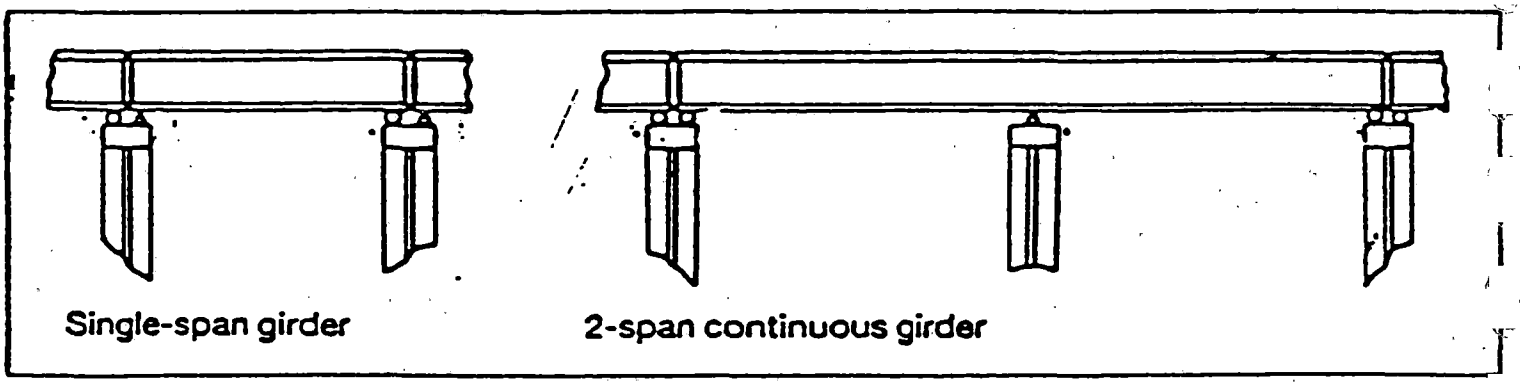

Figure 3.8.4-1 Rigid-Beam Structures

Arch Bridges

Arch bridges can easily span distances from 30 to 300 meters, and are essentially the opposite of suspension bridges. Where suspension cables hang freely from supporting towers, the arch curves rigidly upward from its abutments. While the suspension cable tends to pull its anchorages together, the arch tends to push its abutments apart. Therefore arches must be made of materials that can withstand compression. Arch bridges can be made of bricks or stone and are held together by the compressive forces of the arch. The roadway may be suspended below the arch on vertical cables or supported above it on piers. The cost of span has been estimated at $11,950 per meter. An example of an arch bridge is shown in Figure 3.8.4-2.

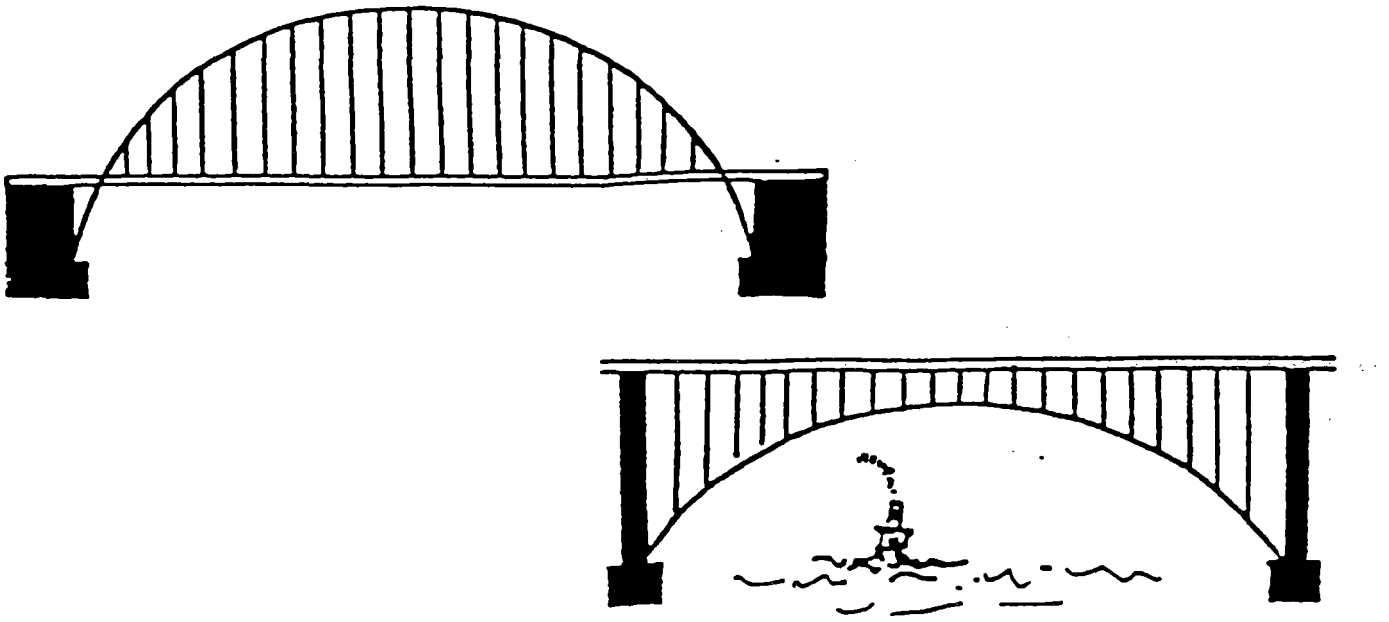

Figure 3.8.4-2 Arch Bridges

Cable-Stayed Bridges

Cable-stayed systems are being increasingly used for spans from 100 to 300 meters. If multiple stays (more than 6 cables per span) are used, these bridges are more economical than suspension bridges for spans up to 800 meters.

Cable-stayed bridges present a space system, consisting of stiffening girders, steel or concrete deck, and supporting parts as towers acting in compression and inclined cables in tension. By their structural behavior cable-stayed systems fit between the girder-type and suspension-type bridges. The main structural characteristic of this system is the integral action of the stiffening girders and prestressed or post-tensioned inclined cables, which run from the tower tops down to the anchor points at the stiffening girders. Horizontal compressive forces due to the cable action are taken by the girders and no massive anchorages are required. The deck is supported directly from the towers with stay cables, differing from suspension bridges which support the deck with loosely hung main cables with vertical suspenders. The result is a significantly stiffer structure and less deflections which is desired for maglev systems.

Cable-stayed bridges are geometrically unchangeable under any load position on the bridge, and all cables are always in a state of tension. This characteristic permits them to be built from relatively light, flexible cables. The most important characteristic of such a three-dimensional bridge is the full participation of the transverse structural parts in the work of the main structure in the longitudinal direction. This means a considerable increase in the moment of inertia of the construction, which permits a reduction in the depth of the girders and consequent savings in steel. The cost of span has been estimated at $13,930 per meter. An example is shown in Figure 3.8.4-3.

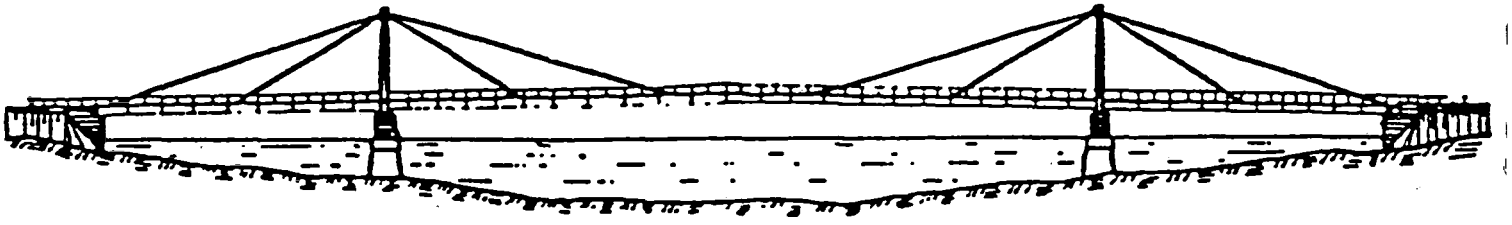

Figure 3.8.4-3 Cable-Stayed Bridge

Suspension Bridges

Suspension bridges, shown in Figure 3.8.4-4, can span distances from 300 to 1500 meters. The supporting members of a suspension bridge are continuous flexible cables, with each cable anchored at both ends. Cables hang freely from supporting towers and tends to pull the anchorages together. The cost of suspended spans has been estimated at $16,157 per meter.

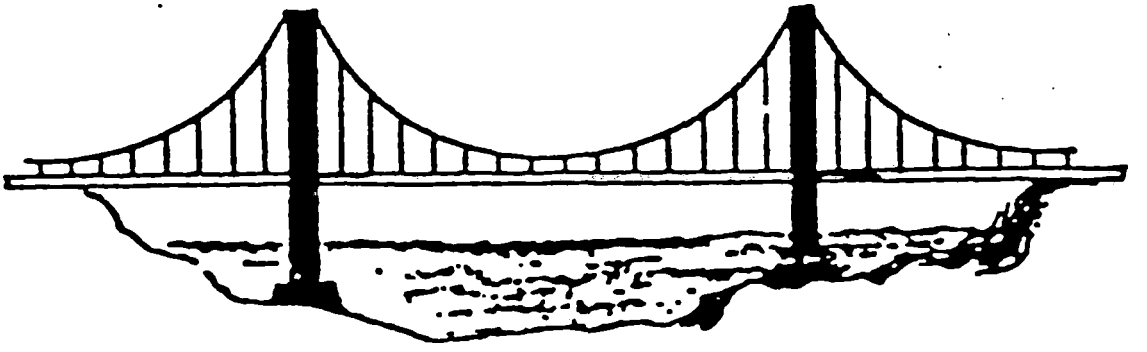

Figure 3.8.4-4 Suspension Bridge

Table 3.8.4-1 gives the range of length for each viable span alternative and an estimate for cost per meter of span length.

Table 3.8.4-1 Optimal Span Ranges and Costs for Various Bridge Types

Bridge Type	Span Range	Cost Per Meter ($1992)
Rigid Beam Bridge	6 to 30 meters for single span girder 30 to 60 meters for 2-span continuous girder	$7,760
Arch Bridge	30 to 300 meters	$11,950
Cable-Stayed Bridge	100 to 800 meters	$13,930
Suspension Bridge	300 to 1500 meters	$16,157

3.8.5 Highway Span

The final structural alternative for span lengths is a multiple span structure in which the pillars straddles the highway. In this configuration the length between pillar structure remains the default of 25 meters, however, on top of the two pillars lays a superstructure which spans the width of the highway. A cost estimate for this structure is given in Table 3.8.5-1 assuming a total structural length of 200 meters (8 pillar sets) supporting a double-elevated guideway. Cost categories are similar to the ones specified in Table 3.8.3-1 above. An example is shown in Figure 3.8.5-1. The cost per meter is $9,436.

Table 3.8.5-1 Cost Estimate for System Over Highway System (200 meters)

Description	1992 Dollars
Footing	254,400
Form/Pour Concrete Columns	219,000
Install Bearings	60,800
Prestressed Concrete Guideway	1,157,000
Other costs	196,400
Total Structure Cost	1,887,200

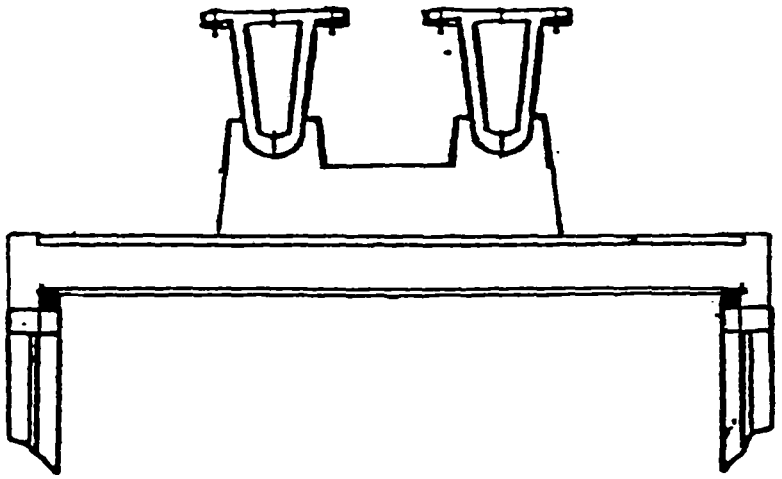

Figure 3.8.5-1 Structure Spanning Highway

3.9 INFORMATION SYNTHESIS

The use of existing rights-of-way (ROW) is assessed for maglev systems by estimating trip times and land acquisition requirements for potential maglev corridors while meeting passenger comfort limits. Right-of-way excursions improve trip time but incur a cost for purchasing land. This final report documents findings of the eight tasks in establishing right-of-way feasibility by examining three city-pair corridors in detail and developing an approximation method for estimating route length and travel times in 20 additional city-pair corridor portions and 21 new corridors. The use of routes independent of existing railroad or highway rights-of-way have trip time advantages and significantly reduce the need for aggressive guideway geometries on intercity corridors.

Selection of the appropriate alignment is determined by many corridor specific issues. Use of existing intercity rights-of-way may be appropriate for parts of routes on a corridor-specific basis and for urban penetration where vehicle speeds are likely to be reduced by policy due to noise and safety considerations, and where land acquisition costs are high. Detailed aspects of available rights-of-way, land acquisition costs, geotechnical issues, land use, and population centers must be examined in more detail on a specific corridor basis before the final maglev alignment can be chosen. Other issues affecting the viability of maglev transportation include ridership, fare structures, and competition which are outside the scope of this research.

The examination of new and existing ROW for use in siting maglev guideway alignments has yielded quantitative evidence from which the advantages and disadvantages of the alternatives may be assessed. The candidate city-pairs examined in this study are linked by existing highway and railroad rights-of-way. The existing rights-of-way offer the following advantages:

- Highway land is owned publicly and access rights could be granted by government entities to a maglev developer for minimal cost.

- Use of an existing rights-of-way will require less time and expense for environmental impact studies (EIS), expedite government approvals, and reduce overall risk and uncertainty associated with the development project compared to using new ROW.

- Existing rights-of-way are especially useful in dense urban areas where land acquisition for alternative routes is prohibitively expensive.

The disadvantages of using existing ROW include:

- The incompatibility of high speed transportation with existing ROW alignment because frequent short radius curves limit vehicle speeds.

- Significant increases in average speed are achieved through mitigating unbalanced lateral accelerations in short radius curves at the expense of passenger comfort through increased bank angles (up to 30 degrees), roll rates (as high as 10 degrees per second), and vertical accelerations (up to 1.3g's).

- Safety risks of shared ROW are mitigated using raised guideway, but new risks to the existing mode from guideway crossings, possible collisions with columns, falling debris, and startle effects from sighting high speed vehicles are added.

- Increased column heights (~12 meters) required throughout the ROW because of relatively frequent overpasses and vertical curvature limits imposed by high speed in conjunction with comfort constraints add significantly to guideway costs.

As an alternative to the use of existing ROW, independent routes were examined in each of the 23 city-pair corridors that were constrained only by terrain and population centers. Advantage was taken of existing ROW for penetrating urban areas. The advantages for these routes include:

- The independent alignment includes longer straight segments and larger radius curved segments such that speeds are not limited very often, allowing sustained high speeds for long distances, and high average speeds over the entire route.

- Higher average speeds combined with generally shorter routes result in significantly reduced trip times that compare favorably with airline flight times.

- The infrequency of speed limiting curved segments allows conservative geometry (12 degree bank angles) and comfort limits (5 degree per second roll rates and 1.2 g's vertical acceleration) to be used with little increase to travel times.

- Competitive travel times, together with familiar comfort conditions, will maximize passenger acceptance and attract ridership.

- Savings in guideway construction costs accrue through shorter routes, less average guideway heights, and less severe guideway geometries.

However, there are disadvantages:

- Additional expenses are incurred for land that must be surveyed, acquired and cleared.
- Complete environmental impact studies are required for all new proposed rights-of-way, and they will introduce risks and uncertainties into the overall project as well as contribute time and expense to schedules and budgets.
- Straighter routes require more special construction such as tunneling, cut and fill, bridge structures, and structure relocation.

Alignment geometries require aggressive superelevation, roll rate and vertical acceleration comfort limits to stay within the existing intercity rights-of-way. Comfort limited speed on existing alignment curvatures of 2000 meters or less can be overcome using superelevations of 30 degrees or more to control lateral loads, downward vertical accelerations of 1.3g or greater at high speed, and roll rates of 10 degrees per second or more to shorten transition spirals to stay within right-of-way constraints. These aggressive alignment geometries result in intercity trip time improvements on the order of 30 percent from more conservative approaches which use 12 degrees superelevation, 1.2g maximum downward vertical acceleration, and 5 degrees per second roll rate limits. However, passengers are subjected to comfort attributes unprecedented in previously implemented public transportation systems.

Short-radius curvature exhibited by the existing intercity transportation alignments can be reduced significantly when the constraint to use the existing right-of-way is removed. Topographic and land use considerations still require alignment curvature, but greater flexibility is available in eliminating the extensive use of short-radius curves. Independent route alignments examined in this study were on the order of 10 percent shorter in overall length and trip times averaged 25 percent less than the best right-of-way constrained routes in each corridor. Trip times are only minimally improved (about 3 percent) when aggressive comfort limits are used. Elimination of significant alignment curvature permits high average vehicle speed and the preservation of more commonly experienced passenger comfort attributes.

Representative Corridor Analysis In the subsequent discussion, the New York City to Syracuse corridor is used as an example to compare maglev travel times using different alignment parameters. Extra trip time runs are included to extend the lateral unbalanced comfort limit to 0.15g and examine bank angles of 24 and 30 degrees. The bulk of the analysis performed in this corridor included local service with station stops in Albany and Utica. Express runs saved about

six minutes over local trip times for each alignment due by eliminating two minute station dwell times and approach deceleration and departure acceleration at each intermediate station stop.

The existing right-of-way alignments do not benefit significantly from maximum vehicle speeds above 110 m/s unless the most aggressive comfort limits are invoked. This is because the alignment curvature constrains the average speed to meet comfort limits. This is illustrated in Figure 3.9-1 for the highway centerline route. Although comfort increases are shown for unbalanced lateral load and total bank angle, it is the bank angle that most effects the increase in average speed and reduced trip times. The sensitivity of average speed to changes in unbalanced lateral load limits is much reduced at the higher bank angles.

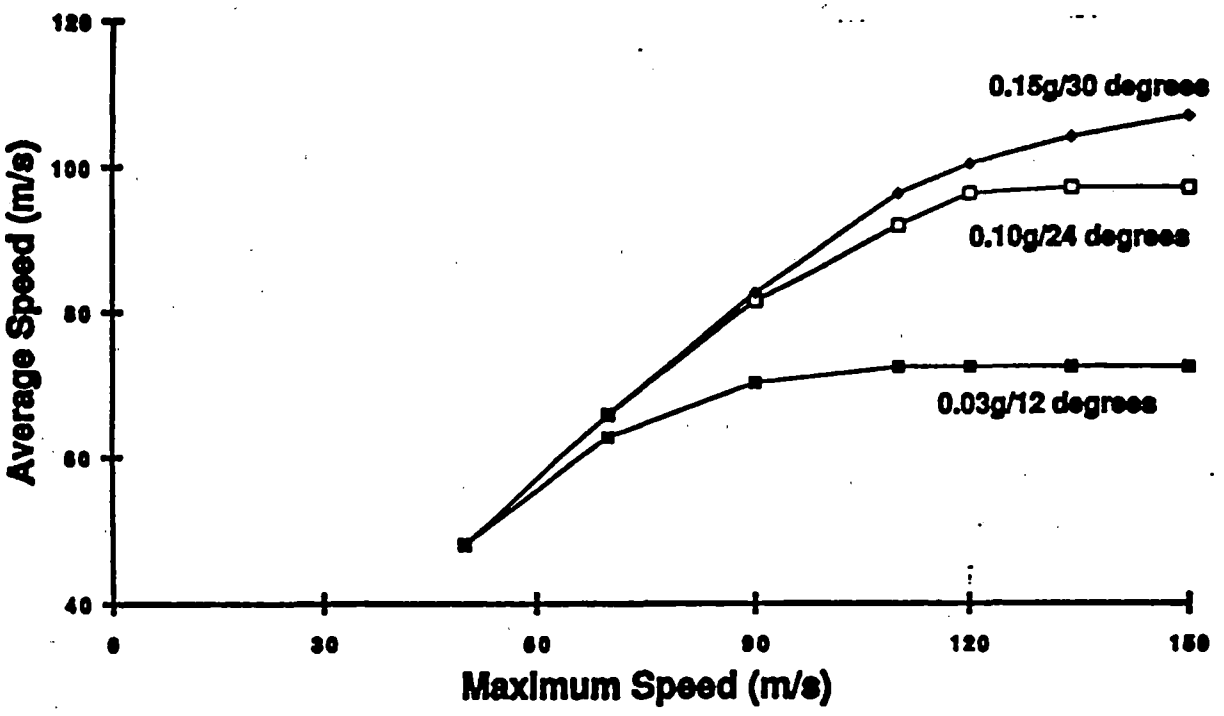

Figure 3.9-1 Average Speed Saturation for Comfort Constrained Alignment

Five route alignments were developed for the New York City to Syracuse corridor. These included the existing highway and railroad rights-of-way, judicious excursion routes for each, and a route independent of ROW constraints. Table 3.9-1 includes the trip time and average speed for all five routes and compares trip times and average speeds for varying comfort constraints.

Table 3.9-1 New York to Syracuse Travel Times and Average Speeds

Superelevation	12 degrees			24 degrees			30 degrees		
Unbalanced Lateral Load	0.03g	0.10g	0.15g	0.03g	0.10g	0.15g	0.03g	0.10g	0.15g
	h:mm / m/s	h:mm / m/s	h:mm / m/s	h:mm / m/s	h:mm / m/s	h:mm / m/s	h:mm / m/s	h:mm / m/s	h:mm / m/s
Highway ROW									
Centerline (425.8 km)									
150 m/s	1:38 / 72.79	1:29 / 79.80	1:25 / 84.13	1:17 / 92.18	1:13 / 96.86	1:11 / 99.78	1:11 / 99.91	1:08 / 103.74	1:07 / 106.27
134 m/s	1:38 / 72.77	1:29 / 79.77	1:25 / 84.05	1:17 / 91.89	1:14 / 96.12	1:12 / 98.70	1:12 / 98.81	1:10 / 102.10	1:08 / 104.12
110 m/s	1:38 / 72.49	1:30 / 78.99	1:26 / 82.57	1:20 / 88.47	1:17 / 91.39	1:16 / 93.04	1:16 / 93.11	1:15 / 94.88	1:14 / 95.79
Excursion (419.8 km)									
150 m/s	1:55 / 75.17	1:25 / 82.14	1:21 / 86.45	1:14 / 94.38	1:11 / 98.91	1:09 / 101.72	1:08 / 101.85	1:06 / 105.53	1:02 / 107.98
134 m/s	1:33 / 75.15	1:25 / 82.04	1:21 / 86.23	1:14 / 93.75	1:11 / 97.82	1:10 / 100.26	1:10 / 100.37	1:08 / 103.49	1:07 / 105.41
110 m/s	1:34 / 74.49	1:27 / 80.64	1:23 / 84.05	1:18 / 89.59	1:16 / 92.28	1:14 / 93.77	1:14 / 93.83	1:13 / 95.40	1:13 / 96.17
Railroad ROW									
Centerline (423.7 km)									
150 m/s	1:43 / 68.71	1:34 / 75.03	1:29 / 78.91	1:22 / 86.31	1:18 / 90.65	1:16 / 93.41	1:16 / 93.53	1:13 / 97.25	1:11 / 99.66
134 m/s	1:43 / 68.67	1:34 / 74.93	1:29 / 78.77	1:23 / 86.05	1:18 / 90.24	1:16 / 92.98	1:16 / 93.10	1:13 / 96.51	1:11 / 98.59
110 m/s	1:43 / 68.35	1:35 / 74.37	1:31 / 77.93	1:24 / 84.14	1:21 / 87.18	1:19 / 88.90	1:19 / 88.97	1:17 / 91.02	1:17 / 92.27
Excursion (420.7 km)									
150 m/s	1:38 / 71.68	1:29 / 78.18	1:25 / 82.08	1:19 / 89.33	1:15 / 93.48	1:13 / 96.12	1:13 / 96.24	1:10 / 99.67	1:09 / 101.90
134 m/s	1:38 / 71.64	1:30 / 77.91	1:26 / 81.65	1:19 / 88.58	1:16 / 92.46	1:14 / 94.88	1:14 / 94.99	1:12 / 98.07	1:10 / 99.97
110 m/s	1:39 / 70.83	1:32 / 76.49	1:28 / 79.76	1:22 / 85.35	1:20 / 88.06	1:18 / 89.63	1:18 / 89.70	1:17 / 91.53	1:16 / 92.66
Independent (402.3 km)									
150 m/s	0:59 / 112.88	0:59 / 113.38	0:59 / 113.94	0:59 / 114.03	0:59 / 114.22	0:59 / 114.28	0:59 / 114.25	0:59 / 117.40	0:59 / 114.49
134 m/s	1:04 / 104.43	1:03 / 106.43	1:02 / 106.78	1:02 / 107.02	1:02 / 107.23	1:02 / 107.28	1:02 / 107.28	1:02 / 107.33	1:02 / 107.36
110 m/s	1:12 / 93.13	1:11 / 94.66	1:11 / 94.74	1:11 / 93.92	1:11 / 94.25	1:11 / 94.62	1:11 / 94.62	1:11 / 94.64	1:11 / 94.64

The aggressive comfort limits result in a 30 percent decrease in trip time for existing rights-of-way and much less significantly (about 3 percent) for the independent alignment. Figure 3.9-2 illustrates trip time on the New York to Syracuse corridor with respect to airline flight times using the underlined entries from Table 3.9-1 for highway centerline, highway excursion and independent alignments. The airline flight time is obtained from the Official Airline Guide. These comparisons do not include the access and egress times associated with either transportation mode. In each city pair case, specific station locations can be arranged to make these direct comparisons. It is anticipated that the relative performance of maglev travel on a flight time basis alone, coupled with anticipated access/egress advantages of city-center stations will warrant further study for these direct comparisons.

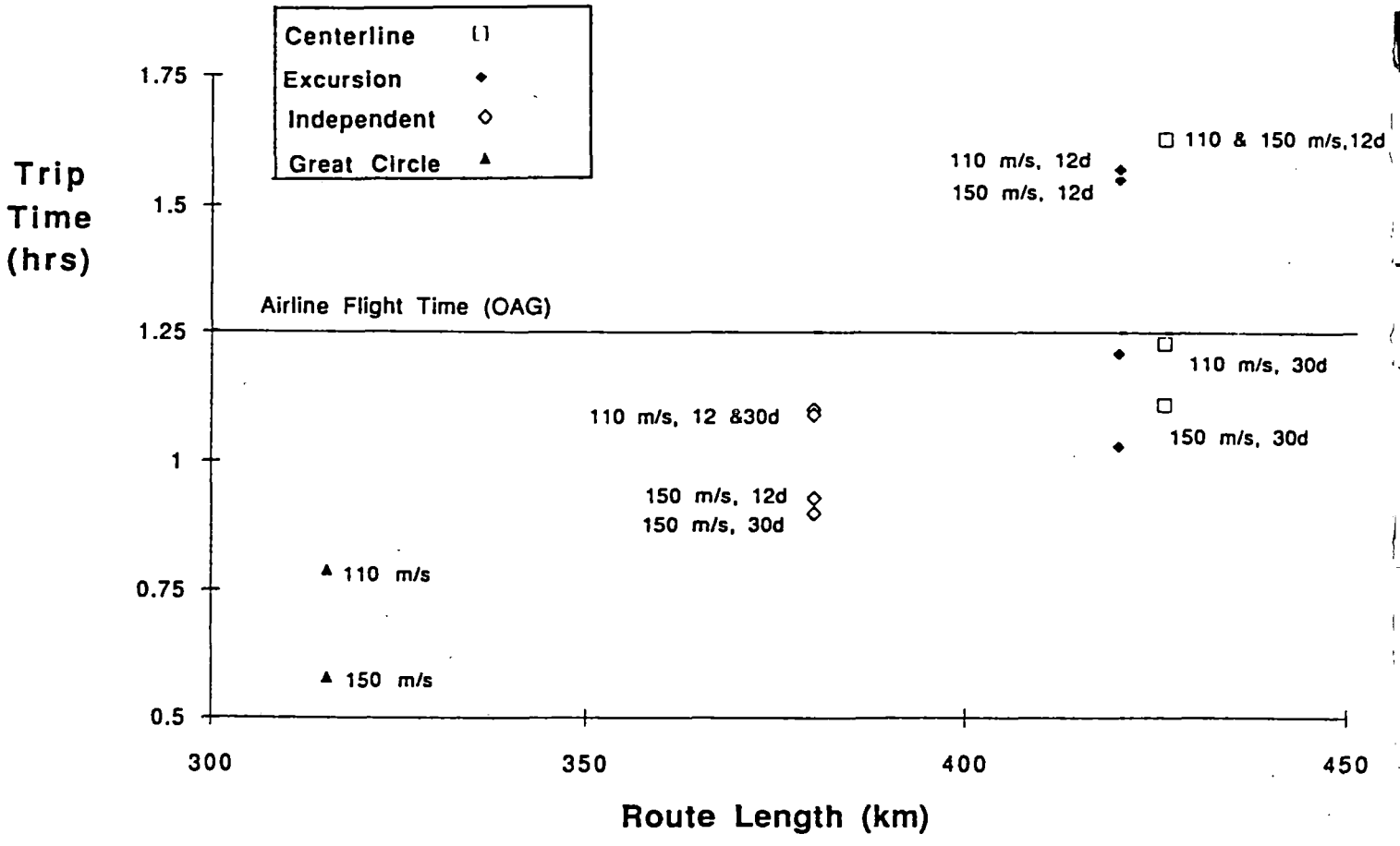

Figure 3.9-2 New York to Syracuse Trip Times Compared to Airline Travel Time

Trip time can be reduced by minimizing short-radius curvature and decreasing route length. Average speed is sensitive to maximum vehicle speed , short-radius curvature in the alignment and comfort limits. Length depends more on the terrain, the relative straightness of the route and of course the distance between city pairs. The limit to which trip time can be reduced is defined by the great circle distance between the city pairs divided by the maximum allowed vehicle speed. As shown in the Figure 3.9-2, all of the trip time improvements begin to approach these minimum trip time limits. Although guideway cost is reduced if the length is shortened, the need for special structures, bridges, tunnels, and land increase costs for the shorter, more direct route. Table 3.9-2 summarizes cost impact of special structures on the New York to Syracuse corridor.

Table 3.9-2 New York to Syracuse Alternative Structures

Route	Total Length	Outside ROW		Non-default Span Lengths				Default Span	Total Span
TappanZee-Syracuse	(Km)	Length (Km)	Land Used (m2)	25-100m	100-200m	200-300m	> 300m	Cost ($M)	Cost ($M)
Highway									
Centerline	425.8	0.0	0	21	13	2	1	3274.7	3321.7
Excursion	419.8	58.2	1,065,060	54	16	2	2	3209.5	3285.8
Railroad									
Centerline	423.7	0.0	0	29	4	1	1	3267.7	3299.9
Excursion	420.7	47.3	865,590	52	5	1	2	3232.0	3283.9
Independent	379.7	379.7	6,948,510	29	2	1	2	2926.3	2959.0
			Maglev ROW Width = 18.3 m	$11950/m	$11950/m	$13930/m	$13930/m	$7760/m	

Similar results were obtained for the Los Angeles to San Francisco and the Chicago to Detroit corridors. Table 3.9-3 illustrates that the travel times in these two corridors exhibit the same effects of speed saturation on the existing highway route as described above for New York, Increases in maximum speed capability exhibit significant reductions in travel time on the independent alignments where speed limiting curves have been minimized. Tables 3.9-4 and 3.9-5 report the incidences of special structures in these two corridors and reflect the guideway cost estimates for the highway and independent routes.

Table 3.9-3 Other Corridor Travel Time Comparisons

Superelevation	12 degrees	30 degrees	Superelevation	12 degrees	30 degrees
Unbalanced Lateral Load	0.03g	0.15g	Unbalanced Lateral Load	0.03g	0.15g
	h:mm / m/s	h:mm / m/s		h:mm / m/s	h:mm / m/s
Chicago to Detroit			Los Angeles to San Fran		
Highway ROW			Highway ROW		
Centerline (433.6 km)			Centerline (587.5 km)		
150 m/s	1:39 / 72.70	1:12 / 100.54	150 m/s	1:45 / 93.06	1:25 / 114.62
110 m/s	1:41 / 71.67	1:19 / 91.88	110 m/s	1:59 / 82.63	1:42 / 96.30
Excursion (433.1 km)			Excursion (583.4 km)		
150 m/s	1:34 / 76.56	1:10 / 103.49	150 m/s	1:38 / 99.57	1:24 / 115.19
110 m/s	1:36 / 75.04	1:18 / 92.91	110 m/s	1:52 / 86.89	1:40 / 97.35
Independent (399.0 km)			Independent (577.5 km)		
150 m/s	0:54 / 123.90	0:54 / 124.01	150 m/s	1:23 / 115.68	1:18 / 122.68
110 m/s	1:08 / 97.85	1:08 / 97.85	110 m/s	1:40 / 95.82	1:37 / 99.64

Table 3.9-4 Los Angeles to San Francisco Alternative Structures

Route	Total Length	Outside ROW		Non-default Span Lengths				Default Span	Total Span
LosAngeles-SanFran	(Km)	Length (Km)	Land Used (m2)	25-100m	100-200m	200-300m	> 300m	Cost ($M)	Cost ($M)
Highway									
Centerline	587.5	0.0	0	46	3	3	0	4531.8	4575.2
Excursion	583.4	38.6	706,380	54	16	2	2	4479.1	4555.3
Independent	577.5	577.5	10,568,250	20	4	0	0	4469.0	4488.1
			Maglev ROW Width = 18.3 m	$11950/m	$11950/m	$13930/m	$13930/m	$7760/m	

Table 3.9-5 Chicago to Detroit Alternative Structures

Route	Total Length	Outside ROW		Non-default Span Lengths				Default Span	Total Span
Detroit-Chicago	(Km)	Length (Km)	Land Used (m2)	25-100m	100-200m	200-300m	> 300m	Cost ($M)	Cost ($M)
Highway									
Centerline	433.6	0.0	0	13	16	1	5	3327.5	3388.3
Excursion	433.1	46.5	850,950	53	17	1	5	3306.9	3393.4
Independent	399.0	399.0	7,301,700	18	1	1	1	3083.8	3104.0
			Maglev ROW Width = 18.3 m	$11950/m	$11950/m	$13930/m	$13930/m	$7760/m	

Investigation of 21 Additional Corridors

The analysis techniques applied to the original 23 corridor portions were used in the examination of 21 new corridors. These corridors are listed in Table 3.9.6 with the intermediate cities along the routes. The new corridors incorporate the 23 corridor portions examined previously.

Table 3.9-6 New Corridors Examined

1. New York Albany Utica Syracuse Rochester Buffalo Niagara Falls	2. Boston Providence Hartford New Haven New York Philadelphia Wilmington Baltimore Washington	3. San Diego Los Angeles Bakersfield Fresno San Jose San Francisco	4. Chicago South Bend Toledo Detroit
5. Dallas Houston	6. Dallas Waco Austin San Antonio 6a. Austin Houston	7. Miami West Palm Orlando Tampa	8. Seattle Tacoma Olympia Portland
9. Los Angeles Las Vegas	10. Washington Richmond Raleigh- Durham Greensboro Charlotte Greenville Atlanta	11. Chicago Milwaukee Madison Minn./St. Paul	12. Chicago Bloomington Springfield St. Louis Columbia Kansas City
13. Philadelphia Lancaster Harrisburg State College Altoona Johnstown Greensburg Pittsburgh	14. Pittsburgh Youngstown Akron Cleveland Toledo	15. Chicago Lafayette Indianapolis Cincinnati	16. Cleveland Akron Columbus Dayton Cincinnati
17. San Diego Phoenix	18. Houston Beaumont Lake Charles Lafayette Baton Rouge New Orleans	19. Los Angeles Phoenix	20. Boston Worcester Springfield Lee (Pittsfield) Albany
21. San Francisco - Sacremento - Lake Tahoe - Carson City - Reno			

Each corridor was assessed for travel times with respect to the highway and independent alignments including multiple station stops and three high speed ground transportation (HSGT) technologies: Transrapid 07, the French TGV high speed rail system, and a proposed United States maglev system. The attributes of each of these technologies affecting the analysis are shown in Table 3.9.7. In addition, acceleration limitations due the power, drag, and grade were included for each technology. Although comfort limited longitudinal acceleration limits were never exceeded, accelerations appreciably less than the limit were encountered at high speeds when climbing grades.

Table 3.9-7 Three High Speed Ground Transportation Technologies

Parameters	TGV	Transrapid 07	U.S. Maglev
Maximum Speed (m/s)	89.4	134.1	134.1
Maximum Bank Angle (degrees)	6	12	30
Unbalanced Lateral Acceleration Limit (g's)	.10	.10	.10
Unbalanced Upward Acceleration Limit (g's)	-.05	-.05	-.25
Unbalanced Downward Acceleration Limit (g's)	0.2	0.2	0.25
Unbalanced Longitudinal Acceleration Limit (g's)	.16	.16	.16
Unbalanced Longitudinal Deceleration Limit (g's)	.075	.15	.16
Maximum Grade (%)	3.5	10	10
Station Dwell Time (min)	2	2	2

Travel times are reported for all 21 new corridors in Appendix D. Several factors augmented the methodology used on the original 23 corridor portions. In many cases on the new corridors, urban

accelerations were incorporated where previous analysis used a constant 0.16g longitudinal acceleration rate at all speeds. As before, route alignments were created using 1:250,000 topographic maps and the results for existing ROW alignments were adjusted as per the regression equations for excursion alignments described in section 3.7.

Railroad alignments were examined in the first eight corridors only for TGV comparisons but the effort was discontinued because it is more advantageous to TGV to consider its relative performance on new straighter alignments. All 21 corridors include TGV travel time estimates on the independent alignments. TGV grade limitations of 3.5 percent required that the independent alignments be adjusted in elevation to stay within this limit. An analysis was performed by identifying those segments where the grade limit along the independent alignment was too steep for TGV This was especially necessary in the California mountain regions and not so significant elsewhere. The elevations of segments were adjusted in the independent alignment description files to accommodate TGV grade capabilities. The plan view alignments were **not** changed in this activity. This resulted in an optimistically shorter route length for TGV in the California mountains considering that much of the elevation adjustments would be avoided with plan view modifications in an actual system.

There are several optimizations possible throughout the alignments examined here. For example, the San Diego-Phoenix corridor follows I-15 north out of San Diego and connects with I-10 and follows it to Phoenix. The more accepted route might be I-8 east out of San Diego and take US80 north to Phoenix. The I-15/I-10 route north is approximately 80 kilometers longer than the I-8/US80 route.

Overall, 12,806 kilometers of highway alignments were examined in the 21 new corridors. The aggregate total length of the independent alignment was 6.70 percent less lengthy, saving 858 kilometers of guideway cost. This potentially large dollar savings, on the order of $1.7 billion at $20 million per guideway kilometer, will significantly contribute to the acquisition of air rights for new ROW. Similarly, the independent alignments were 7.95 percent less lengthy on the average than railroad ROW alignments in the first eight corridors.

Relative travel time comparisons for the three HSGT technologies are shown in Table 3.9-8. The U.S maglev faster in all cases primarily do to a larger maximum bank angle and greater acceleration capabilities at higher speeds. Using the independent alignment from Boston to Washington, D.C., the U. S. maglev would arrive in two hours and sixteen minutes, almost one hour ahead of TGV, on an express run. This U.S. maglev advantage is much less evident when compared to TR07 on

the same corridor alignment, just thirteen minutes faster, because the benefits of higher bank angles are not significant on the independent alignments. This is further supported when considering an express run on the highway alignment in the same corridor where the U.S. maglev is 34 minutes faster than TR07 because the larger bank angle has a more pronounced advantage when an appreciable number of speed limiting curves are present..

Table 3.9-8 HSGT Travel Time Comparisons

Average over 21 Corridors	US vs TR07 on Hwy	US vs TR07 on Ind	US vs TGV on Ind	TR07 vs TGV on Ind	TR07 Hwy vs Ind	USComp Hwy vs Ind	TGV RR* vs Ind
Travel Time Imprv Local Service (%)	17.70%	5.92%	30.49%	26.13%	21.75%	10.68%	21.63%
Travel Time Imprv Express Service (%)	18.66%	4.84%	30.94%	27.44%	24.50%	11.78%	21.85%

* statistics based on the first eight corridors only

Table 3.9-9 shows that the travel time penalty for stopping frequently, every 20 to 30 minutes on the average in the 21 corridors, has a significant effect on end-to-end travel times. The express service would save approximately 19 minutes in travel time over a local service trip lasting two hours on the independent alignments. The major contributor to this savings is the station dwell time, two minutes for every station stop was used in this analysis, in the cases of the two maglev technologies. As expected, TGV station stop service times exhibited a larger contribution from the deceleration and acceleration times associated with making the stop.

Table 3.9-9 Comparison of Station Stop Effects

Average over 21 Corridors	TR07 on Hwy	USComp on Hwy	TGV on RR*	TR07 on Ind	TGV on Ind	USComp on Ind
Avg Travel Time Saved Per Corridor with Express (%)	12.38%	14.01%	13.01%	16.63%	15.51%	16.10%
Avg Time Saved Per Stop with Express (min)	3.5	3.2	4.4	3.7	4.6	3.3
Avg Time Saved Per Stop From Accl/Decl with Express (min)	1.5	1.2	2.4	1.7	2.6	1.3
Avg Time Between Stations (min)	26.9	21.8	33.3	20.3	28.3	19.1

* statistics based on the first eight corridors only

The Boston to Washington, D.C., corridor is an extreme case in that it includes 16 intermediate station stops. The average time between stations is between 10 and 16 minutes. The express run on the independent alignment saves 52 minutes, 32 of them coming from two minute dwell times at the 16 intermediate stations, over the full local service travel times. In practice, skip-stop operations will mitigate the effects of so many station stops on the end-to-end traveller's travel time.

APPENDIX A. REFERENCES

1. "Acceleration and Comfort in Public Ground Transportation", J.W. Gebhard, Transportation Programs Report, TPR 002, February 1970.

2. "United States - Federal Republic of Germany Cooperative Study of Advanced Ground Vehicle Ride Quality", E. Donald Sussman et al, U.S. DOT-TSC, November 1979, Internal TSC working paper.

3. "The Development of Interior Noise and Vibration Criteria", J.D. Leatherwood, Clevenson, S.A., Stephens, D.G., NASA Langley Research Center, October 1990.

4. "New York State Technical & Economical Maglev Evaluation", Grumman Space And Electronics Division, Grumman Corporation, for the New York State Energy Research and Development Authority and the New York State Thruway Authority, June 1991.

5. "The Transrapid06 Trial Operations up to Service Readiness", in Transrapid Maglev System, Hestra-Verlag Darmstadt, Transrapid International Gesellschaft fur Magnetbahnsysteme, 1989.

6. Abraham, E., Private communication, Otis Elevator Co., Farmington, CT.

7. "Development of Techniques and Data for Evaluating Ride Quality", R.D. Peplar et al, U.S. DOT-TSC, Volume I: Summary, February 1978.

8. "Development of Techniques and Data for Evaluating Ride Quality", R.D. Peplar et al, U.S. DOT-TSC, Volume II: Ride-Quality Research, February 1978.

9. "Development of Techniques and Data for Evaluating Ride Quality", R.D. Peplar et al, U.S. DOT-TSC, Volume III: Guidelines for Development of Ride-Quality Models and Their Application, February 1978.

10. "Guideway Alignment and Surveying", in Transrapid Maglev System, Hestra-Verlag Darmstadt, Transrapid International Gesellschaft fur Magnetbahnsysteme, 1989.

11. Means 1992 Building Construction Cost Data 50th Annal Edition, R.S. Means Company, Inc.

Additional documents which informed the judgement applied in this report.

12. "The Concrete Guideway", in Transrapid Maglev System, Hestra-Verlag Darmstadt, Transrapid International Gesellschaft fur Magnetbahnsysteme, 1989.

13. "HSST MAGLEV Train at Yokohama Expo '89", Magnetic Levitation Technology for Advanced Transit Systems, Future Transportation Technology Conference and Exposition, Vancouver, British Columbia, Canada, August 1989.

14. "Human Engineering Design Criteria for Military Systems, Equipment, and Facilities", MIL-STD-1472D, 14 March 1989.

15. "Use of Existing Highway Right-of-Way for High Speed Rail Transportation", Richard L. Peterson et al, Texas Transportation Institute, 1985.

16. "Human Factors in Engineering and Design", E.J. McCormick, 1976.

17. "Dynamic Criteria in the Design of Maglev Suspension Systems", R.M. Goodall and R.A. Williams, IME Conference on Magnetic Levitation, 1984.

18. An Introduction to Transportation Engineering, W.W. Hay, Wiley & Son, 1977, New York.

19. Railroad Engineering, W.W. Hay, Wiley & Son, 1982, New York.

20. "Disturbing Effects of Horizontal Acceleration", Electric Railway Presidents Conference Committee, Bulletin No. 3, September 1932.

21. "Recent Developments in Railway Curve Design", Loach, J.C. and Maycock, M.G., Proceedings Institute of Civil Engineers, Part II, October 1952.

22. A Policy on Geometric Design of Highways and Streets, American Association of State Highway and Transportation Officials, 1990.

23. "Evaluation of Train Ride Comfort under Various Speeds at Curves, Quarterly Report, Railway Technical Research Institute, Japanese National Railways, 1966.

24. "Dynamics of High Speed Rolling Stock", Quarterly Report, Railway Technical Research Institute, Japanese National Railways, 1963.

25. Tolerance Criteria of Ride Comfort for Lateral Vibration (Report 1), Quarterly Report, Railway Technical Research Institute, Japanese National Railways, 1966.

26. Thompson, G., Private communication, Westinghouse Electric Corp., Beltsville, MD.

27. Chevy Chase Chevyland Dealership, Private communication, Bethesda, MD.

28. Cheslock, R., Private communication, United States State Department, Washington DC.

29. Wood, J., Private communication, Wyle Laboratories, Hampton, VA.

30. "Maglev Vehicles and Superconductor Technology: Integration of High-Speed Ground Transportation into Air System Travel", L.R. Johnson et al, Center for Transportation Research, Argonne National Laboratory, 1989

31. "Elevated Guideway Cost-Ride Quality Studies for Group Rapid Transit Systems.", Wormley, D.N., et. al., Department of Mechanical Engineering, MIT, Cambridge, MA, U.S. DOT, DOT-TSC-OST-77-54, August 1978.

32. Cable Stayed Bridges: An Approach to Modern Bridge Design., Troitsky, M.S., New York: Van Nostrand Reinhold Company, 1988.

33. "Firm makes bridges easier to build," ENR, March 30, 1992.

34. "Cable-Stayed Guideway: An Analyses and Dynamic Model Tests.", Whitelaw, R.L., et. al., Federal Railroad Administration, April 1974.

35. "Maglev Cost Estimation: Capital Cost Elements", Harrison, J.A., et. al., Interim Report. U.S. DOT, Volpe National Transportation Center, Cambridge, MA, 1992.

36. Building Bridges: History, Technology, Construction, Wittfoht, H., Dusseldorf: Beton-Verlag, 1984.

37. Maglev Transit, Inc. Magnetic Levitation Demonstration Project: Executive Summary. 1988.

38. Maglev Transport: Now and For the Future,.Railway Division of the Institution of Mechanical Engineers, The Institution of Civil Engineers, and the Institution of Electrical Engineers, 1984.

39. "Civil Aspects of Maglev Design", Zicha, J.H., Paper presented at the International Conference on Maglev and Linear Drives, 1986.

40. Benefits of Magnetically Levitated High-Speed Transportation for the United States, Vol. 1, Executive Report.

41. "Bridge Vulnerability to Earthquakes," Appendix II, in GAO/RCED-92-59, Highway Bridges at Risk From Earthquakes.

42. Johnson, R., Private communication, Howard Needles, Tammen, and Burgendoff, Minneapolis, MN.

APPENDIX B. REFERENCE SYSTEM

The following coordinate system was used in the completion of the tasks relating to passenger comfort and maximum speed derivations. The solid lines represent the reference coordinate system; dotted lines represent the passenger coordinate system (denoted by subscript letter "p") as a result of guideway banking and gradient. Comfort values (see section 3.2) are calculated through the passenger coodinate system. Summation of acceleration forces to derive maximum speeds (see section 3.3) are applied in the reference system but decomposed to the passenger system for the calculation of vehicle speed.

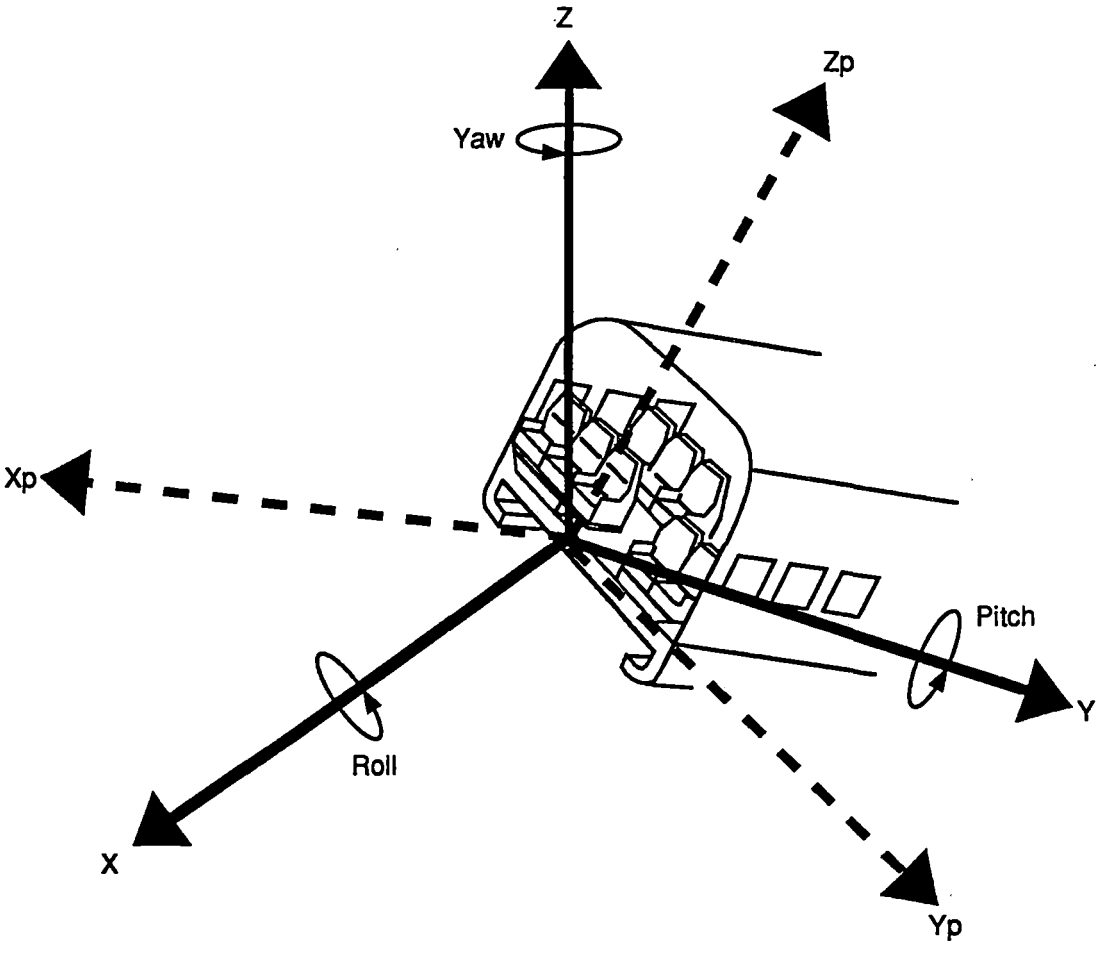

APPENDIX C. SPEED TABLES

	Speed Table for Horizontal Curvature			
Horizontal Radius (meters)	6 degrees (m/s)	12 degrees (m/s)	18 degrees (m/s)	24 degrees (m/s)
0	0.00	0.00	0.00	0.00
150	17.39	21.51	25.14	28.57
300	24.59	30.42	35.56	40.40
450	30.11	37.26	43.55	49.48
600	34.77	43.02	50.29	57.13
750	38.88	48.10	56.23	63.87
900	42.59	52.69	61.59	69.97
1050	46.00	56.91	66.53	75.58
1200	49.18	60.84	71.12	80.80
1350	52.16	64.53	75.43	85.70
1500	54.98	68.02	79.52	90.33
1650	57.66	71.34	83.40	94.74
1800	60.23	74.51	87.10	98.95
1950	62.69	77.56	90.66	102.99
2100	65.05	80.48	94.08	106.88
2250	67.34	83.31	97.39	110.63
2400	69.55	86.04	100.58	114.26
2550	71.69	88.69	103.68	117.78
2700	73.76	91.26	106.68	121.19
2850	75.79	93.76	109.60	124.51
3000	77.75	96.20	112.45	127.75
3150	79.67	98.57	115.23	130.90
3300	81.55	100.89	117.94	133.98
3450	83.38	103.16	120.59	137.00
3600	85.18	105.38	123.18	139.94
3750	86.93	107.55	125.72	142.83
3900	88.65	109.68	128.21	145.66
4050	90.34	111.77	130.66	148.43
4200	92.00	113.82	133.05	151.15
4350	93.63	115.83	135.41	153.83
4500	95.23	117.82	137.72	156.46
4650	96.80	119.76	140.00	159.05
4800	98.35	121.68	142.24	161.59
4950	99.88	123.57	144.45	164.10
5100	101.38	125.42	146.62	166.56
5250	102.86	127.25	148.76	169.00
5400	104.32	129.06	150.87	171.39

	Speed Table for Horizontal Curvature			
Horizontal Radius (meters)	6 degrees (m/s)	12 degrees (m/s)	18 degrees (m/s)	24 degrees (m/s)
5550	105.76	130.84	152.95	173.76
5700	107.18	132.60	155.00	176.09
5850	108.58	134.33	157.03	178.39
6000	109.96	136.04	159.03	180.66
6150	111.33	137.73	161.01	182.91
6300	112.68	139.40	162.96	185.13
6450	114.01	141.05	164.89	187.32
6600	115.33	142.68	166.79	189.48
6750	116.63	144.29	168.68	191.62
6900	117.92	145.89	170.54	193.74
7050	119.19	147.47	172.38	195.84
7200	120.46	149.03	174.21	197.91
7350	121.70	150.57	176.01	199.96
7500	122.94	152.10	177.80	201.99
7650	124.16	153.61	179.57	204.00
7800	125.37	155.11	181.32	205.99
7950	126.57	156.60	183.06	207.96
8100	127.76	158.07	184.78	209.91
8250	128.94	159.52	186.48	211.85
8400	130.11	160.97	188.17	213.76
8550	131.26	162.40	189.84	215.66
8700	132.41	163.82	191.50	217.55
8850	133.55	165.22	193.14	219.42
9000	134.67	166.62	194.77	221.27
9150	135.79	168.00	196.39	223.10
9300	136.90	169.37	197.99	224.92
9450	138.00	170.73	199.58	226.73
9600	139.09	172.08	201.16	228.52
9750	140.17	173.42	202.72	230.30
9900	141.25	174.75	204.28	232.07
10050	142.31	176.07	205.82	233.82
10200	143.37	177.38	207.35	235.56
10350	144.42	178.68	208.87	237.28
10500	145.46	179.97	210.38	239.00
10650	146.50	181.25	211.87	240.70
10800	147.53	182.52	213.36	242.39
10950	148.55	183.78	214.84	244.06

	Speed Table for Horizontal Curvature			
Horizontal Radius (meters)	6 degrees (m/s)	12 degrees (m/s)	18 degrees (m/s)	24 degrees (m/s)
11100	149.56	185.04	216.30	245.73
11250	150.57	186.28	217.76	247.38
11400	151.57	187.52	219.21	249.03
11550	152.56	188.75	220.65	250.66
11700	153.55	189.97	222.07	252.28
11850	154.53	191.19	223.49	253.90
12000	155.51	192.39	224.90	255.50
12150	156.48	193.59	226.30	257.09
12300	157.44	194.78	227.70	258.67
12450	158.40	195.97	229.08	260.24
12600	159.35	197.14	230.46	261.81
12750	160.29	198.31	231.82	263.36
12900	161.23	199.48	233.18	264.91
13050	162.17	200.63	234.54	266.44
13200	163.10	201.78	235.88	267.97
13350	164.02	202.92	237.22	269.49
13500	164.94	204.06	238.55	271.00
13650	165.85	205.19	239.87	272.50
13800	166.76	206.32	241.18	273.99
13950	167.67	207.43	242.49	275.48
14100	168.57	208.55	243.79	276.95
14250	169.46	209.65	245.08	278.42
14400	170.35	210.75	246.37	279.88
14550	171.24	211.85	247.65	281.34
14700	172.12	212.94	248.92	282.78
14850	172.99	214.02	250.19	284.22
15000	173.86	215.10	251.45	285.65
15150	174.73	216.17	252.70	287.08
15300	175.59	217.24	253.95	288.50
15450	176.45	218.30	255.19	289.91
15600	177.31	219.36	256.43	291.31
15750	178.16	220.41	257.66	292.71
15900	179.00	221.46	258.88	294.10
16050	179.85	222.50	260.10	295.48
16200	180.68	223.54	261.31	296.86
16350	181.52	224.57	262.52	298.23
16500	182.35	225.60	263.72	299.60

	Speed Table for Horizontal Curvature			
Horizontal Radius (meters)	6 degrees (m/s)	12 degrees (m/s)	18 degrees (m/s)	24 degrees (m/s)
16650	183.18	226.62	264.92	300.96
16800	184.00	227.64	266.11	302.31
16950	184.82	228.65	267.29	303.66
17100	185.63	229.66	268.47	305.00
17250	186.45	230.67	269.65	306.33
17400	187.26	231.67	270.82	307.66
17550	188.06	232.67	271.98	308.98
17700	188.86	233.66	273.14	310.30
17850	189.66	234.65	274.30	311.61
18000	190.46	235.63	275.45	312.92
18150	191.25	236.61	276.59	314.22
18300	192.04	237.59	277.73	315.52
18450	192.82	238.56	278.87	316.81
18600	193.61	239.53	280.00	318.09
18750	194.38	240.49	281.13	319.37
18900	195.16	241.45	282.25	320.65
19050	195.93	242.41	283.37	321.92
19200	196.70	243.36	284.48	323.18
19350	197.47	244.31	285.59	324.44
19500	198.23	245.25	286.70	325.70
19650	199.00	246.19	287.80	326.95
19800	199.75	247.13	288.89	328.19
19950	200.51	248.07	289.98	329.43
20100	201.26	249.00	291.07	330.67
20250	202.01	249.92	292.16	331.90
20400	202.76	250.85	293.24	333.13
20550	203.50	251.77	294.31	334.35
20700	204.24	252.69	295.39	335.57
20850	204.98	253.60	296.45	336.78
21000	205.72	254.51	297.52	337.99
21150	206.45	255.42	298.58	339.20
21300	207.18	256.32	299.64	340.40
21450	207.91	257.22	300.69	341.59
21600	208.64	258.12	301.74	342.79
21750	209.36	259.01	302.78	343.97
21900	210.08	259.91	303.83	345.16
22050	210.80	260.79	304.87	346.34

	Horizontal Radius Range To Satisfy Vertical Comfort							
	6 Degrees		12 Degrees		18 Degrees		24 Degrees	
	Minimum	Maximum	Minimum	Maximum	Minimum	Maximum	Minimum	Maximum
Speed	Radius	Radius	Radius	Radius	Radius	Radius	Radius	Radius
(m/s)	(m)	(m)	(m)	(m)	(m)	(m)	(m)	(m)
0	0.00	infinite	0.00	infinite	0.00	infinite	0.00	infinite
2	0.21	infinite	0.38	infinite	0.51	infinite	0.58	4.54
4	0.83	infinite	1.53	infinite	2.03	infinite	2.32	18.16
6	1.87	infinite	3.44	infinite	4.56	infinite	5.22	40.87
8	3.33	infinite	6.12	infinite	8.11	infinite	9.28	72.66
10	5.20	infinite	9.56	infinite	12.67	infinite	14.49	113.53
12	7.49	infinite	13.77	infinite	18.24	infinite	20.87	163.48
14	10.19	infinite	18.74	infinite	24.83	infinite	28.41	222.51
16	13.31	infinite	24.48	infinite	32.43	infinite	37.10	290.63
18	16.85	infinite	30.98	infinite	41.04	infinite	46.96	367.82
20	20.80	infinite	38.25	infinite	50.67	infinite	57.97	454.10
22	25.16	infinite	46.28	infinite	61.31	infinite	70.14	549.47
24	29.95	infinite	55.07	infinite	72.96	infinite	83.48	653.91
26	35.15	infinite	64.64	infinite	85.63	infinite	97.97	767.44
28	40.76	infinite	74.96	infinite	99.31	infinite	113.62	890.04
30	46.79	infinite	86.05	infinite	114.01	infinite	130.43	1021.73
32	53.24	infinite	97.91	infinite	129.71	infinite	148.40	1162.51
34	60.10	infinite	110.53	infinite	146.44	infinite	167.53	1312.36
36	67.38	infinite	123.92	infinite	164.17	infinite	187.82	1471.30
38	75.08	infinite	138.07	infinite	182.92	infinite	209.27	1639.32
40	83.19	infinite	152.98	infinite	202.68	infinite	231.88	1816.42
42	91.72	infinite	168.66	infinite	223.45	infinite	255.65	2002.60
44	100.66	infinite	185.11	infinite	245.24	infinite	280.58	2197.86
46	110.02	infinite	202.32	infinite	268.04	infinite	306.66	2402.21
48	119.79	infinite	220.30	infinite	291.86	infinite	333.91	2615.64
50	129.98	infinite	239.04	infinite	316.69	infinite	362.32	2838.15
52	140.59	infinite	258.54	infinite	342.53	infinite	391.88	3069.74
54	151.61	infinite	278.81	infinite	369.38	infinite	422.60	3310.42
56	163.05	infinite	299.85	infinite	397.25	infinite	454.49	3560.18
58	174.91	infinite	321.65	infinite	426.13	infinite	487.53	3819.02
60	187.18	infinite	344.21	infinite	456.03	infinite	521.73	4086.94
62	199.86	infinite	367.54	infinite	486.94	infinite	557.10	4363.94
64	212.96	infinite	391.64	infinite	518.86	infinite	593.62	4650.03

	Horizontal Radius Range To Satisfy Vertical Comfort							
	6 Degrees		12 Degrees		18 Degrees		24 Degrees	
	Minimum	Maximum	Minimum	Maximum	Minimum	Maximum	Minimum	Maximum
Speed	Radius	Radius	Radius	Radius	Radius	Radius	Radius	Radius
(m/s)	(m)	(m)	(m)	(m)	(m)	(m)	(m)	(m)
66	226.48	infinite	416.50	infinite	551.79	infinite	631.30	4945.19
68	240.42	infinite	442.12	infinite	585.74	infinite	670.14	5249.44
70	254.77	infinite	468.51	infinite	620.70	infinite	710.14	5562.78
72	269.53	infinite	495.67	infinite	656.68	infinite	751.30	5885.19
74	284.72	infinite	523.59	infinite	693.67	infinite	793.62	6216.68
76	300.31	infinite	552.27	infinite	731.67	infinite	837.09	6557.26
78	316.33	infinite	581.72	infinite	770.69	infinite	881.73	6906.92
80	332.76	infinite	611.93	infinite	810.71	infinite	927.53	7265.67
82	349.60	infinite	642.91	infinite	851.76	infinite	974.48	7633.49
84	366.86	infinite	674.66	infinite	893.81	infinite	1022.60	8010.40
86	384.54	infinite	707.17	infinite	936.88	infinite	1071.87	8396.38
88	402.64	infinite	740.44	infinite	980.96	infinite	1122.31	8791.46
90	421.15	infinite	774.48	infinite	1026.06	infinite	1173.90	9195.61
92	440.07	infinite	809.28	infinite	1072.17	infinite	1226.65	9608.84
94	459.41	infinite	844.85	infinite	1119.29	infinite	1280.57	10031.16
96	479.17	infinite	881.18	infinite	1167.43	infinite	1335.64	10462.56
98	499.34	infinite	918.28	infinite	1216.58	infinite	1391.87	10903.04
100	519.93	infinite	956.15	infinite	1266.74	infinite	1449.26	11352.60
102	540.94	infinite	994.77	infinite	1317.92	infinite	1507.81	11811.25
104	562.36	infinite	1034.17	infinite	1370.11	infinite	1567.52	12278.97
106	584.20	infinite	1074.33	infinite	1423.31	infinite	1628.39	12755.78
108	606.45	infinite	1115.25	infinite	1477.53	infinite	1690.42	13241.68
110	629.12	infinite	1156.94	infinite	1532.76	infinite	1753.61	13736.65
112	652.20	infinite	1199.39	infinite	1589.00	infinite	1817.95	14240.70
114	675.70	infinite	1242.61	infinite	1646.26	infinite	1883.46	14753.84
116	699.62	infinite	1286.59	infinite	1704.53	infinite	1950.13	15276.06
118	723.95	infinite	1331.34	infinite	1763.81	infinite	2017.95	15807.36
120	748.70	infinite	1376.85	infinite	1824.11	infinite	2086.94	16347.75
122	773.87	infinite	1423.13	infinite	1885.42	infinite	2157.08	16897.21
124	799.45	infinite	1470.17	infinite	1947.74	infinite	2228.38	17455.76
126	825.45	infinite	1517.98	infinite	2011.08	infinite	2300.85	18023.39
128	851.86	infinite	1566.55	infinite	2075.43	infinite	2374.47	18600.10
130	878.69	infinite	1615.89	infinite	2140.79	infinite	2449.25	19185.90

	Horizontal Radius Range To Satisfy Vertical Comfort							
	6 Degrees		12 Degrees		18 Degrees		24 Degrees	
	Minimum	Maximum	Minimum	Maximum	Minimum	Maximum	Minimum	Maximum
Speed	Radius	Radius	Radius	Radius	Radius	Radius	Radius	Radius
(m/s)	(m)	(m)	(m)	(m)	(m)	(m)	(m)	(m)
132	905.93	infinite	1665.99	infinite	2207.17	infinite	2525.19	19780.77
134	933.59	infinite	1716.86	infinite	2274.56	infinite	2602.29	20384.73
136	961.67	infinite	1768.49	infinite	2342.97	infinite	2680.55	20997.77
138	990.16	infinite	1820.88	infinite	2412.38	infinite	2759.97	21619.90
140	1019.07	infinite	1874.05	infinite	2482.81	infinite	2840.55	22251.10
142	1048.39	infinite	1927.97	infinite	2554.26	infinite	2922.29	22891.39
144	1078.13	infinite	1982.66	infinite	2626.72	infinite	3005.19	23540.76
146	1108.29	infinite	2038.12	infinite	2700.19	infinite	3089.24	24199.21
148	1138.86	infinite	2094.34	infinite	2774.67	infinite	3174.46	24866.74
150	1169.85	infinite	2151.33	infinite	2850.17	infinite	3260.84	25543.36

	Maximum Speeds for Vertical Curves					
Vertical Radius (m)	Max Speed Summit (m/s)	Max Speed Sag (m/s)		Vertical Radius (m)	Max Speed Summit (m/s)	Max Speed Sag (m/s)
150	8.57	17.15		5400	51.44	102.88
300	12.12	24.25		5550	52.15	104.30
450	14.85	29.70		5700	52.85	105.70
600	17.15	34.29		5850	53.54	107.08
750	19.17	38.34		6000	54.22	108.44
900	21.00	42.00		6150	54.90	109.79
1050	22.68	45.37		6300	55.56	111.12
1200	24.25	48.50		6450	56.22	112.44
1350	25.72	51.44		6600	56.87	113.74
1500	27.11	54.22		6750	57.51	115.02
1650	28.43	56.87		6900	58.15	116.29
1800	29.70	59.40		7050	58.77	117.55
1950	30.91	61.82		7200	59.40	118.79
2100	32.08	64.16		7350	60.01	120.02
2250	33.20	66.41		7500	60.62	121.24
2400	34.29	68.59		7650	61.22	122.45
2550	35.35	70.70		7800	61.82	123.64
2700	36.37	72.75		7950	62.41	124.83
2850	37.37	74.74		8100	63.00	126.00
3000	38.34	76.68		8250	63.58	127.16
3150	39.29	78.57		8400	64.16	128.31
3300	40.21	80.42		8550	64.73	129.45
3450	41.12	82.23		8700	65.29	130.58
3600	42.00	84.00		8850	65.85	131.70
3750	42.87	85.73		9000	66.41	132.82
3900	43.71	87.43		9150	66.96	133.92
4050	44.55	89.10		9300	67.51	135.01
4200	45.37	90.73		9450	68.05	136.10
4350	46.17	92.34		9600	68.59	137.17
4500	46.96	93.91		9750	69.12	138.24
4650	47.73	95.47		9900	69.65	139.30
4800	48.50	96.99		10050	70.17	140.35
4950	49.25	98.50		10200	70.70	141.39
5100	49.99	99.98		10350	71.21	142.43
5250	50.72	101.44		10500	71.73	143.46

	Maximum Speeds for Vertical Curves					
Vertical Radius (m)	Max Speed Summit (m/s)	Max Speed Sag (m/s)		Vertical Radius (m)	Max Speed Summit (m/s)	Max Speed Sag (m/s)
10650	72.24	144.48		15900	88.27	176.53
10800	72.75	145.49		16050	88.68	177.36
10950	73.25	146.50		16200	89.10	178.19
11100	73.75	147.50		16350	89.51	179.01
11250	74.25	148.49		16500	89.92	179.83
11400	74.74	149.48		16650	90.32	180.65
11550	75.23	150.46		16800	90.73	181.46
11700	75.72	151.43		16950	91.13	182.27
11850	76.20	152.40		17100	91.54	183.07
12000	76.68	153.36		17250	91.94	183.87
12150	77.16	154.32		17400	92.34	184.67
12300	77.63	155.27		17550	92.73	185.47
12450	78.11	156.21		17700	93.13	186.26
12600	78.57	157.15		17850	93.52	187.05
12750	79.04	158.08		18000	93.91	187.83
12900	79.50	159.01		18150	94.31	188.61
13050	79.97	159.93		18300	94.69	189.39
13200	80.42	160.85		18450	95.08	190.16
13350	80.88	161.76		18600	95.47	190.93
13500	81.33	162.67		18750	95.85	191.70
13650	81.78	163.57		18900	96.23	192.47
13800	82.23	164.46		19050	96.62	193.23
13950	82.68	165.35		19200	96.99	193.99
14100	83.12	166.24		19350	97.37	194.75
14250	83.56	167.12		19500	97.75	195.50
14400	84.00	168.00		19650	98.12	196.25
14550	84.44	168.87		19800	98.50	197.00
14700	84.87	169.74		19950	98.87	197.74
14850	85.30	170.60		20100	99.24	198.48
15000	85.73	171.46		20250	99.61	199.22
15150	86.16	172.32		20400	99.98	199.96
15300	86.59	173.17		20550	100.35	200.69
15450	87.01	174.02		20700	100.71	201.42
15600	87.43	174.86		20850	101.08	202.15
15750	87.85	175.70		21000	101.44	202.88

	Maximum Speeds for Vertical Curves					
Vertical Radius (m)	Max Speed Summit (m/s)	Max Speed Sag (m/s)		Vertical Radius (m)	Max Speed Summit (m/s)	Max Speed Sag (m/s)
21150	101.80	203.60		26400	113.74	227.47
21300	102.16	204.32		26550	114.06	228.12
21450	102.52	205.04		26700	114.38	228.76
21600	102.88	205.76		26850	114.70	229.40
21750	103.24	206.47		27000	115.02	230.04
21900	103.59	207.18		27150	115.34	230.68
22050	103.94	207.89		27300	115.66	231.32
22200	104.30	208.60		27450	115.98	231.95
22350	104.65	209.30		27600	116.29	232.59
22500	105.00	210.00		27750	116.61	233.22
22650	105.35	210.70		27900	116.92	233.85
22800	105.70	211.40		28050	117.24	234.47
22950	106.04	212.09		28200	117.55	235.10
23100	106.39	212.78		28350	117.86	235.72
23250	106.74	213.47		28500	118.17	236.35
23400	107.08	214.16		28650	118.48	236.97
23550	107.42	214.84		28800	118.79	237.59
23700	107.76	215.53		28950	119.10	238.21
23850	108.10	216.21		29100	119.41	238.82
24000	108.44	216.89		29250	119.72	239.44
24150	108.78	217.56		29400	120.02	240.05
24300	109.12	218.24		29550	120.33	240.66
24450	109.46	218.91		29700	120.64	241.27
24600	109.79	219.58		29850	120.94	241.88
24750	110.12	220.25		30000	121.24	242.49
24900	110.46	220.92		30150	121.55	243.09
25050	110.79	221.58		30300	121.85	243.70
25200	111.12	222.24		30450	122.15	244.30
25350	111.45	222.90		30600	122.45	244.90
25500	111.78	223.56		30750	122.75	245.50
25650	112.11	224.22		30900	123.05	246.10
25800	112.44	224.87		31050	123.35	246.69
25950	112.76	225.53		31200	123.64	247.29
26100	113.09	226.18		31350	123.94	247.88
26250	113.41	226.83		31500	124.24	248.48

Maximum Speeds for Vertical Curves						
Vertical Radius (m)	Max Speed Summit (m/s)	Max Speed Sag (m/s)		Vertical Radius (m)	Max Speed Summit (m/s)	Max Speed Sag (m/s)
31650	124.53	249.07		36900	134.47	268.93
31800	124.83	249.66		37050	134.74	269.48
31950	125.12	250.24		37200	135.01	270.02
32100	125.42	250.83		37350	135.28	270.57
32250	125.71	251.42		37500	135.55	271.11
32400	126.00	252.00		37650	135.83	271.65
32550	126.29	252.58		37800	136.10	272.19
32700	126.58	253.16		37950	136.37	272.73
32850	126.87	253.74		38100	136.63	273.27
33000	127.16	254.32		38250	136.90	273.81
33150	127.45	254.90		38400	137.17	274.34
33300	127.74	255.48		38550	137.44	274.88
33450	128.03	256.05		38700	137.71	275.41
33600	128.31	256.62		38850	137.97	275.95
33750	128.60	257.20		39000	138.24	276.48
33900	128.88	257.77		39150	138.50	277.01
34050	129.17	258.34		39300	138.77	277.54
34200	129.45	258.91		39450	139.03	278.07
34350	129.74	259.47		39600	139.30	278.60
34500	130.02	260.04		39750	139.56	279.12
34650	130.30	260.60		39900	139.82	279.65
34800	130.58	261.17		40050	140.09	280.17
34950	130.86	261.73		40200	140.35	280.70
35100	131.14	262.29		40350	140.61	281.22
35250	131.42	262.85		40500	140.87	281.74
35400	131.70	263.41		40650	141.13	282.27
35550	131.98	263.97		40800	141.39	282.79
35700	132.26	264.52		40950	141.65	283.31
35850	132.54	265.08		41100	141.91	283.82
36000	132.82	265.63		41250	142.17	284.34
36150	133.09	266.18		41400	142.43	284.86
36300	133.37	266.74		41550	142.69	285.37
36450	133.64	267.29		41700	142.94	285.89
36600	133.92	267.84		41850	143.20	286.40
36750	134.19	268.38		42000	143.46	286.91

	Maximum Speeds for Vertical Curves					
Vertical Radius (m)	Max Speed Summit (m/s)	Max Speed Sag (m/s)		Vertical Radius (m)	Max Speed Summit (m/s)	Max Speed Sag (m/s)
42150	143.71	287.43		47400	152.40	304.80
42300	143.97	287.94		47550	152.64	305.28
42450	144.22	288.45		47700	152.88	305.76
42600	144.48	288.96		47850	153.12	306.24
42750	144.73	289.47		48000	153.36	306.72
42900	144.99	289.97		48150	153.60	307.20
43050	145.24	290.48		48300	153.84	307.68
43200	145.49	290.98		48450	154.08	308.16
43350	145.74	291.49		48600	154.32	308.64
43500	146.00	291.99		48750	154.56	309.11
43650	146.25	292.50		48900	154.79	309.59
43800	146.50	293.00		49050	155.03	310.06
43950	146.75	293.50		49200	155.27	310.54
44100	147.00	294.00		49350	155.50	311.01
44250	147.25	294.50		49500	155.74	311.48
44400	147.50	295.00		49650	155.98	311.95
44550	147.75	295.50		49800	156.21	312.42
44700	148.00	295.99		49950	156.45	312.89
44850	148.24	296.49		50100	156.68	313.36
45000	148.49	296.98		50250	156.92	313.83
45150	148.74	297.48		50400	157.15	314.30
45300	148.99	297.97		50550	157.38	314.77
45450	149.23	298.47		50700	157.62	315.23
45600	149.48	298.96		50850	157.85	315.70
45750	149.72	299.45		51000	158.08	316.16
45900	149.97	299.94		51150	158.31	316.63
46050	150.21	300.43		51300	158.55	317.09
46200	150.46	300.92		51450	158.78	317.56
46350	150.70	301.41		51600	159.01	318.02
46500	150.95	301.89		51750	159.24	318.48
46650	151.19	302.38		51900	159.47	318.94
46800	151.43	302.87		52050	159.70	319.40
46950	151.68	303.35		52200	159.93	319.86
47100	151.92	303.84		52350	160.16	320.32
47250	152.16	304.32		52500	160.39	320.78

APPENDIX D ROUTE TRIP TIME RESULTS

The data within this appendix contains tables with route lengths, mileposts and vehicle travel times for the 21 new corridors. The tables reflect travel times for different alignment/technology combinations taking into account vehicle acceleration characteristics, effects of grades, mandatory urban speed limits as well as the comfort limits used in earlier analyses. Each of the 21 corridors report station-to-station travel times as well as total local and express service. Travel times and route lengths have been adjusted using the regression equations in section 3.7 for the judicious excursion routes.

Also included with Appendix D is a diskette containing the input files used for the analysis. These input files contain segment information for route alignments, including segment length, horizontal radius, sample elavation points, urban speed limits, and station stops. Files include a highway alignment, a railroad alignment (for the first 8 corridors), and an independent alignment. For some corridors it was necessary to supply an additional input file for the independent alignment with modified grades for the TGV technology (3.5% grade limitation).

City-Pair	Hwy Length (km)	TR07 Trip Time (min)	USComp Trip Time (min)	RR Length (km)	TGV Trip Time (min)	Ind Length (km)	TR07 Trip Time (min)	TGV Trip Time (min)	USComp Trip Time (min)
1. NY-NFalls									
LaGuardia-Tarrytown									
Penn Station-Tarrytown	42.3	15.9	14.0	42.3	19.4	42.3	15.9	19.4	14.0
Tarrytown-Albany	262.1	46.9	34.5	242.0	57.7	253.7	35.7	50.8	30.9
Albany-Utica	403.4	31.8	23.7	386.3	41.4	396.6	21.5	32.6	20.4
Utica-Syracuse	472.5	13.4	11.0	473.9	22.8	459.9	11.0	16.3	10.1
Syracuse-Rochester	607.1	27.2	20.8	604.2	44.8	601.5	24.5	34.8	21.5
Rochester-Buffalo	702.8	18.5	14.5	713.8	29.0	696.3	14.9	22.2	14.1
Buffalo-Niagara	727.1	8.9	8.3	738.6	10.5	721.2	8.4	10.5	7.7
Local Service		174.5	138.9		237.6		143.8	198.5	130.6
Express Service		152.7	117.5		210.3		120.7	170.4	109.4
2. Bos-Wash									
Boston-Newton	20.3	6.5	6.3	20.5	8.0	20.5	6.7	8.0	6.4
Newton-Worcester	71.8	13.7	11.1	72.9	17.2	71.1	10.4	14.6	9.3
Worcester-Springfield	143.6	17.9	13.3	156.3	29.0	136.5	12.7	18.8	11.0
Springfield-Hartford	187.2	10.8	8.2	196.5	14.9	178.9	9.2	12.5	7.7
Hartford-New Haven	246.0	14.4	10.7	255.6	18.7	236.3	12.4	16.8	9.6
New Haven-New Rochelle	336.7	25.4	19.4	344.6	30.9	327.6	16.8	23.5	15.1
NewRochelle-LaGuardia	361.9	9.3	8.8	365.6	9.0	348.5	7.8	9.0	7.6
LaGuardia to Penn Station	372.0	4.6	4.3	375.7	5.9	358.6	4.6	5.9	4.3
Penn Stn to Newark Airprt	393.9	9.0	8.0	397.6	11.0	380.5	9.0	11.0	8.0
Airport to NE Philadelphia	493.1	19.9	16.8	486.5	24.3	472.0	15.7	21.9	14.7
NE Phil to 30th St Station	527.6	12.8	11.8	520.7	14.0	506.1	12.3	14.0	11.7
30th to Phil Airport	538.3	4.9	4.4	538.7	8.4	524.2	7.1	8.4	6.6
Airport to Wilmington	571.5	11.0	9.9	570.0	12.0	557.5	9.1	11.7	8.4
Wilmington to NE Balt	667.5	23.6	17.4	665.8	26.2	653.8	15.6	22.6	14.3
NE Balt to Camden	684.1	7.2	6.3	679.5	6.7	671.4	6.7	7.9	6.5
Camden to Greenbelt	725.4	11.2	9.6	729.9	19.1	712.4	9.9	12.8	9.0
Greenbelt to Union Station	741.3	6.7	6.1	744.9	6.7	729.4	6.8	8.2	6.3
Local Service		240.9	204.4		294.1		204.8	259.6	188.7
Express Service		186.0	152.0		229.0		149.2	190.0	136.5
3. SD-SF									
San Diego-La Jolla	25.5	8.9	7.8	26.5	11.4	25.4	8.9	10.8	7.8
La Jolla-Anaheim	162.1	35.7	27.3	166.2	37.6	161.9	23.7	33.4	22.4
Anaheim-Los Angeles	201.7	14.0	13.4	210.9	17.1	201.5	14.0	15.9	13.4
Los Angeles-Bakersfield	378.0	40.6	33.6	582.9	117.4	370.5	33.1	44.5	30.9
Bakersfield to Fresno	550.9	31.3	25.6	755.7	38.7	541.5	24.9	37.3	24.1
Fresno to San Jose Airport	793.1	55.4	43.0	1046.9	77.0	795.9	37.8	54.6	36.0
SJ Airport to SF Airport	842.4	16.6	16.3	1097.7	18.7	845.2	16.6	17.6	16.3
Airport to San Francisco	865.7	9.2	8.3	1121.3	10.1	868.5	9.2	11.4	8.3
Local Service		225.7	189.2		342.0		182.3	239.5	173.0
Express Service		200.0	165.5		311.7		156.2	205.2	153.1
4. Chi-Det									
Chi O'Hare to Chi Loop	30.4	10.5	9.6	32.8	12.8	32.8	10.9	12.8	10.6
Chi Loop to Hammond, IN	76.1	16.3	15.2	60.7	12.8	60.7	10.7	12.8	10.0
Hammond to South Bend	193.3	28.4	21.0	175.0	29.2	166.4	16.4	24.4	15.6
South Bend to Toledo	414.9	47.1	35.4	400.1	52.7	386.3	31.3	46.5	30.3
Toledo to Ann Arbor	486.7	18.0	13.4	482.2	25.6	457.0	11.9	17.7	11.0
Ann Arbor to Det Airport	516.6	11.3	10.6	577.6	15.0	487.4	10.7	11.7	10.5
Airport to Detroit	537.0	7.7	7.4	538.5	8.7	508.3	7.7	8.7	7.5
Local Service		151.2	124.6		168.8		111.5	146.6	107.3
Express Service		130.6	104.9		142.0		89.2	118.0	86.7
5. Dal-Hou									
Ft Worth to Airport	39.3	12.8	12.2	30.9	10.6	30.9	9.7	10.6	9.6
Airport to Dallas	64.4	9.0	8.8	55.8	9.9	55.8	9.0	9.9	8.7
Dallas to Hou Airport	441.4	69.2	55.1	467.2	105.8	426.6	52.5	77.1	51.2
Airport to Houston	468.4	9.6	9.4	491.7	10.0	451.1	8.9	10.0	8.6
Local Service		106.7	91.6		142.2		86.1	113.5	84.2
Express Service		96.7	82.3		127.7		76.3	101.1	74.9

City-Pair	Hwy Length (km)	TR07 Trip Time (min)	USComp Trip Time (min)	RR Length (km)	TGV Trip Time (min)	Ind Length (km)	TR07 Trip Time (min)	TGV Trip Time (min)	USComp Trip Time (min)
6. Dal-SA									
Ft Worth to Airport	39.3	12.8	12.2	30.9	10.6	30.9	9.7	10.6	9.6
Airport to Dallas	64.4	9.0	8.8	55.8	9.9	55.8	9.0	9.9	8.7
Dallas to Waco	223.7	30.6	25.1	231.2	49.3	201.0	23.0	33.2	22.0
Waco to Austin	386.6	31.8	25.7	405.1	52.2	361.7	25.8	35.6	24.2
Austin to SA Airport	508.1	23.6	19.7	525.2	39.5	472.6	18.7	26.0	18.0
SA Airport to San Antonio	517.9	6.6	6.1	533.8	7.8	482.3	6.5	7.7	6.1
Local Service		124.5	107.7		179.3		102.8	132.9	98.7
Express Service		105.1	89.6		156.4		84.1	112.2	80.7
San Antonio to Houston	314.2	54.7	46.0	337.2	101.2	332.5	47.1	68.4	46.1
Austin to Houston	347.8	57.4	49.0			338.5	48.2	69.8	47.6
7. Mia-Tmp									
Miami to Hialeah	9.4	3.5	3.0	9.4	4.6	9.4	3.5	4.6	3.0
Hialeah to Ft Lauderdale	41.9	11.4	11.1	44.4	14.6	44.2	12.0	13.2	11.8
Ft Laud to W. Palm Beach	110.0	19.2	17.1	111.8	23.4	111.6	17.1	20.3	16.5
W.PalmBch to Kissimmee	359.6	52.3	39.2	405.1	74.8	342.6	33.0	48.9	31.8
Kissimmee to Orlando	383.7	9.0	8.5	428.1	9.4	365.7	8.4	9.4	8.2
Local Service		103.5	86.9		134.9		82.0	104.4	79.3
Express Service		90.9	75.3		117.6		67.1	85.7	65.6
Orlando-Tampa Express	151.8	36.5	31.0	156.5	48.4	140.6	27.4	34.7	26.6
8. Sea-Port									
Seattle to Sea-Tac Airport	22.8	8.0	7.2	25.5	10.1	19.5	6.4	7.7	6.1
Airport to Tacoma	59.9	10.6	8.0	74.8	19.0	52.1	8.7	12.3	6.7
Tacoma to Olympia	104.4	12.4	9.0	123.9	22.1	96.8	9.5	13.7	7.9
Olympia to Portland	284.1	42.9	32.4	321.3	64.0	275.2	29.6	41.4	27.9
Local Service		79.9	62.6		121.1		60.3	81.1	54.6
Express Service		69.1	52.7		108.9		49.6	67.4	44.2
9. LA-LV									
Anaheim to Los Angeles	42.8	14.0	13.4			45.0	14.2	15.2	14.0
Los Angeles to Ontario Apt	102.3	19.9	19.5			104.5	19.9	22.5	19.5
Airport to Las Vegas	482.9	76.2	61.4			461.3	54.8	83.8	51.7
Local Service		114.1	98.2				92.9	125.5	89.2
Express Service		107.4	92.2				84.3	114.8	81.1
10. DC-Atl									
WashDC to National Arpt	26.4	9.0	8.3			26.4	9.0	11.2	8.3
Airport to I-95 Beltway	41.1	5.8	5.6			41.1	5.8	6.9	5.6
I-95 Beltway to Richmond	191.4	31.2	24.6			190.9	25.1	35.4	23.5
Rich to Raleigh-Durham	431.3	50.8	38.9			443.5	37.2	54.3	35.1
Raleigh to Greensboro	518.9	19.8	14.9			529.2	14.0	21.0	13.0
Greensboro to Charlotte	662.3	30.9	24.4			674.4	23.6	33.5	22.8
Charlotte to Greenville	804.3	29.3	22.2			813.3	21.0	31.1	19.9
Greenville to NE Atlanta	1018.6	36.2	30.2			1027.9	30.4	45.4	29.6
NE Atlanta to Downtown	1037.9	7.5	7.1			1047.4	7.5	8.4	7.1
Atlanta to Airport	1054.6	6.4	6.2			1064.0	6.4	7.7	6.2
Local Service		246.9	202.3				200.1	274.9	191.2
Express Service		213.7	170.4				164.8	229.9	158.4
11. Chi-Minn									
Chi Loop to O'hare Airport	30.4	10.6	9.6			32.8	10.9	12.5	10.3
Airport to Kenosha	101.5	18.0	14.0			103.2	14.0	19.2	12.5
Kenosha to Milwaukee	154.9	12.0	9.7			154.1	9.9	14.1	8.7
Milwaukee to W. Milwaukee	164.6	4.4	4.0			165.6	4.4	5.8	3.7
W. Mil to Madison	268.2	19.8	15.9			268.0	16.0	23.8	15.1
Madison to Eau Claire	542.1	57.2	43.4			533.9	37.0	55.3	36.2
Eau Claire to St Paul	678.0	27.7	20.9			667.0	19.8	29.4	19.1
St Paul to Minneapolis	692.5	6.2	5.5			680.2	5.3	7.5	4.4
Local Service		169.9	137.2				131.2	181.6	124.0
Express Service		144.3	113.0				103.3	147.8	99.0

City-Pair	Hwy Length	TR07 Trip	USComp Trip	RR Length	TGV Trip	Ind Length	TR07 Trip	TGV Trip	USComp Trip
	(km)	Time (min)	Time (min)	(km)	Time (min)	(km)	Time (min)	Time (min)	Time (min)
12. Chi-KC									
Chicago Loop to I-294	29.6	9.6	9.2			29.6	9.6	11.1	9.2
I-294 to Bloomfield	210.4	36.3	27.3			204.2	25.4	37.9	24.5
Bloomfield to Springfield	311.2	23.8	17.3			299.7	15.0	22.3	14.2
Springfield to StLouis	469.4	29.5	23.9			443.4	22.3	32.3	21.0
StLouis to StLou Airport	492.8	9.2	8.4			466.8	9.2	11.3	8.4
StLouis to Columbia	668.6	33.1	25.9			639.1	25.0	37.1	24.2
Columbia to I-435	858.9	30.8	27.0			828.2	27.3	40.5	26.3
I-435 to Kansas City	869.4	4.6	4.3			838.7	4.6	5.7	4.3
Local Service		191.0	157.3				152.4	212.3	146.1
Express Service		166.1	133.7				126.0	179.0	121.9
13. Phi-Pitt									
Philadelphia to Radnor	23.7	8.4	7.5			23.7	8.4	10.4	7.5
Radnor to Harrisburg	169.1	35.7	26.1			157.5	20.9	30.8	19.5
Harris to Greensburg	450.7	77.4	56.8			413.2	36.4	54.2	34.9
Greensburg to Pittsburgh	494.8	16.6	14.9			457.3	16.6	20.2	14.9
Local Service		144.1	111.3				88.3	121.6	82.8
Express Service		133.9	101.5				77.2	107.9	72.5
14. Pit-Tol									
Pittsburgh to Airport	30.8	14.8	11.5			30.8	14.8	19.3	11.5
Airport to Youngstown	117.0	20.7	16.0			115.2	13.8	20.1	12.9
Youngstown to Akron	186.5	17.6	13.2			183.2	11.4	16.9	10.7
Akron to S. Cleveland	235.8	14.2	10.8			228.7	8.9	12.7	7.9
S. Cleveland to Cleveland	246.6	4.6	4.4			239.5	4.6	5.8	4.4
Cleveland to Airport	262.7	6.2	6.0			255.6	6.2	7.4	6.0
Airport to Toledo	425.6	32.6	25.1			418.4	24.2	35.6	22.9
Local Service		122.7	98.9				95.9	129.7	88.2
Express Service		102.1	79.0				73.6	101.5	67.7
15. Chi-Cinn									
Chi O'Hare to Chi Loop	30.4	10.5	9.6			32.8	10.9	12.8	10.6
Chi Loop to Hammond	76.1	16.3	15.2			60.7	10.7	12.8	10.0
Hammond to Lafayette	223.6	30.0	23.1			206.5	22.5	32.9	20.9
Lafayette to Indianapolis	323.9	20.5	16.8			305.4	16.4	24.1	15.4
Indianapolis to Cinncinnati	499.1	38.6	30.1			474.6	28.0	39.0	26.6
Local Service		123.8	102.9				96.4	129.4	91.6
Express Service		109.8	89.9				82.0	111.1	78.2
16. Clev-Cin									
Cleveland to S. Cleveland	14.1	4.7	4.4			14.1	4.7	5.6	4.4
S. Clevelend to Akron	62.0	14.8	11.5			59.6	8.9	12.5	7.9
Akron to Columbus	257.0	35.1	28.2			243.8	27.3	40.3	25.9
Columbus to Dayton	376.6	24.3	19.1			355.6	19.5	27.6	17.1
Dayton to Cinncinnati	459.7	19.7	16.9			435.5	17.0	22.3	15.7
Local Service		106.6	88.0				85.3	116.3	78.9
Express Service		92.8	74.5				70.0	97.6	64.7
17. SD-Pho									
Express Service	657.4	114.2	94.6			625.7	88.4	131.7	85.4
18. Hou-NO									
Houston to East I-610	13.1	4.4	4.2			13.1	4.4	5.5	4.2
Houston to Beaumont	135.7	20.9	18.0			132.0	18.1	26.9	17.3
Beaumont to Lake Charles	343.6	35.9	30.1			337.5	29.2	43.6	28.4
Lake Charles to Lafayette	427.2	13.8	12.7			421.2	13.5	20.0	12.8
Lafayette to Baton Rouge	532.4	19.7	15.8			521.0	15.6	23.1	14.8
Baton Rouge to New Orlear	550.3	7.1	6.5			538.8	7.1	8.7	6.5
Local Service		111.7	97.2				97.8	137.8	94.0
Express Service		93.0	79.4				78.9	113.7	76.2

City-Pair	Hwy Length (km)	TR07 Trip Time (min)	USComp Trip Time (min)	RR Length (km)	TGV Trip Time (min)	Ind Length (km)	TR07 Trip Time (min)	TGV Trip Time (min)	USComp Trip Time (min)
19. LA-Pho									
Los Angeles to Ontario	62.7	19.9	19.5			62.7	19.9	22.5	19.5
Ontario Airport to Phoenix	605.1	88.1	76.1			600.7	74.8	112.6	73.3
Local Service		110.0	97.6				96.7	137.1	94.8
Express Service		106.5	94.3				93.2	132.4	91.5
20. Bos-Alb									
Boston-Newton	20.3	6.5	6.3			20.5	6.7	8.1	6.4
Newton-Worcester	71.8	13.7	11.1			71.1	10.4	14.6	9.3
Worcester-Springfield	143.6	17.9	13.3			136.5	12.7	18.8	11.0
Springfield-Lee(Pittsfield)	208.0	18.6	11.7			199.2	12.5	18.4	8.5
Lee to Albany	283.3	20.9	15.3			272.8	13.1	17.6	11.4
Local Service		79.1	59.4				56.6	77.4	48.2
Express Service		70.5	53.5				47.5	65.4	42.5
21. SF-Reno									
SanFran to Sacramento	15.9	5.2	5.0			15.9	5.2	8.2	5.0
Sacramento to Lake Tahoe	139.6	27.8	22.3			137.3	23.1	31.5	21.6
Lake Tahoe to Carson City	300.8	51.0	34.8			286.4	23.3	40.1	21.2
Carson City to Reno	392.6	28.2	20.7			368.1	14.3	20.5	12.5
Local Service		118.2	88.8				71.9	106.4	66.2
Express Service		106.0	78.8				60.5	90.2	55.7

APPENDIX E: THE VALUE OF EXCURSIONS

This appendix provides the alignment information for improvements to route trip times based on judicious departures from the right-of-way. Departures were identified off USGS quadrangle topographic maps and evaluated for their potential reduction in trip time. The information for each detailed route is listed in table format to include the segment number at which the departure begins, the centerline guideway length, length of departure measured from the centerline, time saved, and a savings ratio of time saved (in seconds) to land needed for departure. An adjustment is made to the length outside the right-of-way (ROW) for the entry and exit distances associated with leaving the centerline for departure. Excursions are sorted by the savings ratio. Additional statistics including total time saved, total land acquired, percentage of route applicable to departure criteria, and average savings ratio are also provided.

Tappan Zee Bridge to Syracuse Highway 150 m/s

Segment Number	Length Base (m)	Length Alt (m)	Length (m) Outside ROW	Time Saved (sec)	Savings Ratio (sec/km)
72	10115	4115	1250	56.52	45.22
260	9470	9400	1250	39.82	31.86
373	8560	8400	1500	21.63	14.42
313	5970	4600	2525	32.82	13.00
9	6350	6300	600	7.57	12.62
149	4970	4700	2850	23.92	8.39
31	13310	13300	10100	40.55	4.01
346	2300	2100	1000	3.64	3.64
87	4060	4060	1700	5.15	3.03
92	8980	8950	4850	8.93	1.84
381	5450	5300	4275	4.70	1.10
209	4960	4900	2575	2.52	0.98
156	7650	7150	6250	4.92	0.79
102	5970	5800	2900	2.14	0.74

Total Time Saved = 254.83 sec (4.25 min)
Total Land Acquired = 43,625 m x 18.3 = 798,338 m^2
Excursion Percentage = 10.4%
Average Saving Ratio (sec/km) = 5.84

Yonkers to Syracuse Railroad 150 m/s

Segment Number	Length Base (m)	Length Alt (m)	Length (m) Outside ROW	Time Saved (sec)	Savings Ratio (sec/km)
500	10300	10200	500	37.02	74.04
477	21710	21500	2700	72.36	26.80
413	6470	6300	1600	22.24	13.90
369	3810	3650	1750	23.06	13.18
252	4430	4100	3300	26.38	7.99
401	4540	3600	2400	15.10	6.29
457	7640	7500	2150	12.97	6.03
437	7255	7000	6450	38.01	5.89
186	4350	4200	2750	12.36	4.49
339	2720	2650	0*	3.48	3.48

Total Time Saved = 276.93 sec (4.6 min)
Total Land Acquired = 23,600 m x 18.3 = 431,880 m^2
Excursion Percentage = 5.6%
Average Saving Ratio (sec/km) = 11.73

* No area outside the right-of-way was needed due to a large median. This excursion was listed to show trip time savings and could be used to adjust the centerline route but was not in this analysis.

Detroit to Chicago Highway 150 m/s

Segment Number	Length Base (m)	Length Alt (m)	Length (m) Outside ROW	Time Saved (sec)	Savings Ratio (sec/km)
111	2840	2800	200	18.00	90.00
2	6330	6300	600	23.97	39.95
162	10760	10600	1100	43.61	39.65
169	7580	7500	600	17.33	28.88
179	10610	10500	1300	35.57	27.36
273	3030	2700	2100	54.46	25.93
236	14850	14850	700	15.08	21.54
21	5830	5700	1100	21.96	19.96
197	7850	7700	1000	18.36	18.36
174	9560	9400	700	11.23	16.04
58	2920	2850	1500	18.85	12.57
101	8900	8900	1400	16.84	12.03
39	3350	3300	2200	14.32	6.51
89	10430	10400	1200	0.60	0.50
224	7670	7650	900	0.27	0.30
149	3070	3050	1000	0.21	0.21

Total Time Saved = 310.66 sec (5.2 min)
Total Land Acquired = 17,600 m x 18.3 = 322,080 m^2
Excursion Percentage = 4.1%
Average Saving Ratio (sec/km) = 17.65

Detroit to Chicago Railroad 150 m/s

Segment Number	Length Base (m)	Length Alt (m)	Length (m) Outside ROW	Time Saved (sec)	Savings Ratio (sec/km)
93	2930	2930	0*	23.63	23.63
1	8660	8600	600	12.80	21.33
43	6000	4350	3700	58.77	15.88
75	4570	4550	2700	30.13	11.16
84	4700	4200	3600	40.10	11.14
175	6160	5840	4300	42.21	9.82
114	11820	11800	9300	62.85	6.76
68	10330	10200	3400	17.00	5.00
57	6850	6600	5700	24.04	4.22
52	1300	1300	850	3.38	3.98

Total Time Saved = 314.91 sec (5.25 min)
Total Land Acquired = 34,150 m x 18.3 = 624,945 m^2
Excursion Percentage = 8.4%
Average Saving Ratio (sec/km) = 9.22

* No area outside the right-of-way was needed due to a large median. This excursion was listed to show trip time savings and could be used to adjust the centerline route but was not in this analysis.

Los Angeles to San Francisco Highway 150 m/s

Segment Number	Length Base (m)	Length Alt (m)	Length (m) Outside ROW	Time Saved (sec)	Savings Ratio (sec/km)
213	15625	14950	200	13.82	69.10
57	14030	14020	1400	73.64	52.60
129	8950	8700	700	32.55	46.50
253	3785	3770	1500	50.43	33.62
273	1410	1100	600	16.91	28.18
76	16300	16300	2750	73.76	26.82
194	13789	13700	200	3.08	15.40
102	12370	12350	3700	56.00	15.14
29	3600	3600	0*	12.43	12.43
235	8475	8450	1100	13.10	11.91
268	3815	3770	700	6.33	9.04
173	2700	2700	0*	4.95	4.95
205	5760	4900	1700	7.35	4.32
142	8860	8250	2700	10.27	3.80
248	5140	5140	500	1.79	3.58
178	1415	1415	0*	3.54	3.54
168	8900	8750	400	1.21	3.03
219	17060	16250	3700	10.93	2.95
192	2000	2000	0*	1.77	1.77
162	5475	5450	1900	2.79	1.47
186	2200	2200	0*	0.13	0.13

Total Time Saved = 399.10 sec (7 min)
Total Land Acquired = 23,750 m x 18.3 = 434,625 m^2
Excursion Percentage = 4.1%
Average Saving Ratio (sec/km) = 16.80

* No area outside the right-of-way was needed due to a large median. This excursion was listed to show trip time savings and could be used to adjust the centerline route but was not in this analysis.

Los Angeles to San Francisco Railroad 150 m/s

Segment Number	Length Base (m)	Length Alt (m)	Length (m) Outside ROW	Time Saved (sec)	Savings Ratio (sec/km)
214	14250	11100	0*	378.84	378.84
273	7115	2300	2300	229.78	99.90
193	10900	8700	1700	131.02	77.07
292	2800	1500	0*	54.23	54.23
314	4650	4550	0*	45.06	45.06
424	8750	6550	1800	68.24	37.91
428	3375	3550	300	9.09	30.30
67	11600	10700	7500	180.63	24.08
309	4625	4600	0*	20.13	20.13
391	6850	6800	1000	16.96	16.96
26	4500	4425	2800	47.00	16.79
408	24700	19210	15800	116.35	7.36
174	4075	3400	2500	18.36	7.34
367	4450	4350	0*	5.90	5.90
39	2550	2450	2200	12.48	5.67
129	1350	1200	1100	6.17	5.61
352	3400	3300	2350	7.93	3.37
122	1300	1275	700	1.96	2.80
346	1400	1400	0*	1.79	1.79
398	8200	8200	1150	1.14	0.99
329	5300	5300	0*	0.23	0.23

Total Time Saved = 1353.29 sec (22.5 min.)
Total Land Acquired = 43,200 m x 18.3 = 790,560 m^2
Excursion Percentage = 6.1%
Average Saving Ratio (sec/km) = 31.33

* No area outside the right-of-way was needed due to a large median. This excursion was listed to show trip time savings and could be used to adjust the centerline route but was not in this analysis.

APPENDIX F: ROUTE DESCRIPTIONS

This appendix provides a description of route paths and station stops for centerline and independent routes in the 20 additional corridors specified in section 3.7. The location of station stops for each corridor is dependent on the type of right-of-way used. Station stops for routes using the highway were placed on the outskirts of cities since most major U.S. highways do not penetrate city centers. Station stops for rail routes tend to stop in city centers at the existing rail stations. Independent right-of-way routes tried, where possible, to end at major transportation centers (i.e., airports and train stations).

1. Boston - Hartford

Highway: The highway route starts just west of Boston in Newton and travels west on I-90. Route bears southwest at the I-90 and I-84 split and proceeds to Hartford where it stops at the interchange of I-84 and I-91.

Railroad: The rail route starts near Boston University and travels the Penn Central line west towards Springfield. At Springfield, the Penn Central line bears south towards Hartford. The route ends at the bank of the Connecticut River.

Independent: The route starts on the rail line near Boston University and follows the railroad out of the city. In Newton the route switches to the centerline of I-90 to egress urban areas to Framington. The route leaves the centerline in Framington for independent right-of-way and passes south of Millbury and east of Southbridge. After Southbridge the route heads directly south and continues adjacent to I-86 and passes north of Manchester and stops at the Hartford airport.

2. Hartford - New York City

Highway: The highway route starts at the intersection of Interstate 84 and 91 and takes I-91 south towards New Haven. The route picks up I-95 south in New Haven, continues on I-95 through Bridgeport and Stamford, and ends at La Guardia airport in New York.

Railroad: The rail route follows Penn Central railroad starting in Hartford, south to New Haven, and southwest through Stamford. The route continues along the rail lines into New York City where it ends at the Queens midtown tunnel.

Independent: The route begins at the Hartford airport and follows I-5 out of Hartford. The route breaks off I-5 and heads west across country traveling north of the cities of Norwalk and Stamford. Pick up NYS route 15 in White Plains and follow it into New York City. Inside the city switch to the Metro Transit Authority rail line and follow it to La Guardia airport.

3. New York City - Philadelphia

Highway: The highway route starts at La Guardia airport and follows I-287 across New York Bay (bridge needed) to the New Jersey Turnpike. Travel south on the turnpike centerline down through the state past Trenton. The route switches to I-295 north of Woodbury and continues to the ending station in Gibbstown, south of Philadelphia.

Railroad: The rail route starts at La Guardia airport and travels the Metro Transit Authority rail line across New York Bay (bridge needed) into New Jersey. A connection is made with the Amtrak mainline near Newark international airport. The route continues on the Amtrak line through the state of New Jersey through New Brunswick and Trenton. In Trenton, the route crosses the Delaware River, goes through Philadelphia, and stops at the 30th Street station.

Independent: The route starts at La Guardia airport and follows the Conrail line towards New Jersey. The route switches to I-287 and crosses New York Bay (bridge needed). Follow I-287 to the New Jersey Turnpike and head south. Break off turnpike centerline north of Hightstown and continue south. Enter back into the turnpike centerline near Willingboro and follow to Woodbury where the route departs for the ending station at the bank of the Delaware River across from the airport.

4. Philadelphia - Wilmington

Highway: The highway route starts at the intersection of turnpike, I-295, and I-76. The route continues south on the turnpike, crosses the Delaware River parallel to the Delaware Memorial Bridge, and stops at the airport in Wilmington at the intersection of I-95.

Railroad: The rail route begins at the 30th Street station and travels the Amtrak route along the Delaware River. The ending station is near the Wilmington airport at the intersection of the Amtrak line and route 141.

Independent: The route starts at the Philadelphia station on the south side of the Delaware River, opposite the airport, and egresses to I-295. Follow centerline across the Delaware River (bridge needed) to the station at the Wilmington airport.

5. Wilmington - Baltimore

Highway: The highway route begins at the Wilmington airport and travels south on I-95 through the state of Maryland to Baltimore. Once entering Baltimore, the route travels through the city along I-895 and stops near the entrance of the Harbor Tunnel.

Railroad: The rail route starts at the Wilmington airport and travels on the Amtrak line through Maryland. The route follows Amtrak through the city of Baltimore and stops at Penn Station.

Independent: The route starts at the Wilmington airport and follows I-95 south out of Wilmington. Break from the I-95 centerline near Bay View and continue to travel southwest crossing the Susquehanna River (bridge needed). Continue along independent right-of-way until Baltimore Beltway (I-695) interchange and follow centerline to a station located in center city.

6. Baltimore - Washington

Highway: The highway route starts at Camden Yards in downtown Baltimore and travels along the Baltimore-Washington Parkway towards Washington. The route follows the parkway into the city of Washington and switches to US route 50 where it stops at a station downtown near the Capitol.

Railroad: The rail route starts at Penn Station in Baltimore and follows the Amtrak line to Union Station in downtown Washington.

Independent: The route starts in center city Baltimore and follows I-95 out of city (tunnel needed). Break from centerline and pass by Baltimore-Washington International airport. Travel adjacent to Baltimore-Washington Parkway heading south. Switch to the Amtrak rail line in Beltsville and follow rail to Union Station in downtown Washington.

7. Syracuse - Rochester - Buffalo

Highway: The highway route starts at the intersection of the New York Thruway (I-90) and I-81. The maglev travels west along the Thruway and crosses the Seneca River. The maglev makes a station stop in Rochester at the intersection of I-390 near the town of Henrietta. The route continues along the Thruway to the ending station in Buffalo at the airport.

Railroad: The rail route starts just south of Lake Onondaga and travels west along the Conrail line. The maglev makes a station stop at the existing train station in Rochester and continues along the Conrail railroad to Buffalo. The ending station is located in the town of Sloan, a suburb of Buffalo with closest proximity to the airport.

Independent: The route starts in downtown Syracuse and follows the Conrail railroad line out of the city. Leave railroad at city limits and travel on independent right-of-way towards Rochester. Pick up Conrail again in East Rochester and follow to center city for intermediate station stop. Egress Rochester using I-490 and travel cross-country again towards Buffalo. The route ends at the Greater Buffalo International airport.

8. Buffalo - Niagara Falls

Highway: The highway route starts at the Greater Buffalo International Airport and travels west along route 234. The route heads north when route 234 intersects with I-190. The route takes I-190 across the Niagara River and proceeds west on the Moses Parkway to the base of the river which is the Canadian border.

Railroad: The rail route starts at the downtown rail station and proceeds north on the Conrail line, passes Niagara Falls International Airport and turns west to follow another Conrail line to a station stop at the Canadian border.

Independent: The route starts at the Buffalo airport and heads directly north on independent right-of-way, joins the Conrail line and follows it to the station at the Canadian border.

9. Chicago - Milwaukee

Highway: The highway route begins at the Chicago Loop and follows I-94 north out of Chicago. The route continues along I-94 across the Wisconsin border to the city limits of Milwaukee. The route turns west onto I-894 and continues to a station at the Wisconsin State Fairgrounds.

Railroad: The rail route starts at Chicago Harbor and uses Conrail and the Chicago and Northwestern (CNW) lines to exit the city. Once out of Chicago the route follows a CNW line through Waukegan across the Wisconsin border. The route ends at a station in center city Milwaukee.

Independent: The route begins at the Chicago Loop and follows I-94 out of Chicago and picks up the Chicago Milwaukee St. Paul and Pacific railroad (CMSP&P) heading north. The route travels

parallel to the railroad through the town of Sturtevant and past General Mitchell airport to a station in the center of Milwaukee.

10. Milwaukee - Madison

Highway: The highway route begins at the Wisconsin State Fairgrounds and travels west on I-94 to an ending station in Madison near the banks of Lake Mendota.

Railroad: The rail route starts in downtown Milwaukee and travels along the CNW railroad through the towns of Sullivan and Deerfield. The route travels through Monona and ends at Marshalling yards near the bank of Lake Mendota.

Independent: The route begins at the city center of Milwaukee and follows the Chicago Milwaukee St. Paul and Pacific railroad (CMSP&P) out of the city. Once out of Milwaukee the route picks up I-94 and travels parallel to I-94 crossing the highway twice, once near Lake Mills and again near Seminary Springs. The route ends in eastern Madison on the bank of Lake Monona.

11. Dallas - Houston

Highway: The highway route begins at the intersection of I-20 and I-45. The route travels southeast along the centerline of I-45 through the towns of Corsicana, Huntsville, and Conroe before ending at the intersection of I-610 on the north side of Houston.

Railroad: The rail route starts at the intersection of I-20 and follows the Southern Pacific railroad. The route travels south to Corsicana where it switches to the Fort Worth & Denver line and continues in a southeasterly fashion toward Houston. The route ends at the intersection of I-45 just north of the city.

Independent: The route begins at the intersection I-45 and US route 12 and egresses the Dallas area following the centerline of I-45 south. Once outside city limits the route leaves the centerline and travels west of the highway between Ennis and Bardwell Lake. Continuing south the route crosses I-45 at Corsicana and passes east of Huntsville and Conroe. Approaching Houston, the route picks up the Missouri-Pacific rail line and follows it into Houston and ends at the intersection of I-610.

12. Dallas - Waco

Highway: The highway route begins at the intersection of I-20 and I-35E. Follow I-35E along the centerline south. I-35E meets I-35W in Hillsboro and continues south. The route ends in Waco at the intersection of I-35 and US route 84.

Railroad: The rail route begins at the intersection of US route 12 and travels the Fort Worth & Denver line south. The railroad becomes part of the Missouri-Kansas-Texas line and continues south through Hillsboro. The route ends at the intersection of the railroad and I-35.

Independent: The route begins at the intersection of I-20 and I-35E. The route heads south along independent right-of-way east of Redbird airfield and Midlothian. Continue to travel south and cross over I-35 near Hillsboro. Pick up abandon railroad line on west side of I-35 and follow it to the city limits of Waco. Ending station is located in the city center at the railroad station.

13. Waco - Austin

Highway: The highway route begins at the intersection of I-35 and US route 84. Follow the I-35 centerline south through the towns of Temple and Georgetown to Austin. The route ends at the intersection of I-35 and US route 183.

Railroad: The rail route begins at the intersection of I-35 on the Missouri-Kansas-Texas line and travels south through the towns of Temple, Taylor, and Elgin. At Elgin the route switches to the Southern Pacific line and heads west to Austin. The route ends at the intersection of US route 183 in the southeastern portion of the city.

Independent: The route begins in center city Waco and uses the Missouri-Kansas-Texas railroad line to exit city. The route travels south on the western side of I-35 and crosses over the highway between the towns of Temple and Benton. Continue south passing just east of Georgetown and stop in Austin at the intersection of I-35 and US route 290.

14. Austin - San Antonio

Highway: The highway route starts at the intersection of I-35 and US route 183. Travel south on I-35 past the towns of San Marcos and New Braunfels to the outskirts of San Antonio. Switch to I-410 and follow to the station stop at the San Antonio airport.

Railroad: The rail route starts in the southeastern portion of the city and follows the Missouri-Pacific railroad southeast past the towns of San Marcos and New Braunfels to the San Antonio airport.

Independent: The route begins at the Austin airport and exits the city using I-35 centerline. Break off centerline travelling east of I-35. Cross over I-35 near San Marcos and pass north of New Braunfels. Continue on to a station at the San Antonio airport.

15. Austin - Houston

Highway: The highway route begins at the intersection of I-35 and US route 183. Traveling along route 183 centerline exit city and pick up route 71. Travel south by southeast and pick up the I-10 centerline in Columbus. Continue on I-10 due east to an ending station in Houston at the interchange of I-10 and I-610.

Railroad: The rail route begins at the intersection of US route 183 and travels along the Southern Pacific railroad to Elgin. Transfer to the Missouri-Kansas-Texas line and follow east. The Missouri-Kansas-Texas line meets with I-10 near the town of Sealy and travels parallel to Houston. The route stops at the I-610 interchange.

Independent: The route begins at the intersection of I-35 and US route 290. The route follows route 290 east passing just south of Brenham and crossing over route 290 to travel just north of Hemstead. The route continues parallel to route 290 until it reaches the station in Houston at the I-610 interchange.

16. Los Angeles - San Diego

Highway: The highway route starts at Elsyian Park and follows I-5 through Anahiem and Santa Ana. The route continues along coast through the towns of Oceanside and Solona Beach. The route ends at the intersection of I-5 and route 163 near the Naval housing area.

Railroad: The rail route starts at Elsyian Park and travel along the Southern Pacific railroad through Anahiem. The route switches to the Atchison Topeka and Santa Fe railroad (ATSF) and continues south adjacent to I-5. The route ends at a station located at Sea World (intersection of railroad and I-8).

Independent: The route begins at Elsyian Park and exits the city using a combination of the Southern Pacific railroad and I-5. South of Anaheim catch the ATSF railroad and follow to Mission Viejo. Break off railroad to independent right-of-way but regain I-5 shortly thereafter in San Juan Capistrano to avoid the mountains. Follow I-5 to Oceanside and switch back to the ATSF railroad. At Sorento leave railroad right-of-way to travel to station at Sea World.

17. Los Angeles - Las Vegas

Highway: The highway route starts at Elsyian Park and follows the I-10 centerline to San Bernadino. In San Bernadino the route switches to I-15 and travels through the Gabriel mountains northwest to Barstow. The route continues on I-15 to Las Vegas to the station at the Las Vegas airport.

Railroad: The rail route starts at Elsyian Park and travel along the Southern Pacific railroad past Rosemead through Baldwin Park. The route then switches to the Atchison Topeka and Santa Fe railroad (ATSF) in San Bernadino and heads north through the Gabriel mountains. The route winds through the mountains of eastern California and ends at Boulder Junction just east of the Las Vegas airport.

Independent: The route begins at Elsyian Park and exits Los Angeles using the Southern Pacific railroad. The route breaks from the railroad just east of San Bernadino and heads on independent right-of-way through the Gabriel mountains crossing a portion of the Cleghorn mountains. The route continues northeast, passes south of Barstow, and travels just south of the Soda mountains. The route ends at a station near the Las Vegas airport.

18. Seattle - Tacoma - Olympia - Portland

Highway: The highway route starts near the Seattle airport and follows I-5 south to a station stop in downtown Tacoma. The route continues on I-5 to a second station stop in Olympia. The route exits Olympia on I-5 and travels south to Portland where it stops at a station at the intersection of I-5 and I-30.

Railroad: The rail route begins at the airport in Seattle and runs south on the Chicago Milwaukee St. Paul and Pacific railroad (CMSP&P) out of the city towards Tacoma. The route turns west and makes a station stop in downtown Tacoma. The route continues along the CMSP&P railroad (shared with the Union Pacific and Burlington Northern) to Olympia and makes a second station stop in the downtown area. The route then heads south through the towns of Chehalis and Longview. The route ends after it runs through the city of Vancouver and crosses the Columbia River.

Independent: The route starts near the Seattle airport and follows I-5. The route leaves the right-of-way at Federal Way and travels independently until Tacoma where it enters back into the I-5 centerline and makes a station stop in the city center. Egress from Tacoma is done using I-5 and

continues on the centerline to the station in Olympia. I-5 is used to exit Olympia. The route leaves the I-5 centerline south of Tumwater and travels west of the highway. The route crosses I-5 near Castle Rock and travels east of the highway past Kelso. The route enters Portland on I-5 and stops at the ending station after crossing the Columbia River.

19. Miami - Fort Lauderdale - West Palm Beach - Orlando

Highway: The highway route begins in northern Miami and travels the centerline of the Florida turnpike. Stops are made at Lauderdale Lakes and Haverhill near the Fort Lauderdale and West Palm Beach airports, respectively. The route continues along the turnpike to Orlando and stops at the intersection of the Bee Line Expressway.

Railroad: The rail route starts in north Miami and travels along the railroad making stops at the Fort Lauderdale and West Palm Beach airports. The route continues up the coast and heads inland along the railroad which runs parallel to route 710. The route passes Lake Istokpoga and continues north through Haines City and Kissimmee. The route ends at where the railroad intersects the Bee Line Expressway.

Independent: The route begins in Hollywood just north of Miami. The route follows the Florida turnpike, stops in Fort Lauderdale and West Palm Beach, and switches to the railroad at Riviera Beach. Following the railroad northwest the route picks up route 441 at Okeechobee County airport to Yeehaw Junction where it joins the Florida turnpike again. The route follows the Florida turnpike just east of Lake Marian and stops at a station at the intersection of the Bee Line Expressway.

20. Orlando - Tampa

Highway: The highway route begins at the intersection of the Florida turnpike and the Bee Line Expressway. The route travels along the Bee Line, switches to I-4, and heads southwest along the centerline. The route goes through Lakeland and continues to a station located at the Tampa airport.

Railroad: The rail route begins at the Bee Line interchange and travels southwest through the city of Lakeland. The route continues to the ending station at the Interbay Peninsula in Tampa near the Gandy Bridge.

Independent: The route begins at the Bee Line Expressway and travels adjacent to an existing powerline southwest. The route then follows I-4 and crosses the highway to travel north of Polk City. The route regains its alignment with I-4 and follows the highway to the ending station at the Tampa airport.

MAGLEV Guideway Route Alignment and Right-of-Way Requirements, October 1992 (Martin Marietta Corporation Report), S Carlton, T Andriola, Martin Marietta Corporation, 1992 -11-Advanced Systems